

GFZ

Helmholtz Centre
POTSDAM

HELMHOLTZ CENTRE POTSDAM
**GFZ GERMAN RESEARCH CENTRE
FOR GEOSCIENCES**

Gottfried Grünthal, Dietrich Stromeyer, Christian Bosse

The data sets of the earthquake model for the probabilistic seismic hazard assessment of Germany, version 2016

**Report on supplementary material
for the respective publication**

Scientific Technical Report STR17/05 - Data

Recommended citation:

Grünthal, G., Stromeyer, D., Bosse, C. (2017): The data sets of the earthquake model for the probabilistic seismic hazard assessment of Germany, version 2016 - Report on supplementary material for the respective publication, (Scientific Technical Report STR - Data; 17/05), Potsdam: GFZ German Research Centre for Geosciences.
DOI: <http://doi.org/10.2312/GFZ.b103-17056>

Supplementary datasets described in this report:

Grünthal, G., Stromeyer, D., Bosse, C. (2018): The Source Model of the Probabilistic Seismic Hazard Assessment (PSHA) of Germany - Version 2016. V. 1.0. GFZ Data Services.
DOI: <http://doi.org/10.5880/GFZ.2.6.2018.001>

Respective publication:

Grünthal G, Stromeyer D, Bosse C, Cotton F, Bindi D (2018) The probabilistic seismic hazard assessment of Germany: version 2016, considering the range of epistemic uncertainties and aleatory variability. Bull Earthquake Engineering: 1-57.
DOI: <http://doi.org/10.1007/s10518-018-0315-y>

Imprint

HELMHOLTZ CENTRE POTSDAM
**GFZ GERMAN RESEARCH CENTRE
FOR GEOSCIENCES**

Telegrafenberg
D-14473 Potsdam

Published in Potsdam, Germany
March 2018

ISSN 2190-7110

DOI: <http://doi.org/10.2312/GFZ.b103-17056>
URN: urn:nbn:de:kobv:b103-17056

This work is published in the GFZ series
Scientific Technical Report (STR)
and electronically available at GFZ website
www.gfz-potsdam.de



G. Grünthal, D. Stromeyer, C. Bosse

**The data sets of the earthquake model for
the probabilistic seismic hazard assessment
of Germany, version 2016**

**Report on supplementary material
for the respective publication**

Table of Contents

Abbreviations.....	3
Abstract.....	4
1. Introduction.....	5
2. Seismicity.....	6
2.1. Induced seismicity.....	6
2.2. Seismicity related to photolineations.....	9
2.3. Completeness of catalogued magnitudes.....	11
3. Models of seismic sources.....	12
4. Probability density functions of maximum magnitudes.....	19
5. Seismicity rates.....	21
6. Depth distributions.....	58
7. Tectonic regimes.....	61
8. Additional results of the probabilistic seismic hazard assessment.....	62
8.1. Probabilistic seismic hazard maps.....	62
8.2. Deaggregations.....	81
8.3. The parameters of the EC 8 elastic design spectral shapes.....	82
9. Comparison with results of the new Swiss earthquake hazard model.....	83
10. Available Datasets.....	85
11. References.....	87

Abbreviations

CSS	composite seismic source
DIBt	Deutsches Institut für Bautechnik
EC 8	Eurocode 8
GMPE	ground motion prediction equation
LASZ	large scale areal source zone
meanSRA	mean of the amplitudes of periods $T(0.1s, 0.15s, 0.2s)$ in the UHS representing the plateau at a grid point [m/s^2]
M_w	moment magnitude
M_{max}	maximum expected magnitude
M_{max}^{obs}	maximum observed magnitude
PDF	probability density function
PGA	peak ground acceleration [m/s^2]
PSHA	probabilistic seismic hazard assessment
RP	mean return period [a]
SRA	spectral response acceleration [m/s^2]
SSAZ	small scale seismic source zone
SSZ	seismic source zone
UHS	uniform hazard response spectrum

Abstract

The Scientific Technical Report describes supplementary material to the publication by *Grünthal et al.* (2018) on the earthquake model for the probabilistic seismic hazard assessment (PSHA) of Germany, version 2016. In particular, it contains detailed information, additional figures, tables and electronic data concerning seismicity, seismic source zone models, maximum magnitudes, seismicity rates of the seismic source zones, model data related to distributions of focal depth and tectonic regime parameters. It also supplies seismic hazard maps for Germany with a broad range of parametrizations.

1. Introduction

The re-evaluation of the probabilistic seismic hazard of Germany, in the version of 2016, has been elaborated on behalf of the German Institute for Civil Engineering (DIBt). The descriptions of the related earthquake model as input for the analysis, as well as the presentation of the respective basic results, are subject of the article by *Grünthal et al.* (2018). However, the earthquake model with all its elements and parameters, including their epistemic uncertainties and aleatory variabilities, is rather complex and beyond the scope of the abovementioned publication. Therefore, the entire set of model parameters and input data are compiled within this report as supporting and supplementary material to *Grünthal et al.* (2018). Moreover, the model parameters and input data are made available also in electronic form (*Grünthal et al.* 2018a). Though, to avoid repetitions, the usage of these data requires detailed information of *Grünthal et al.* (2018).

2. Seismicity

2.1. Induced seismicity

The probabilistic seismic hazard assessment (PSHA) of Germany is based on the needs of the National Annex (NA) [DIN EN 1998-1/NA:2011-01(2011)] to the Eurocode 8 [DIN EN 1998-1:2010-12 (2010)] and in agreement with our research contract with the DIBt on natural tectonic earthquakes (cf. chapter 2 in *Grünthal et al.* 2018). However, the issue of induced seismicity, with several widely felt events in the last decades, has become well-covered by the media and received much public attention. Because of this common interest, some light is shed on this aspect of induced seismicity, where we can rely on the review article by *Grünthal* (2014) on different types of induced seismicity observed in Germany and its immediate surroundings. The differentiation is made therein in induced seismic events due to mining of coal, potash and salt mining, ore mining, hydrocarbon exploitation, geothermal projects, water reservoirs and precipitation. The latter type is in a way a natural phenomenon and rather a triggering mechanism; hence this type of events is used for the presented PSHA. For a clearer distinction between tectonic and induced seismicity, *Grünthal* (2014) suggested to make a clear differentiation in the terminology of both types; i.e. to use strictly the term “induced seismic events” versus “natural tectonic earthquakes” (or simply “earthquakes”).

Fig 2-1 shows the observed seismicity in Germany and its immediate surroundings (tectonic earthquakes and induced seismic events), discriminated into the types mentioned above. The concentration of the induced events on respective coal mining areas or project sites is obvious. The precipitation triggered events are connected with karst areas (see *Grünthal*, 2014, for more details). Particularly revealing is the temporal occurrence of magnitudes of the different types of induced seismic events subdivided into mining districts (Fig. 2-2). We can recognize that the respective activities started with certain human manipulations in the underground. On the other hand, there is obviously a decrease in the magnitudes of several types of induced seismicity connected with a better of exploitation processes, fracking activities or stabilization measures in the underground to avoid “Seismic event of economic concern” (SEECo - introduced as technical term *Grünthal* (2014)). Another issue, which can clearly be noticed in Fig. 2-2, is the termination of seismicity of induced events after the stop of respective projects or

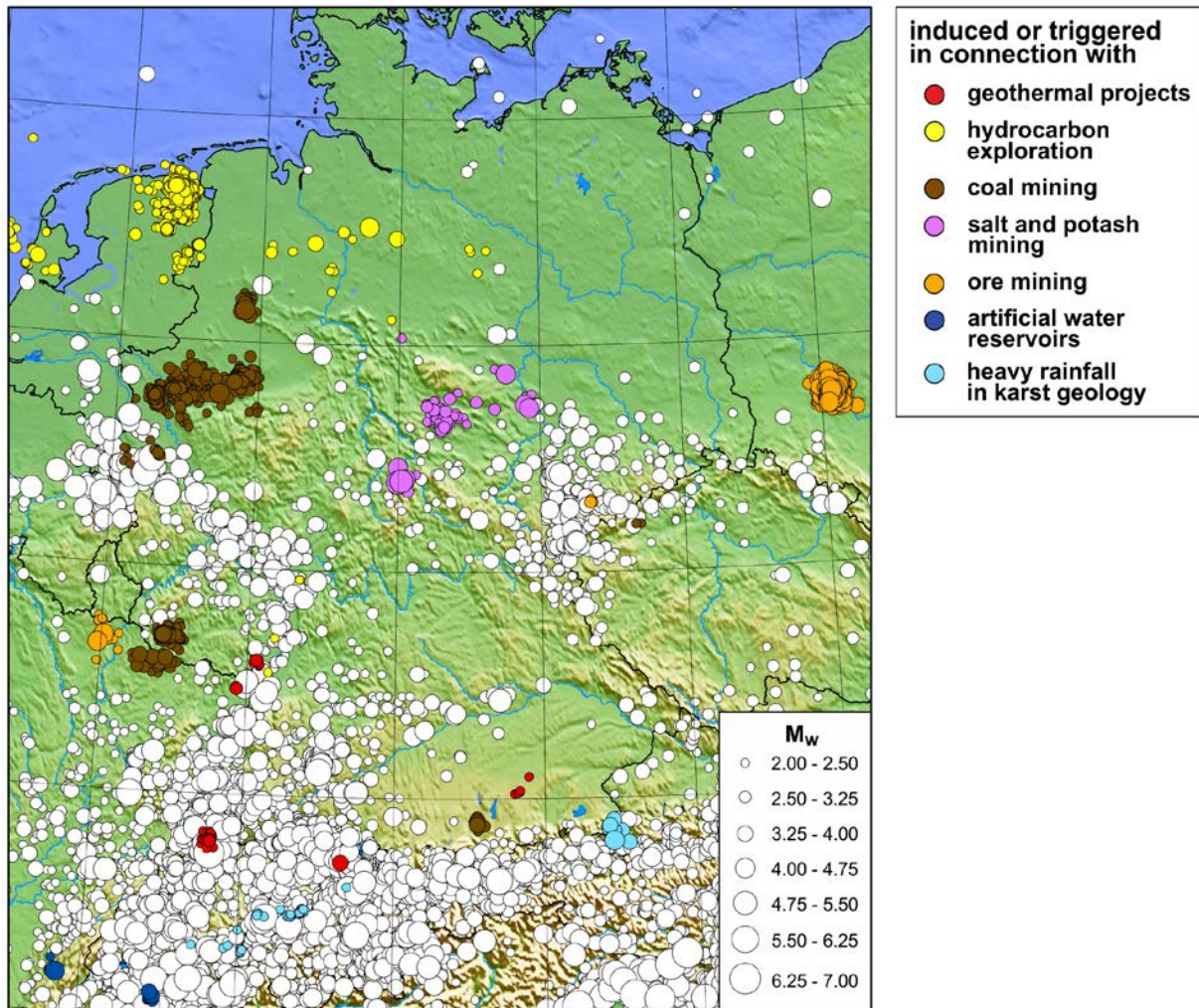


Figure 2-1. Natural tectonic seismicity and induced seismic events in Germany and surroundings; according to Grünthal (2014) – though based on a data file extended up to 2016.

mining activity in certain districts. Such obvious temporal changes in the seismic activities of induced events in dependence of human manipulations in the underground make any probabilistic forecast, such as a PSHA, extremely difficult. Any PSHA concerning induced seismic events which does not consider such striking temporal effects will be of reduced validity.

One of the parameters that provides a preliminary insight into the hazard potential of an area is the maximum observed magnitude M_{max}^{obs} . Fig. 2-3 shows the ranking of M_{max}^{obs} for the different types of induced seismic events in Germany and immediate surroundings. All magnitudes used here are moment magnitudes M_w . The $M_{max}^{obs} = 6.6$ of natural tectonic earthquakes (i.e.; the 1365 Basel earthquake, c.f. Grünthal et al. 2018) is by far the largest event observed in the region. It is followed by the M_w 5.4 Völkershäusen seismic event in a potash mining area, of rank 2, which was caused by an obvious

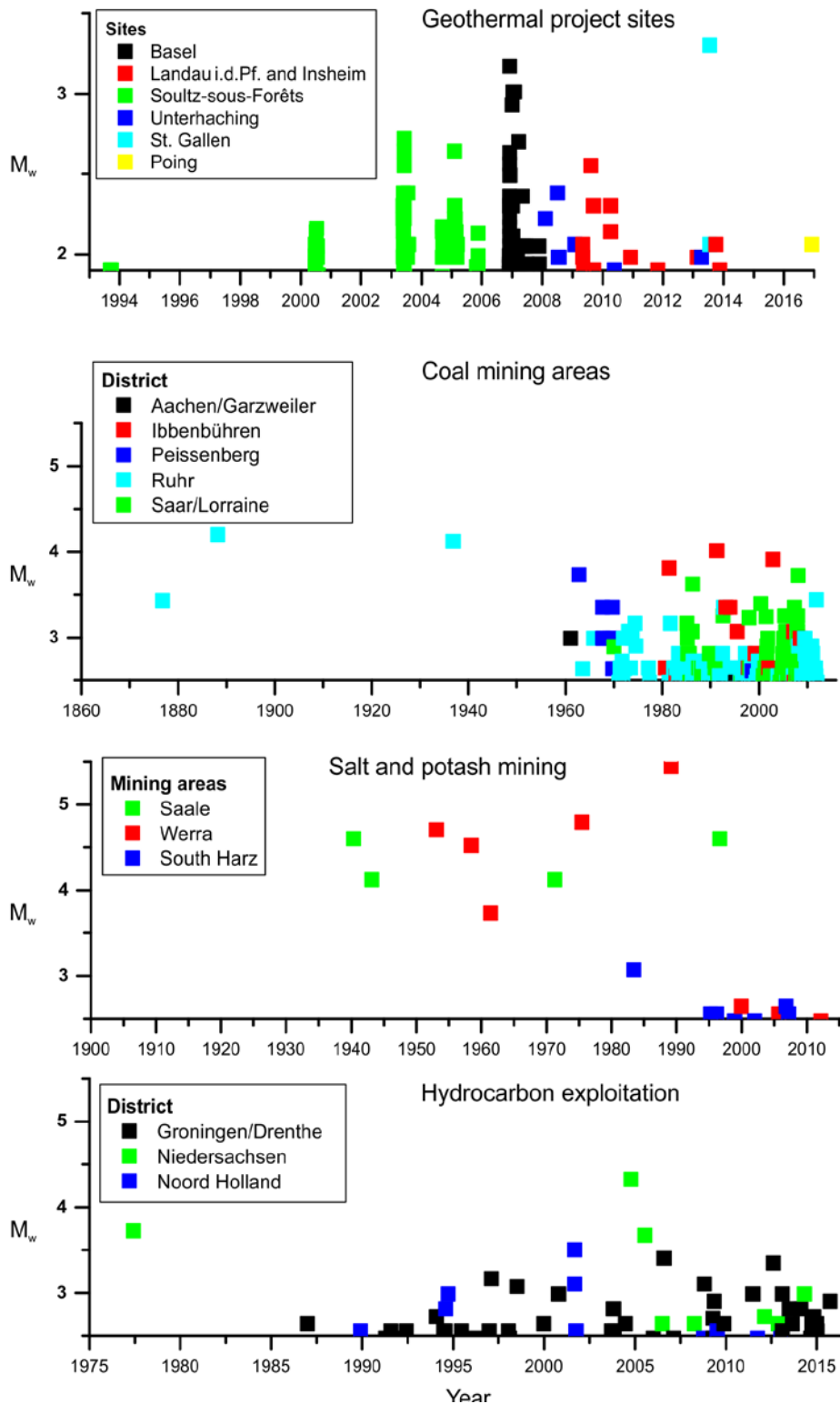


Figure 2-2. Temporal occurrence of induced seismic events specified according to event types and mining districts; according to *Grünthal* (2014) – though based on a data file extended up to 2016.

undersizing of pillars in the potash mining horizon. Since such a mining engineering approach is unlikely to be repeated, a similar event becomes considerably less probable in future. The M_{max}^{obs} values of the other types of induced seismicity are much lower.

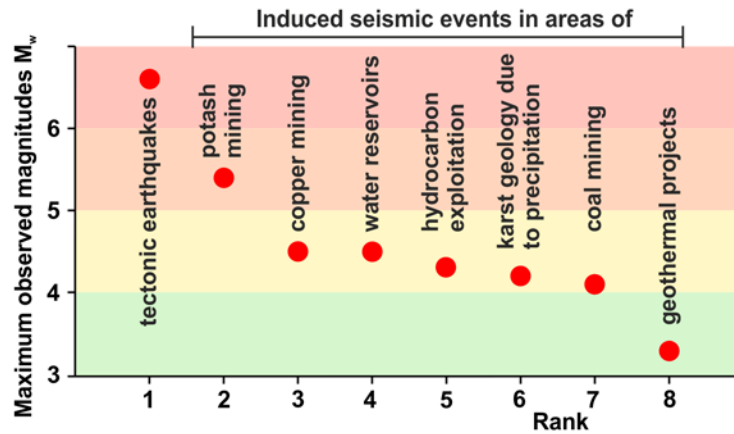


Figure 2-3. Ranking of the maximum observed magnitude M_{max}^{obs} of the different sources of seismicity in Germany and immediate surroundings, differentiated into natural tectonic earthquakes and observed types of induced seismic events up to 2016; modified after *Grünthal* (2014).

A quantitatively more refined comparison is possible with yearly frequency-magnitude relations of the different event types. With respect to such graphs we refer to Fig. 7 of *Grünthal* (2014).

2.2. Seismicity related to photolineations

The relationship of seismicity with regional tectonic settings has already been described to some extent in chapter 3 of *Grünthal et al.* (2018). There, it has been mentioned that prominent seismicity features cannot be associated readily with classical tectonic faults but rather with fracture lineaments detected from high resolution data from ERS-1/2 radar mosaics, Landsat-TM, Aster-DEM, and X-SAR-SRTM. This characteristic shall be supported here with two respective maps. The first example refers to the seismicity of the Hohenzollernalb (HZA), the spot of seismic activity that commenced in 1911 with a M_w 5.7 event, followed by several damaging earthquakes, the most recent in 1978. Ongoing activity can be observed in that focal zone of the HZA, which is located around 9°N and $48.2\text{-}48.5^\circ\text{E}$ (Fig. 2-4). The figure shows both the precisely located seismicity from 1995-2016, alongside the tectonic faults and photolineations of Figs. 3-1, and 3-2 of *Grünthal et al.* (2018) for the southwest part of the target area and surroundings. The coincidence of the seismicity in a narrow band around 9°N and $48.2\text{-}48.5^\circ\text{E}$ with almost N-S striking photolineations is obvious.

The other example, which highlights the importance of photolineations in relation to understanding the seismicity of certain regions, concerns the Vogtland-Leipzig zone (cf.

chapter 3 of Grünthal et al. 2018). Fig. 2-5 shows the well located seismicity of this N-S elongated zone from 1995-2016.

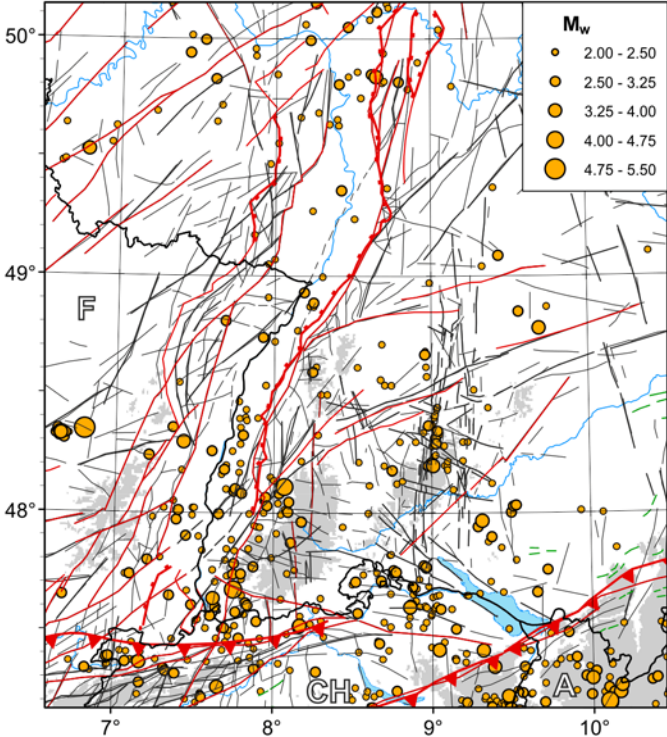


Figure 2-4. Seismicity in the southwest part of the target area and surroundings from 1995-2016 in connection with tectonic faults and photolineations of Figs. 3-1 and 3-2 of Grünthal et al. (2018).

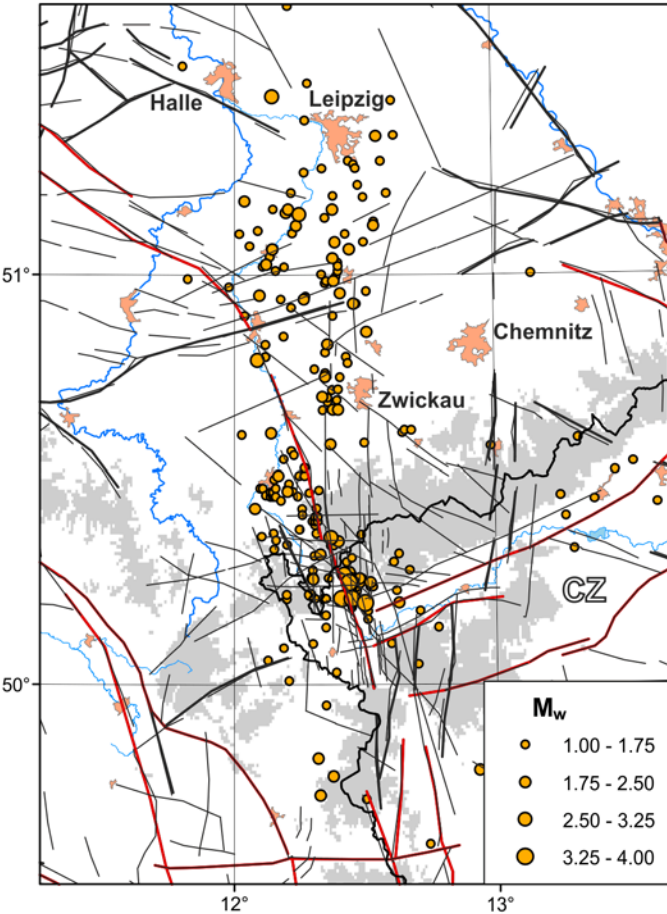


Figure 2-5. Seismicity in the Vogtland-Leipzig zone from 1995-2016 in connection with tectonic faults and photolineations of Fig. 3-1 and 3-2 of Grünthal et al. (2018).

2.3 Completeness of catalogued magnitudes

A basic element for the calculation of yearly rates of catalogued earthquake magnitude classes is the sufficient temporal completeness of events per class. This has been described in many of our earlier seismic hazard studies, such as Grünthal et al. (1998). Therein and in further studies, we have employed an approach for the completeness assessment from a historical perspective in combination with graphs of the cumulative number of events with time; i.e. the slope method. Since the development of our statistical method (Hakimhashemi & Grünthal 2012) we usually apply both methods in parallel. The results based on both approaches are generally very similar. In case of differences, standard deviations of maximum likelihood estimates of Gutenberg-Richter b -values decide which datum to use. As described in Grünthal et al. (2018), we determined the following completeness times for the west and southwest of our target area, i.e. in the regions of elevated seismicity of Germany: for $M_w = 3.5-4.5$ a sufficient completeness time since about 1870, for $M_w = 4.5-5$ since about 1800, $M_w = 5-5.5$ since 1650, $M_w = 5.5-6$ since 1450 and for $M_w = 6-6.5$ since 1250.

For the illustration of the determination of the completeness times, we use here the descriptive slope method, which is intuitively accessible (Fig. 2-6a and b). Both graphs show the cumulative plots of earthquake occurrences with time for half magnitude classes with their centres at $M_w 1.75$ to 5.75 . The abscissae of the graphs were chosen such that they provide sufficient time resolution to determine the point (or time range) where the slopes of the cumulative graphs change. To improve the readability in the graphs, the vertical steps indicating an event with time are normalized in such a way that the end points of the cumulative graphs on the right vertical axis have a small difference with the largest magnitude on top. For the interpretation, the graphs are checked to verify the more or less constant slope of the cumulative plots for each magnitude class viewed from the catalogue end towards historical times and starting with lower magnitude classes. After having determined such a point where the smoothed slope of the cumulative graph of a magnitude class significantly decreases towards history, the procedure is repeated for the next larger class. Its completeness range is assumed to be not shorter than that for the next lower class. Concerning the largest magnitude class (or classes) with usually sparse data, additionally, cultural-historical information is used to determine the likely availability of written testimonies within the respective region.

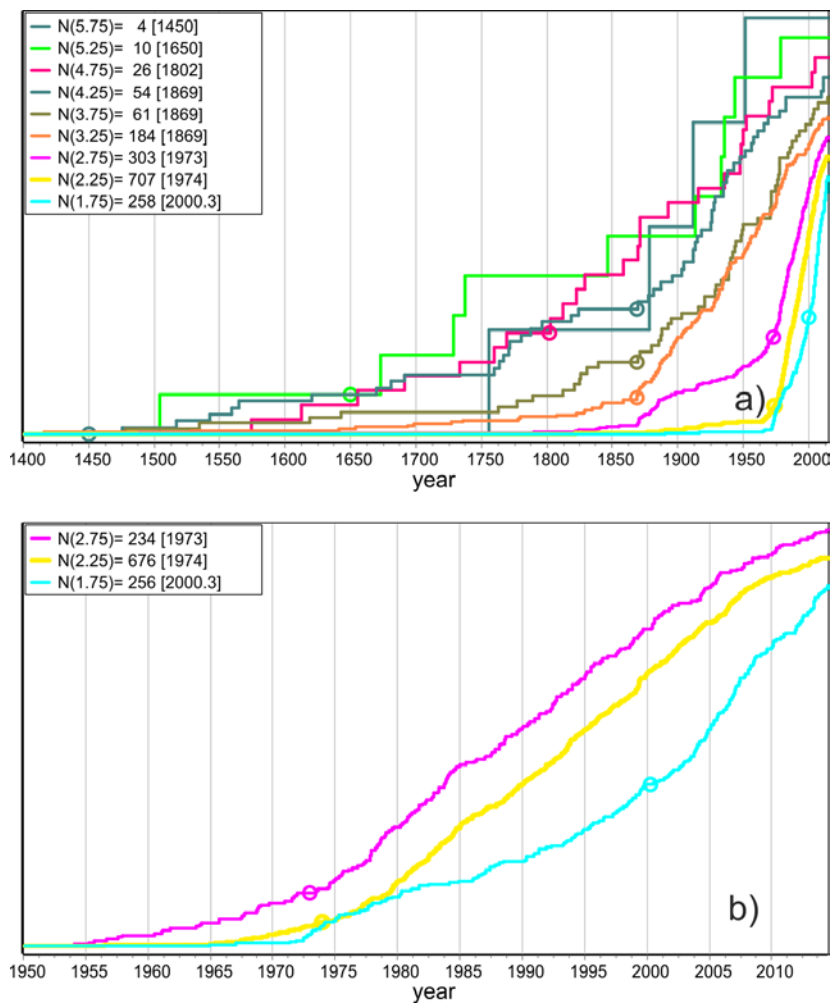


Figure. 2-6 Illustrations of the determination of the completeness times of catalogued earthquakes for the west and southwest regions of Germany with elevated seismicity as cumulative plots of earthquake occurrences with time for half magnitude classes with their centres at 1.75 to 5.75 (a) and with spread horizontal time axis (b) for the three smallest magnitude classes. The determined completeness times are marked as small circles for each magnitude class. The legend contains the numbers of catalogued earthquakes for corresponding magnitude classes within their completeness windows.

3. Models of seismic sources

The input model of the reassessment of the seismic hazard of Germany is composed of five areal seismic source zone (SSZ) models A, B, C, D and E (cf. chapter 4 of *Grünthal et al.* 2018). While this paper shows the configuration of SSZ model A in full, only parts of the others are presented therein. Here, we provide all SSZ models; i.e. the large scale areal seismic source zone (LASZ) models and the small scale areal seismic source zone (SASZ) models, in their entirety together with the enlarged part of the target area for a better readability of the finer SSZ model there (Figs. 3-1 to 3-5). The polygon traces for each SSZ are supplied in the electronic Annex.

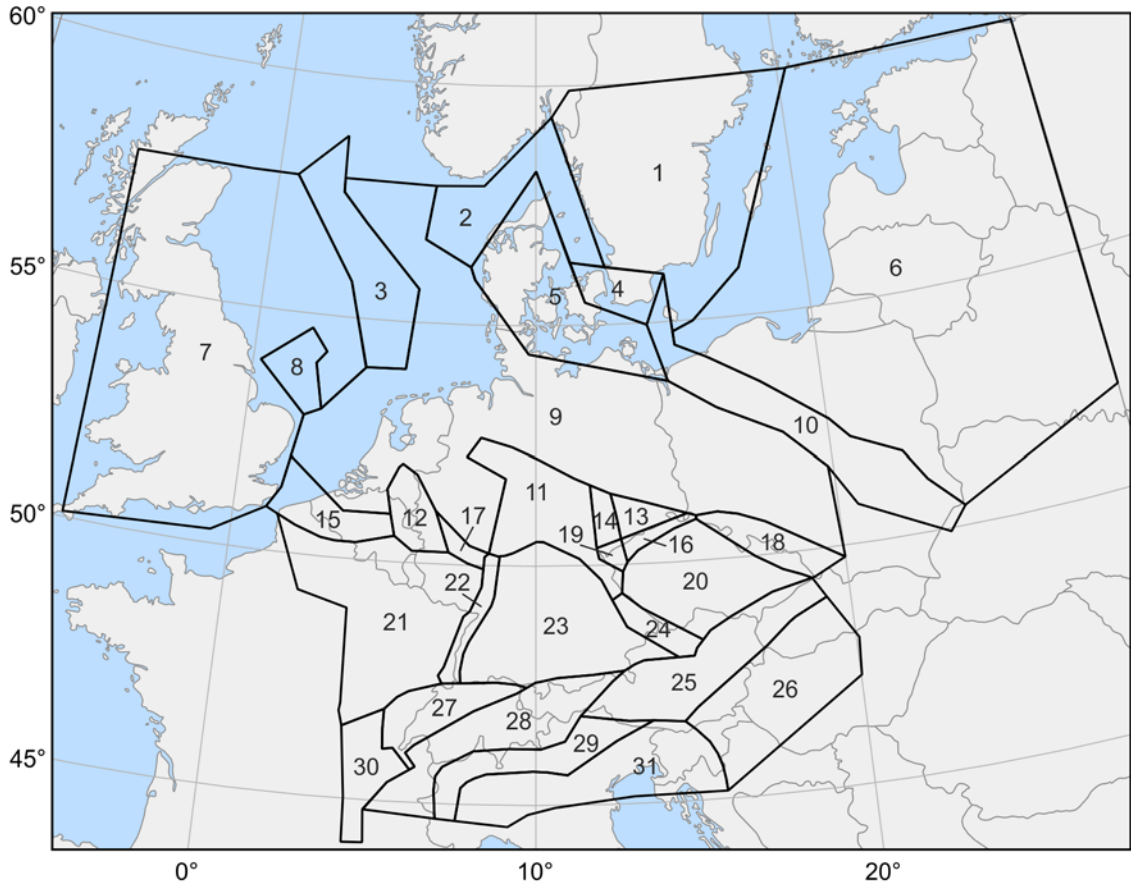


Figure 3-1. The large scale areal seismic source zone (LASZ) model A.

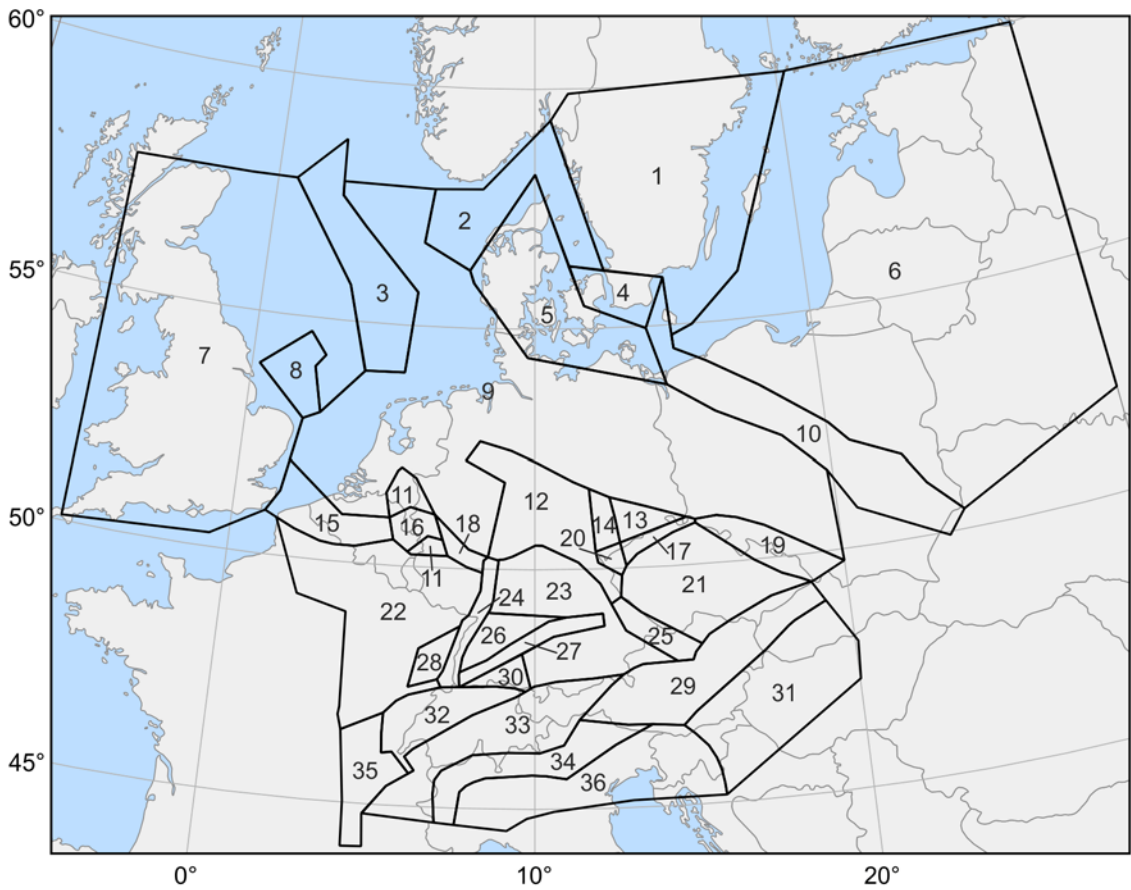


Figure 3-2. The LASZ model B.

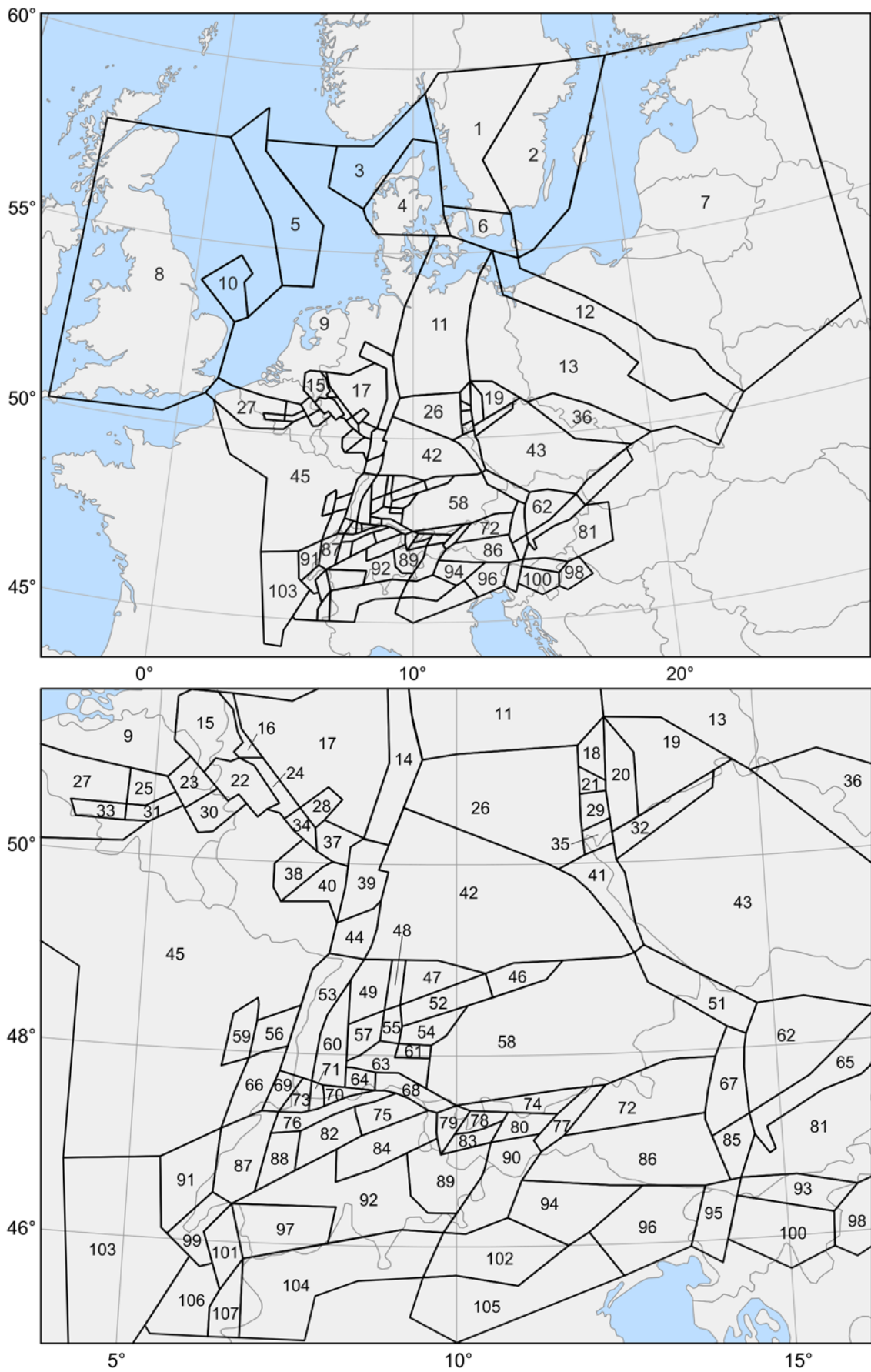


Figure 3-3. The SASZ model C; the entire model above; an enlarged section with the SW part below.

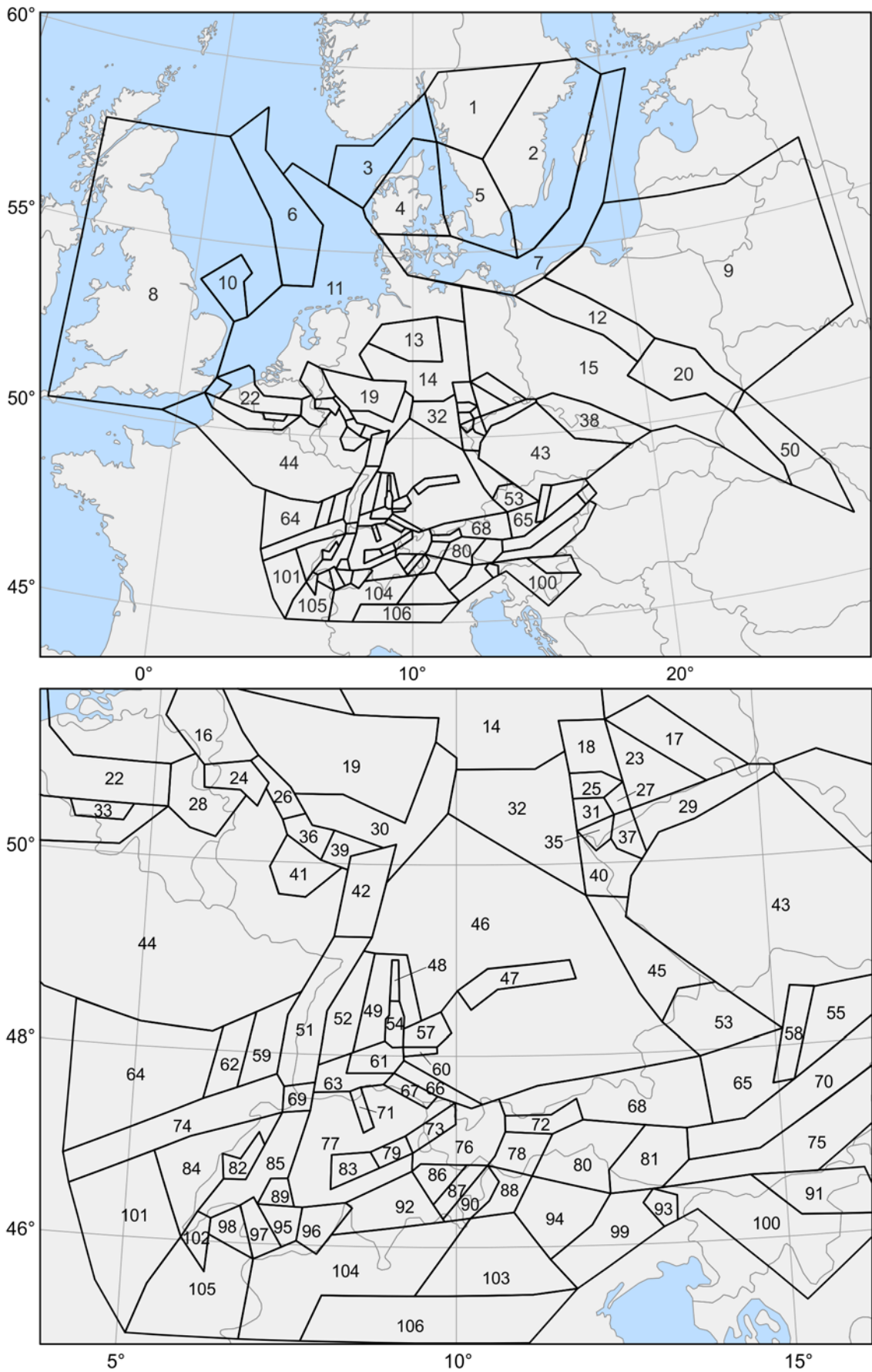


Figure 3-4. The SASZ model D; the entire model above; an enlarged section with the SW part below.

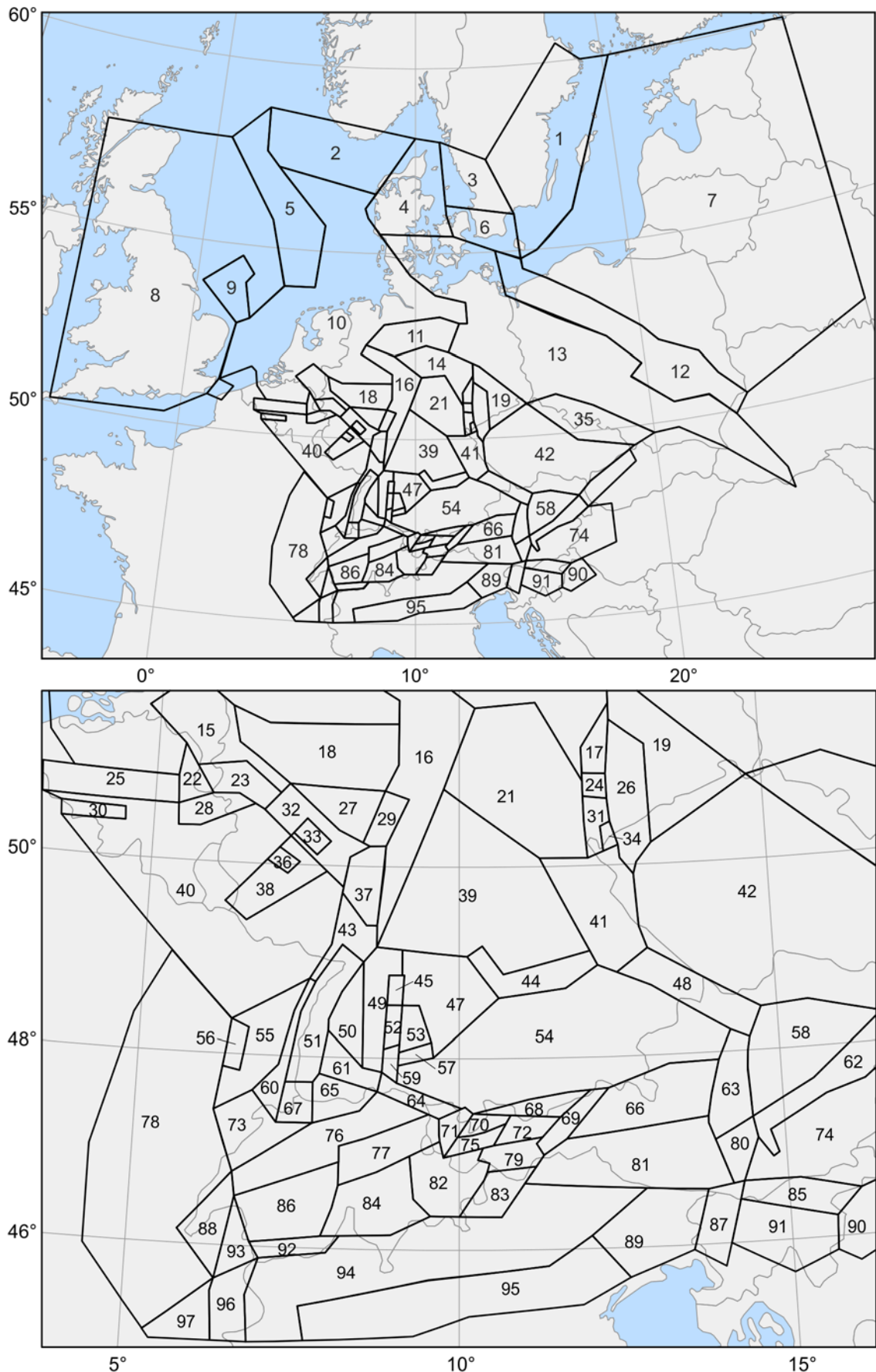


Figure 3-5. The SASZ model E; the entire model above; an enlarged section with the SW part below.

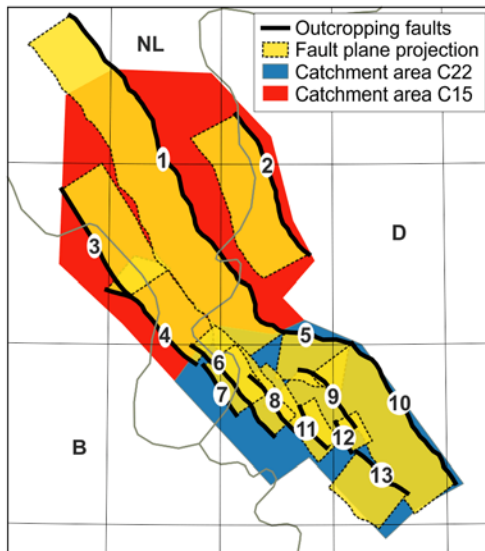


Figure 3-6. Geometry of composite seismic sources for the Lower Rhine Graben (Vanneste *et al.* 2013) and corresponding catchment areas of the SASZ model C.

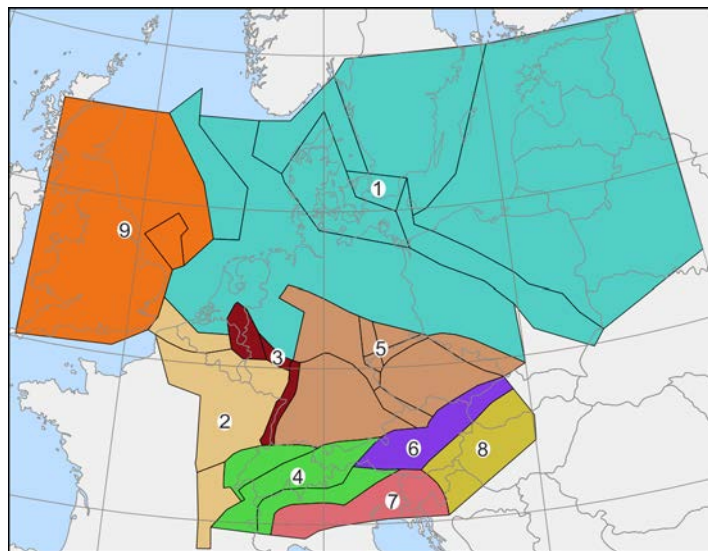


Figure 3-7. The model of superzones, within which separate kernels were derived.

Table 3-1. Parameters of the CSS for the Lower Rhine graben according to Vanneste *et al.* (2013) in the ascending numbering of Fig. 3-6. A dip marked with (*) refers to faults striking from NW to SO otherwise from SO to NW.

No.	Name	Dip [°]	Width [km]	Length [km]	Area [km ²]	Max. depth [km]	Fault type	M_{max}	$\sigma(M_{max})$
1	NLCS001	57.5	29.6	123.8	3664	25.0	normal	7.1	0.3
2	DECS004	57.5	29.6	51.1	1483	25.0	normal	7.1	0.3
3	BECS002	57.5*	27.7	39.2	1086	23.5	normal	6.9	0.3
4	BECS001	57.5*	25.1	37.1	931	21.2	normal	6.9	0.3
5	DECS002	57.5	27.5	21.3	586	23.2	normal	6.6	0.3
6	NLCS002	57.5*	17.7	38.3	678	14.9	normal	6.9	0.3
7	NLCS003	57.5*	22.3	18.4	410	18.8	normal	6.6	0.3
8	DECS005	57.5*	12.1	21.8	264	10.2	normal	6.6	0.3
9	DECS001	57.5	29.6	25.5	755	25.0	normal	6.9	0.3
10	DECS003	57.5	29.6	55.0	1628	25.0	normal	7.1	0.3
11	DECS006	57.5*	10.2	15.3	156	8.7	normal	6.5	0.3
12	DECS007	57.5*	13.8	10.4	144	11.6	normal	6.3	0.3
13	DECS008	57.5	26.2	20.6	540	22.1	normal	6.6	0.3

Model C contains additionally composite seismic fault sources (CSS) for the Lower Rhine graben (Fig. 3-6, Tab. 3-1) derived from the NW-SE striking CSS model by Vanneste *et al.* (2013). The determination of rates is based on the seismicity of two catchment sub-areas C15 and C22 and is described in chapter 4.3 of Grünthal *et al.* (2018).

The PSHA makes use of two zoneless models, which apply procedures of smoothing the observed seismicity. The corresponding bandwidth functions were determined from the areal distribution of the observed seismicity within nine respective superzones. This

superzone model is shown in Fig. 3-7; here related to the SSZ model A. The polygon traces of each superzone for deriving the bandwidth functions are also part of the electronic annex. The parameters of the bandwidth functions of each superzone are provided in Tab. 3-2. Fig. 3-8 presents the shapes of the bandwidth functions together with the data of the mean nearest event distances for all these superzones. This figure also illustrates the truncated version of the bandwidth functions we use for the PSHA.

Table 3-2. Combination of LASZs of model A to build nine kernel superzones KSZ. Parameters c_1 and c_2 of the magnitude dependent bandwidth function $H(M) = c_1 \exp(c_2 M)$.

DSZ	LASZ (model A)	c_1	c_2
1	A09, A05, A04, A01, A10, A06, A03, A02	8.9563	0.5546
2	A21, A30, A15	1.6416	0.7063
3	A12, A17, A22	0.1332	1.0916
4	A27, A28, A29	0.2482	0.8766
5	A11, A23, A14, A13, A19, A16, A24, A20, A18	2.2363	0.4969
6	A25	0.5867	0.7360
7	A31	0.0450	1.0849
8	A26	1.0834	0.5775
9	A07, A08	4.1962	0.5470

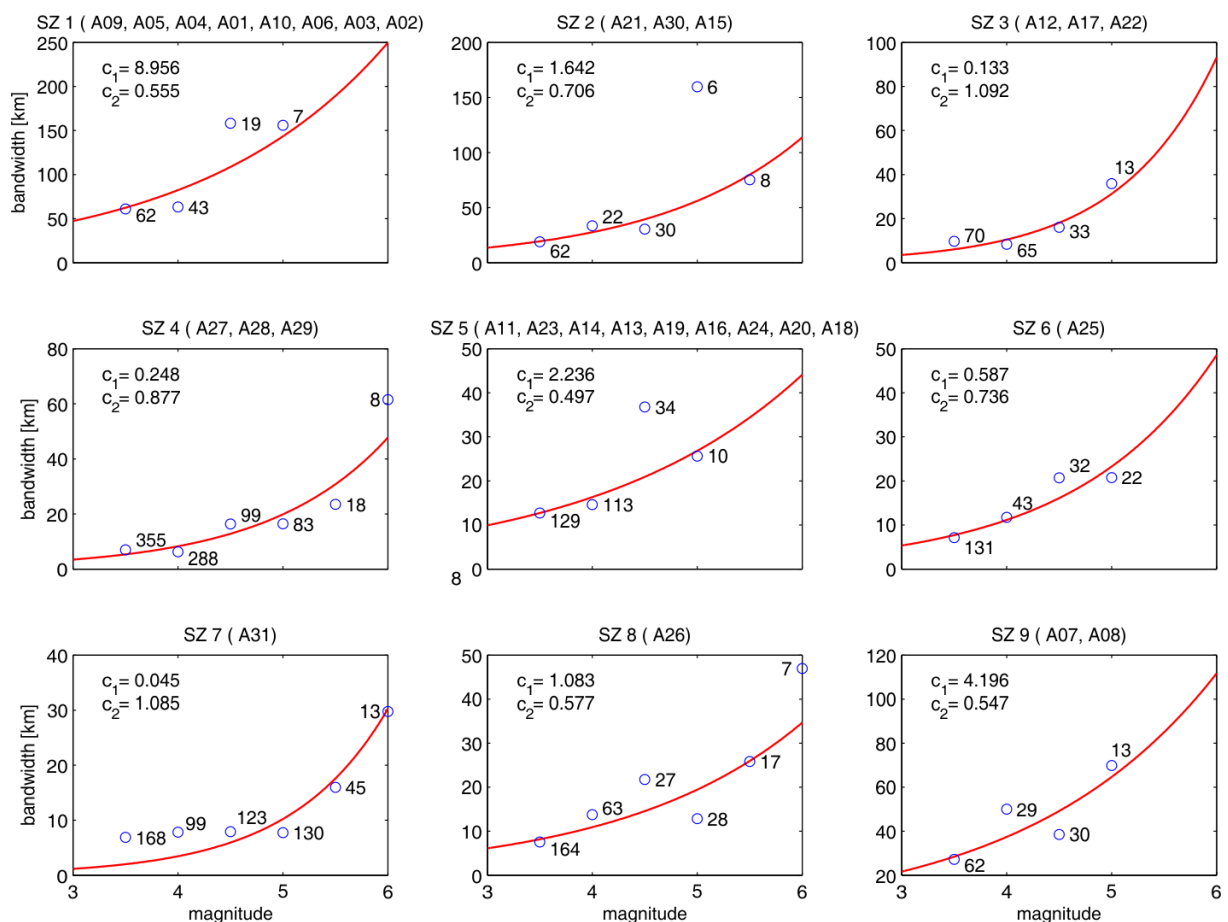


Figure 3-8. Shapes of the bandwidth functions together with the data of the mean nearest event distances for the kernel superzones.

4. Probability density functions of maximum magnitudes

The probability density functions (PDF) of maximum magnitudes (M_{max}) were also derived for the respective M_{max} superzone model (cf. chapter 5.1 of Grünthal et al. 2018). The calculation of the PDF requires different prior functions of M_{max} and different truncation parameters according to different tectonic terranes. The model of tectonic terranes used for the approach is shown in Fig. 4-1. The resulting M_{max} -superzone model, derived from the b -value superzone-model (cf. next chapter) is provided in Fig. 4-2. The polygon traces of each zone are part of the electronic annex. The shapes of the PDFs of each M_{max} -superzone with their discretized five $M_{max,i}$ are presented in Fig. 4-3. Table 4-1 provides the discretized values of the $M_{max,i}$ for each superzone

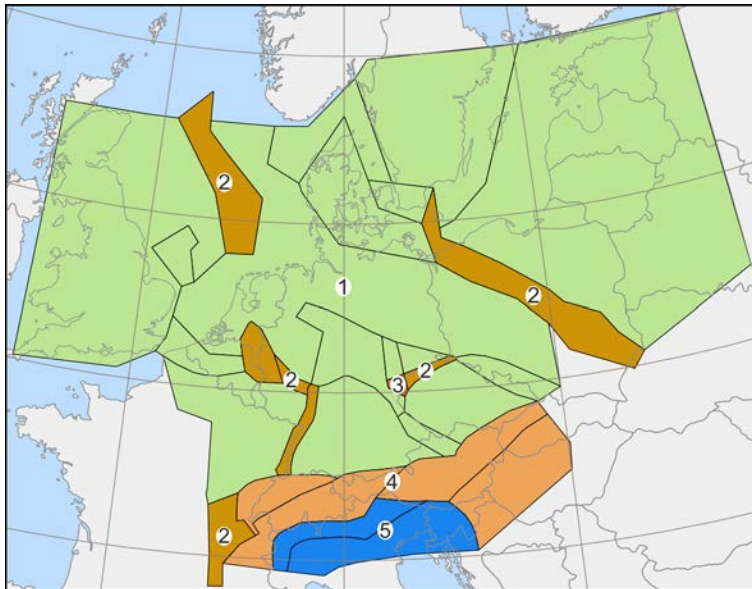


Figure 4-1. The model of tectonic terranes that define the use of different prior functions of M_{max} and truncation parameters.

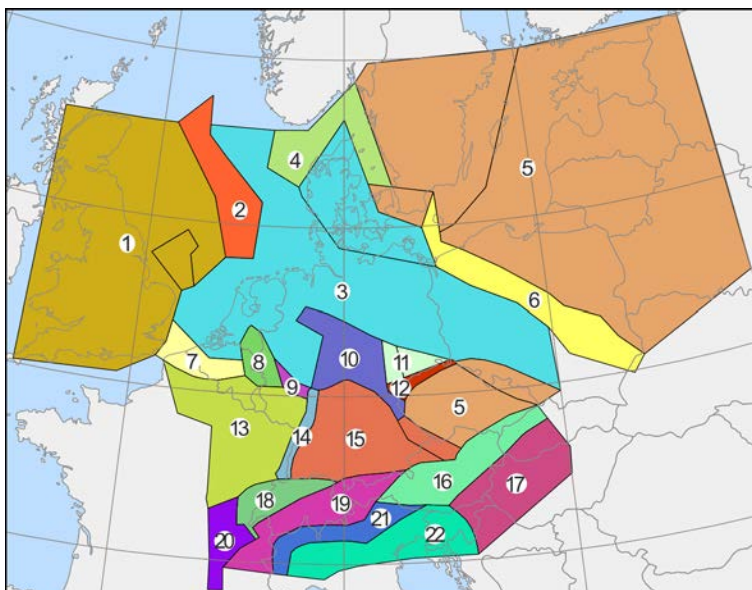


Figure 4-2. The M_{max} -superzone model.

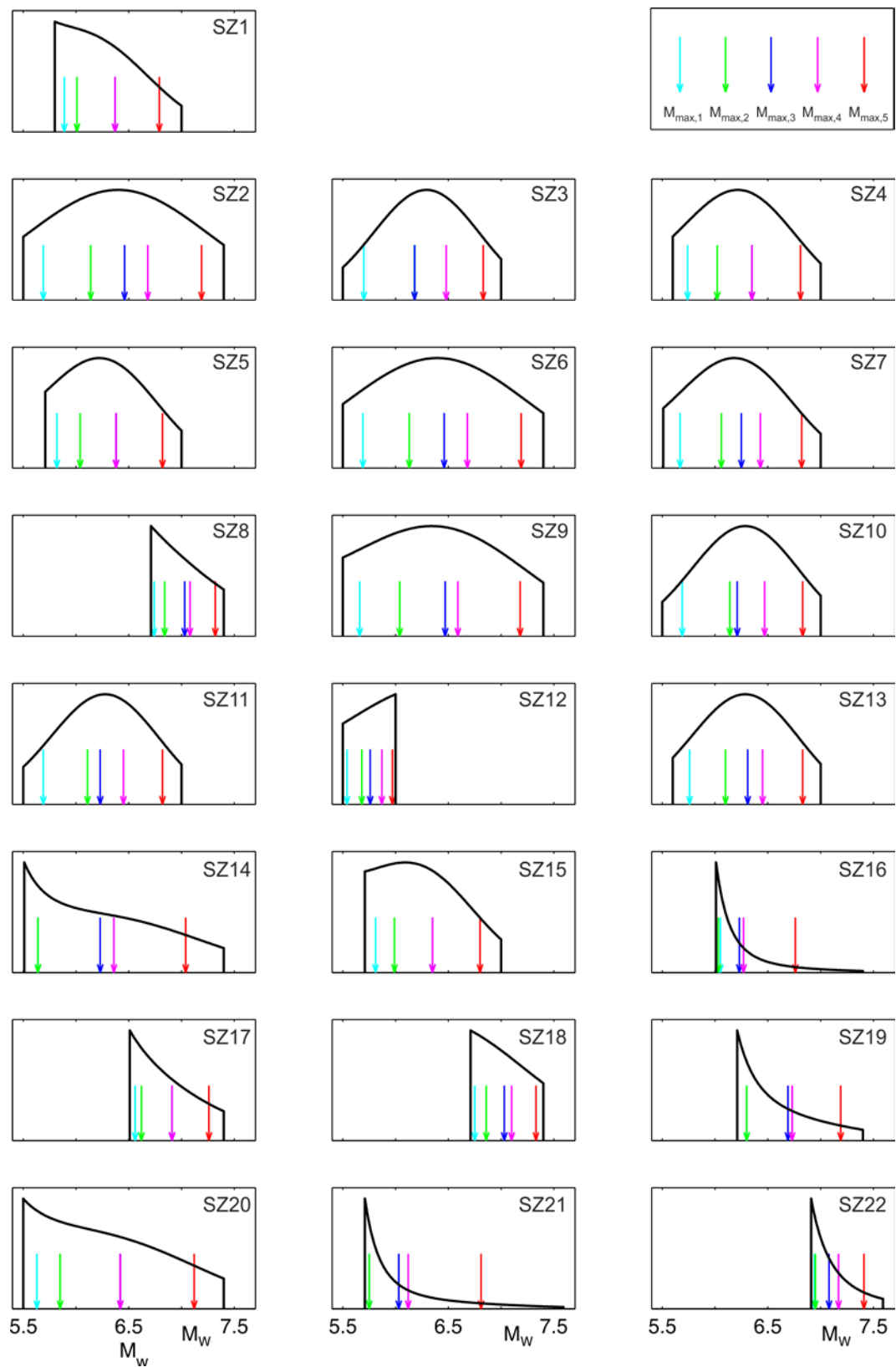


Figure 4-3. Shapes of the PDFs for each M_{max} superzone with their truncations. The discretized $M_{max,i}$ of equal weights are shown as well.

Table 4-1. Discrete M_{max} distribution of model A (Min for Fit High) for all 22 superzones (see Fig. 4-3) with equal weights of 0.2.

SZ Number	$M_{max,1}$	$M_{max,2}$	$M_{max,3}$	$M_{max,4}$	$M_{max,5}$
1	5.89	6.01	6.37	6.37	6.79
2	5.69	6.14	6.46	6.68	7.19
3	5.70	6.18	6.18	6.48	6.83
4	5.74	6.02	6.35	6.35	6.81
5	5.82	6.04	6.38	6.38	6.82
6	5.69	6.13	6.46	6.68	7.19
7	5.67	6.06	6.25	6.43	6.82
8	6.74	6.84	7.03	7.08	7.32
9	5.66	6.04	6.47	6.59	7.18
10	5.69	6.14	6.21	6.47	6.83
11	5.69	6.11	6.23	6.45	6.82
12	5.54	5.68	5.76	5.87	5.97
13	5.76	6.10	6.31	6.45	6.83
14	5.64	5.64	6.23	6.36	7.04
15	5.81	5.99	6.35	6.35	6.80
16	6.05	6.03	6.23	6.27	6.76
17	6.56	6.62	6.91	6.91	7.26
18	6.75	6.86	7.03	7.10	7.33
19	6.30	6.30	6.69	6.73	7.19
20	5.63	5.85	6.42	6.42	7.12
21	5.75	5.75	6.03	6.12	6.81
22	6.94	6.95	7.08	7.17	7.41

5. Seismicity rates

The seismicity rates per superzone (cf. chapter 5.2 of *Grünthal et al. 2018*) were calculated using a minimum of 70 events in each respective zone. The model of these superzones for b values is shown in Fig. 5-1. This superzone model is the basic one of the six superzone models we use for our approach. This prime b -value superzone-model is derived from the large scale seismic source zone model A. Its zones, which are tectonically related to each other, were combined such that at least 70 events would be available for the derivation of the seismicity parameters. This combination of zones is only necessary in areas of very low seismicity. So, it is obvious that the b -value superzone-model (with 18 superzones) is very similar to our SSZ model A.

The M_{max} -superzone model requires a specification of those b -value superzones, which are a combination of different tectonic terranes, which necessitates the use of different prior functions of M_{max} and different truncation parameters. This means that four of the b -value superzone-models needed to be split up which results in 22 M_{max} superzones.

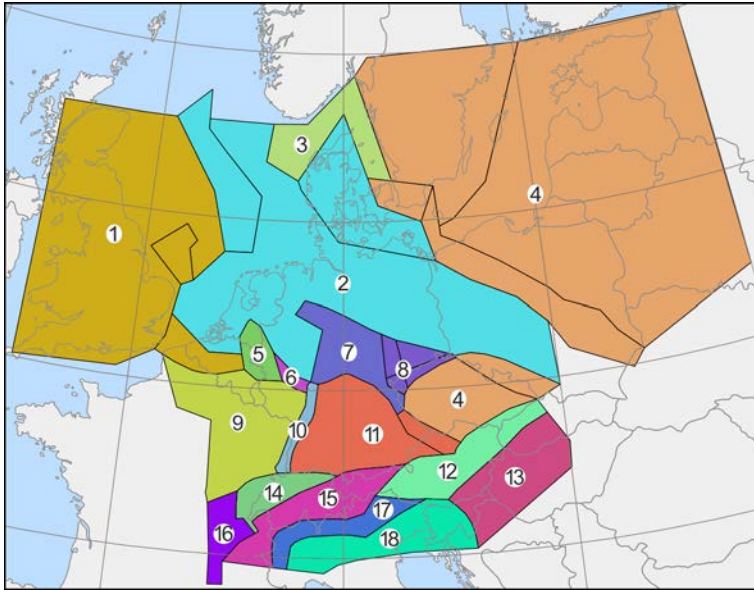


Figure 5-1. The b -value superzone-model with the SSZ of Model A for comparison.

The superzone model of the kernels (see above) is a generalization of the b -value superzone-model to nine superzones. The same model is applied also as superzone model of focal depth (see below). And finally, the superzone model of tectonic regimes required a split up of two superzones of the latter, which results in eleven superzones of the model for the tectonic regime (see below).

The determination of the seismicity rate parameters necessitates the differentiation of two versions for the minimum for fit (cf. chapter 5.2.3 of Grünthal *et al.* 2018). This could be applied in about 35% of the SSZs. The magnitude frequency graphs of the zones of the b -value superzone-model are shown in Fig. 5-2 with the minimum magnitude for the fit at low values and $M_{max,3}$.

Figure 5-2. Frequency-magnitude graphs of the zones of the b -value superzone model with the minimum magnitude for the fit at low values and $M_{max,3}$. The cumulative and the non-cumulative form are given.

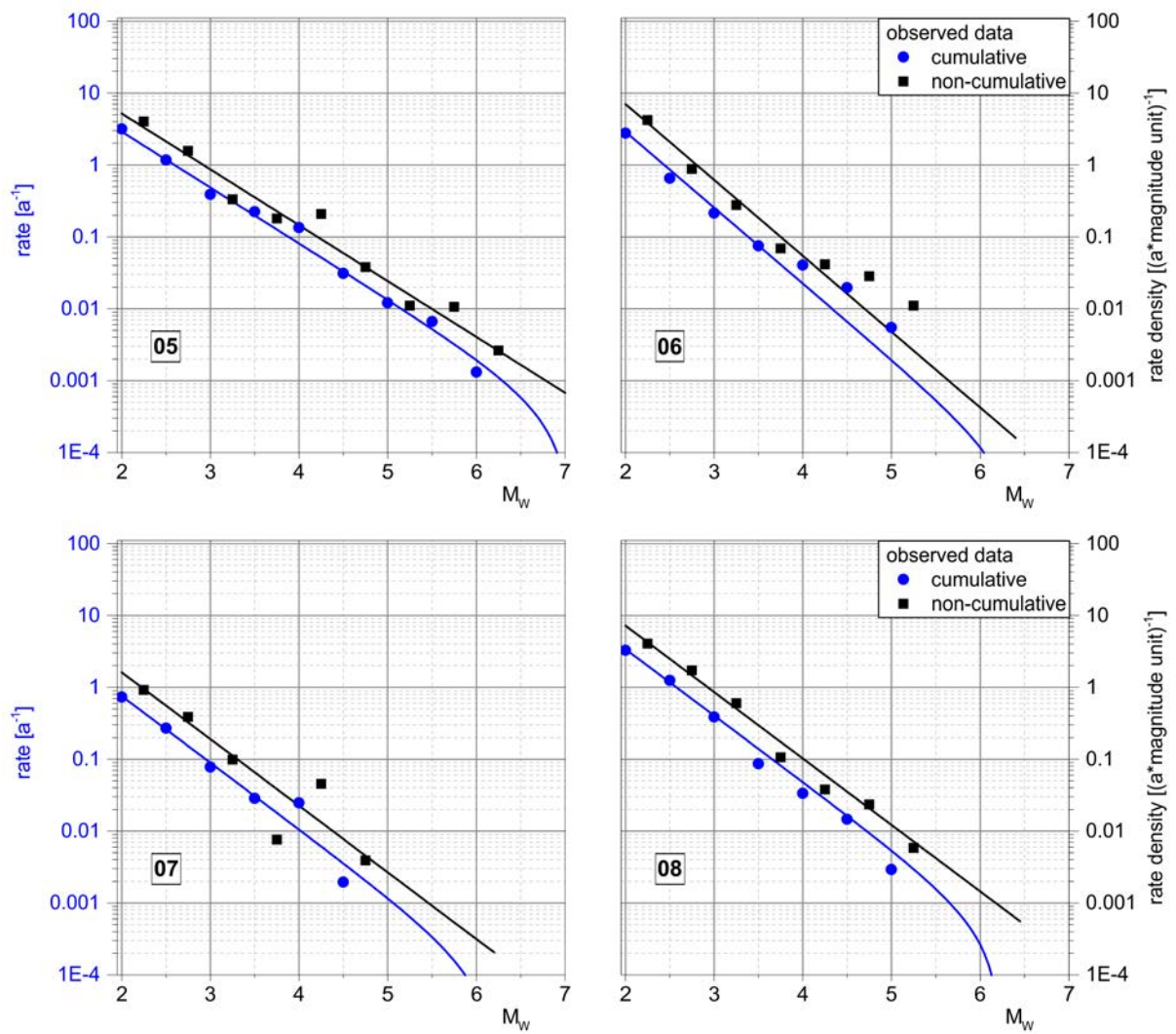


Figure 5-2. Continued.

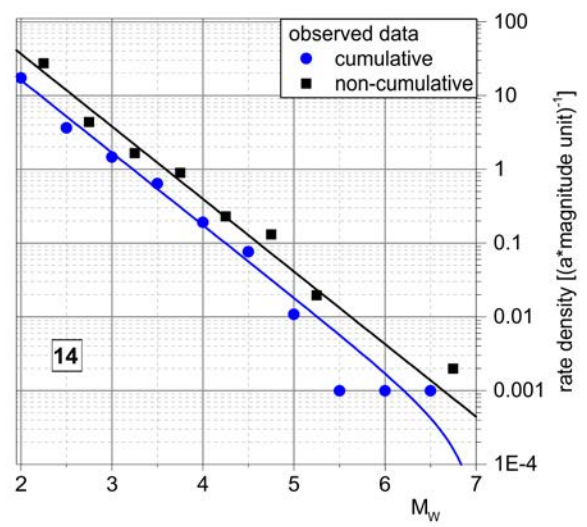
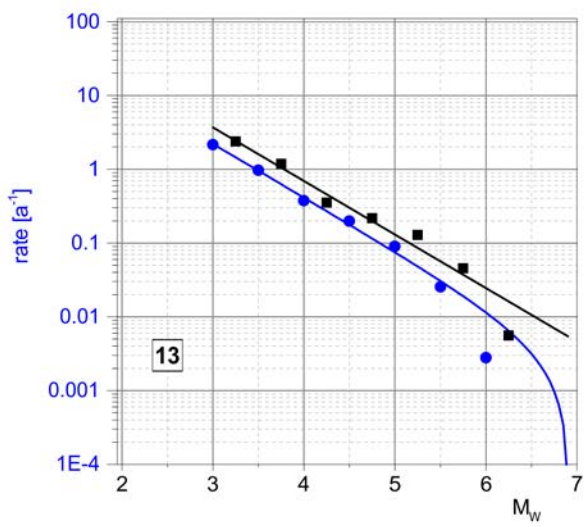


Figure 5-2. Continued.

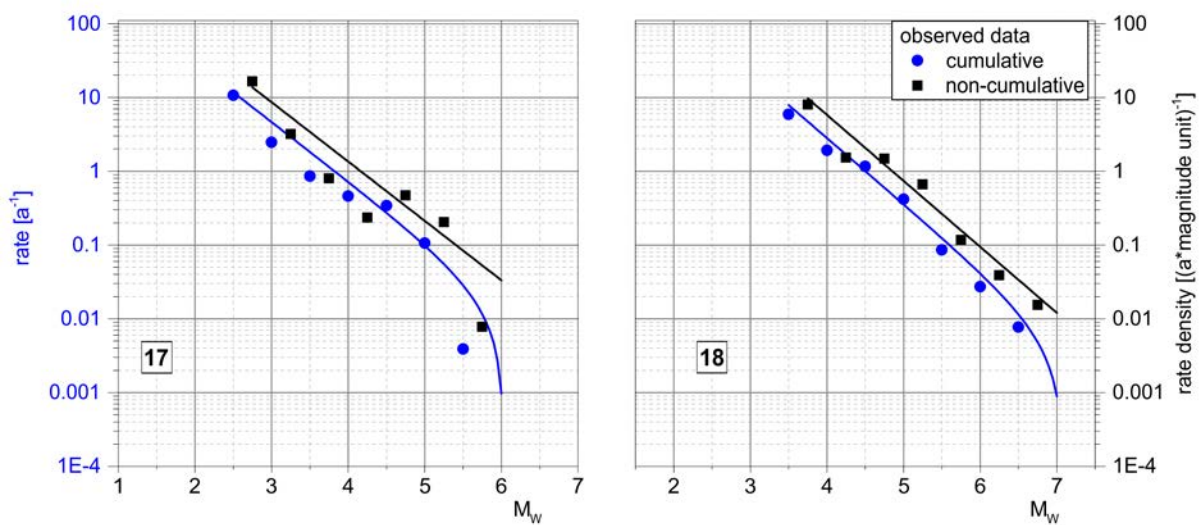


Figure 5-2. Continued.

Fig. 5-3 provides the areal variation of b values in the SSZ of model A. The variation of the a value, given as the rate ν for $M_w = 4.0$ and normalized to 1000 km^2 , is presented in Fig. 5-4. The parameters of the frequency-magnitude relation a and b with the parameters of the covariance matrix as measure of the uncertainty for the different $M_{max,i}$ per zone are provided in Tab. 5-1a-e for the SSZ models A, B, C, D and E. This table contains the two versions for the minimum fit.

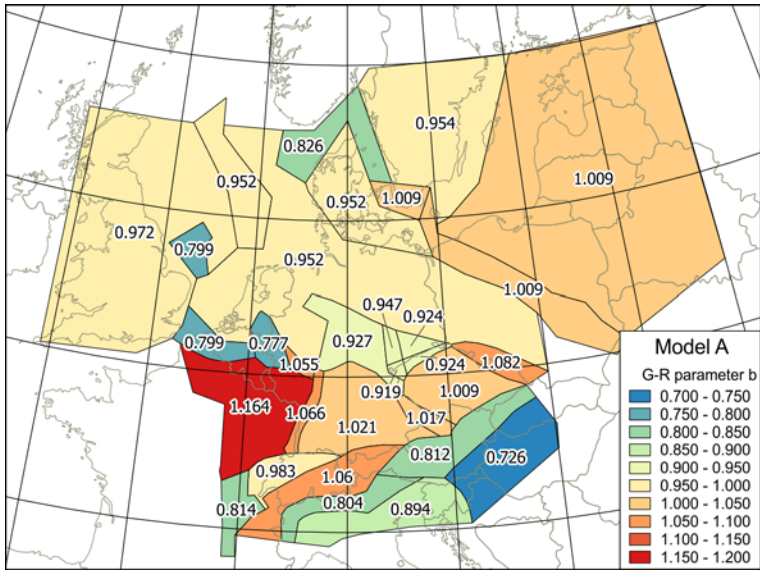


Figure 5-3. The areal variation of b values in the SSZ of model A.

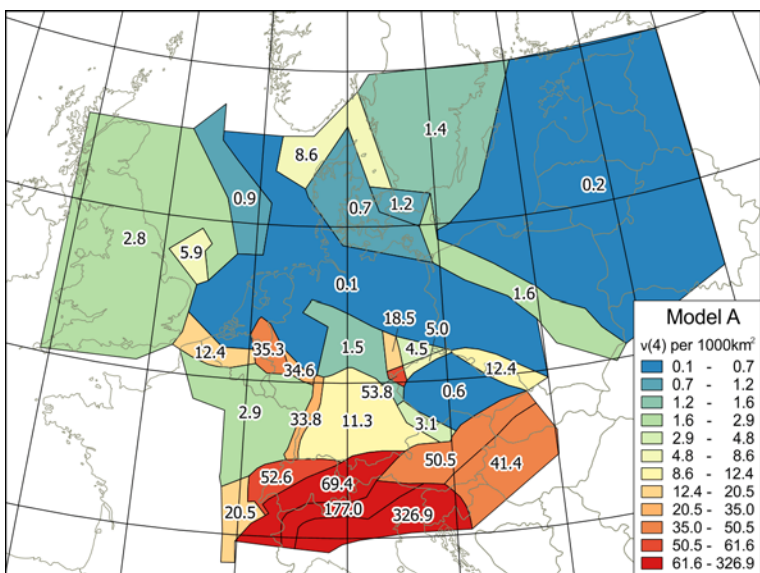


Figure 5-4. The variation of a values, given as the rate $<$ for $M_w = 4.0$ and normalized to 1000 km².

Additionally, those SSZs, where the distinction of the minimum for fit to lower and higher magnitudes could be made, are shown in Fig. 5-5. It enables the easily ascertainable respective information.

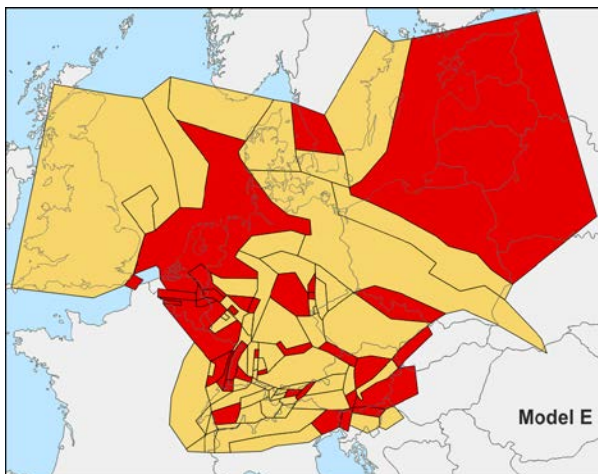
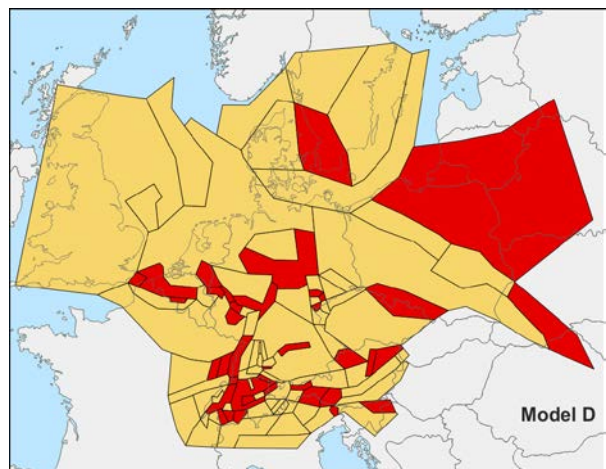
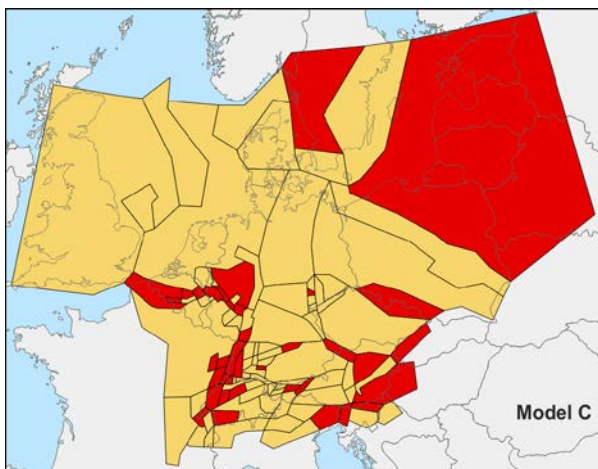
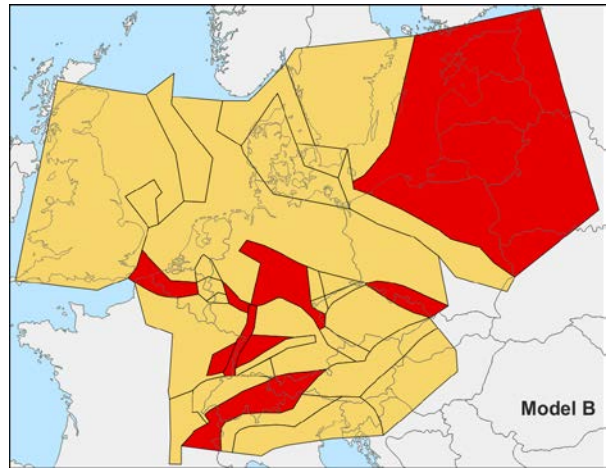
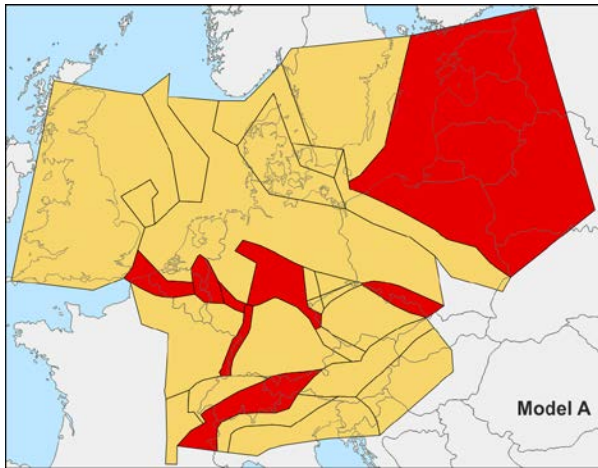


Figure 5-5. The seismic source zone models A to E with the indication for each SSZ, if the differentiation for the minimum for fit to lower or higher magnitudes could be applied (red) or not (yellow)

Tables 5-1. The parameters a and b of the frequency-magnitude relation with the parameters of the covariance matrix as measure of the uncertainty for the different $M_{max,i}$ per zone and for the SSZ models A (Tab. 5-1a), B (Tab. 5-1b), C (Tab. 5-1c), D (Tab. 5-1d) and E (Tab. 5-1e). The parameters are given for both variants of the minimum for fit.

Table 5-1a. Model A.

	minimum for fit high						minimum for fit low					
	$M_{max,i}$	a	b	Caa	Cab	Cbb	$M_{max,i}$	a	b	Caa	Cab	Cbb
A01	5,82	2,803	0,951	0,0267	0,00918	0,00335	5,82	2,803	0,951	0,0267	0,00918	0,00335
	6,04	2,803	0,951	0,0267	0,00918	0,00335	6,05	2,810	0,954	0,0264	0,00905	0,00330
	6,38	2,810	0,954	0,0264	0,00905	0,00330	6,38	2,810	0,954	0,0264	0,00905	0,00330
	6,38	2,810	0,954	0,0264	0,00905	0,00330	6,38	2,810	0,954	0,0264	0,00905	0,00330
	6,82	2,813	0,955	0,0262	0,00899	0,00328	6,82	2,813	0,955	0,0262	0,00899	0,00328
A02	5,74	2,440	0,820	0,0216	0,00689	0,00237	5,74	2,440	0,820	0,0216	0,00689	0,00237
	6,02	2,440	0,820	0,0216	0,00689	0,00237	6,02	2,440	0,820	0,0216	0,00689	0,00237
	6,35	2,455	0,826	0,0211	0,00671	0,00231	6,35	2,455	0,826	0,0211	0,00671	0,00231
	6,35	2,455	0,826	0,0211	0,00671	0,00231	6,35	2,455	0,826	0,0211	0,00671	0,00231
	6,81	2,461	0,828	0,0208	0,00662	0,00228	6,81	2,461	0,828	0,0208	0,00662	0,00228
A03	5,69	2,039	0,949	0,0588	0,0155	0,00575	5,69	2,039	0,949	0,0588	0,0155	0,00575
	6,14	2,047	0,952	0,0582	0,0152	0,00566	6,14	2,047	0,952	0,0582	0,0152	0,00566
	6,46	2,047	0,952	0,0582	0,0152	0,00566	6,46	2,047	0,952	0,0582	0,0152	0,00566
	6,68	2,047	0,952	0,0582	0,0152	0,00566	6,68	2,047	0,952	0,0582	0,0152	0,00566
	7,19	2,049	0,953	0,0580	0,0151	0,00562	7,19	2,049	0,953	0,0580	0,0151	0,00562
A04	5,82	1,748	0,943	0,0343	0,00625	0,00228	5,82	1,923	1,007	0,0232	0,00227	0,000846
	6,04	1,750	0,943	0,0343	0,00625	0,00228	6,05	1,928	1,009	0,0232	0,00224	0,000837
	6,38	1,764	0,949	0,0340	0,00615	0,00224	6,38	1,928	1,009	0,0232	0,00224	0,000837
	6,38	1,765	0,949	0,0340	0,00614	0,00224	6,38	1,928	1,009	0,0232	0,00224	0,000837
	6,82	1,771	0,951	0,0339	0,00609	0,00222	6,82	1,929	1,010	0,0231	0,00224	0,000834
A05	5,70	2,087	0,949	0,0513	0,0157	0,00575	5,70	2,087	0,949	0,0513	0,0157	0,00575
	6,18	2,094	0,952	0,0507	0,0155	0,00566	6,18	2,094	0,952	0,0507	0,0155	0,00566
	6,18	2,094	0,952	0,0507	0,0155	0,00566	6,18	2,094	0,952	0,0507	0,0155	0,00566
	6,48	2,095	0,952	0,0506	0,0155	0,00566	6,48	2,095	0,952	0,0506	0,0155	0,00566
	6,83	2,097	0,953	0,0504	0,0154	0,00562	6,83	2,097	0,953	0,0504	0,0154	0,00562
A06	5,82	2,919	0,943	0,0656	0,0105	0,00228	5,82	2,577	1,007	0,0174	0,00273	0,000846
	6,04	2,921	0,943	0,0656	0,0105	0,00228	6,05	2,583	1,009	0,0173	0,00270	0,000837
	6,38	2,941	0,949	0,0653	0,0104	0,00224	6,38	2,583	1,009	0,0173	0,00270	0,000837
	6,38	2,942	0,949	0,0653	0,0104	0,00224	6,38	2,583	1,009	0,0173	0,00270	0,000837
	6,82	2,950	0,951	0,0650	0,0103	0,00222	6,82	2,585	1,010	0,0172	0,00269	0,000834
A07	5,89	3,384	0,957	0,0734	0,0183	0,00467	5,88	3,384	0,957	0,0734	0,0183	0,00467
	6,01	3,384	0,957	0,0734	0,0183	0,00467	5,94	3,384	0,957	0,0734	0,0183	0,00467
	6,37	3,440	0,972	0,0695	0,0173	0,00442	6,30	3,440	0,972	0,0695	0,0173	0,00442
	6,37	3,440	0,972	0,0695	0,0173	0,00442	6,30	3,440	0,972	0,0695	0,0173	0,00442
	6,79	3,460	0,977	0,0678	0,0169	0,00430	6,73	3,460	0,977	0,0678	0,0169	0,00430
A08	5,89	2,276	0,970	0,0857	0,0159	0,00407	5,88	1,519	0,780	0,0521	0,00700	0,00172
	6,01	2,298	0,975	0,0849	0,0157	0,00402	5,94	1,519	0,780	0,0521	0,00700	0,00172
	6,37	2,345	0,988	0,0820	0,0150	0,00383	6,30	1,590	0,799	0,0505	0,00658	0,00161
	6,37	2,345	0,988	0,0820	0,0150	0,00383	6,30	1,590	0,799	0,0505	0,00658	0,00161
	6,79	2,370	0,994	0,0804	0,0146	0,00373	6,73	1,620	0,807	0,0496	0,00637	0,00156
A09	5,70	1,653	0,871	0,0647	0,0228	0,00848	5,70	1,862	0,949	0,0429	0,0150	0,00575
	6,18	1,663	0,875	0,0635	0,0223	0,00832	6,18	1,869	0,952	0,0423	0,0148	0,00566
	6,18	1,663	0,875	0,0635	0,0223	0,00832	6,18	1,869	0,952	0,0423	0,0148	0,00566
	6,48	1,663	0,875	0,0635	0,0223	0,00832	6,48	1,869	0,952	0,0422	0,0148	0,00566
	6,83	1,667	0,876	0,0629	0,0221	0,00824	6,83	1,872	0,953	0,0420	0,0147	0,00562
A10	5,69	2,364	0,943	0,110	0,0104	0,00228	5,69	2,655	1,007	0,0802	0,00383	0,000846
	6,13	2,358	0,943	0,111	0,0104	0,00228	6,13	2,658	1,009	0,0802	0,00381	0,000837
	6,46	2,384	0,949	0,110	0,0103	0,00224	6,46	2,658	1,009	0,0802	0,00381	0,000837
	6,68	2,382	0,949	0,110	0,0103	0,00224	6,68	2,657	1,009	0,0802	0,00381	0,000837
	7,19	2,392	0,951	0,110	0,0102	0,00222	7,19	2,659	1,010	0,0802	0,00380	0,000834
A11	5,69	1,983	0,919	0,0196	0,00250	0,000688	5,69	2,055	0,925	0,0395	0,0142	0,00540
	6,14	1,994	0,922	0,0194	0,00245	0,000674	6,14	2,062	0,927	0,0389	0,0140	0,00531
	6,22	1,994	0,922	0,0194	0,00245	0,000674	6,21	2,062	0,927	0,0389	0,0140	0,00531
	6,47	1,994	0,922	0,0194	0,00245	0,000674	6,47	2,062	0,927	0,0389	0,0140	0,00531
	6,83	1,996	0,923	0,0194	0,00245	0,000672	6,83	2,065	0,929	0,0386	0,0139	0,00528
A12	6,74	2,795	0,850	0,226	0,0454	0,00943	6,74	2,268	0,777	0,00824	0,00276	0,00103
	6,84	2,795	0,850	0,226	0,0454	0,00943	6,83	2,268	0,777	0,00824	0,00276	0,00103
	7,03	2,981	0,889	0,208	0,0419	0,00878	7,05	2,268	0,777	0,00824	0,00276	0,00103
	7,08	3,042	0,902	0,199	0,0400	0,00836	7,05	2,274	0,779	0,00812	0,00271	0,00101
	7,32	3,113	0,917	0,191	0,0384	0,00806	7,32	2,274	0,779	0,00812	0,00271	0,00101
A13	5,69	1,721	0,919	0,00882	0,00182	0,000688	5,69	1,726	0,921	0,00893	0,00186	0,000705
	6,11	1,730	0,922	0,00872	0,00178	0,000674	6,11	1,734	0,924	0,00883	0,00182	0,000691
	6,23	1,730	0,922	0,00872	0,00178	0,000674	6,23	1,734	0,924	0,00883	0,00182	0,000691
	6,45	1,730	0,922	0,00872	0,00178	0,000674	6,45	1,734	0,924	0,00883	0,00182	0,000691
	6,82	1,731	0,923	0,00871	0,00178	0,000672	6,82	1,735	0,924	0,00882	0,00182	0,000689

	minimum for fit high						minimum for fit low					
	$M_{max,i}$	a	b	Caa	Cab	Cbb	$M_{max,i}$	a	b	Caa	Cab	Cbb
A14	5,69	2,323	0,945	0,0191	0,00713	0,00282	5,69	2,323	0,945	0,0191	0,00713	0,00282
	6,11	2,328	0,947	0,0189	0,00704	0,00278	6,11	2,328	0,947	0,0189	0,00704	0,00278
	6,23	2,328	0,947	0,0189	0,00704	0,00278	6,23	2,328	0,947	0,0189	0,00704	0,00278
	6,45	2,328	0,947	0,0189	0,00704	0,00278	6,45	2,328	0,947	0,0189	0,00704	0,00278
	6,82	2,330	0,948	0,0188	0,00700	0,00277	6,82	2,330	0,948	0,0188	0,00700	0,00277
A15	5,67	3,120	0,970	0,100	0,0192	0,00407	5,66	2,012	0,780	0,0201	0,00540	0,00172
	6,06	3,138	0,975	0,100	0,0191	0,00402	6,01	2,012	0,780	0,0201	0,00540	0,00172
	6,25	3,198	0,988	0,0960	0,0182	0,00383	6,28	2,068	0,799	0,0188	0,00504	0,00161
	6,43	3,198	0,988	0,0960	0,0182	0,00383	6,37	2,068	0,799	0,0188	0,00504	0,00161
	6,82	3,226	0,994	0,0939	0,0177	0,00373	6,81	2,092	0,807	0,0182	0,00486	0,00156
A16	5,54	1,555	0,919	0,0107	0,00181	0,000688	5,54	1,559	0,921	0,0108	0,00186	0,000705
	5,68	1,563	0,922	0,0106	0,00178	0,000674	5,68	1,567	0,924	0,0107	0,00182	0,000691
	5,76	1,563	0,922	0,0106	0,00178	0,000674	5,76	1,567	0,924	0,0107	0,00182	0,000691
	5,87	1,563	0,922	0,0106	0,00178	0,000674	5,87	1,567	0,924	0,0107	0,00182	0,000691
	5,97	1,564	0,923	0,0106	0,00177	0,000672	5,97	1,568	0,924	0,0107	0,00182	0,000689
A17	5,66	2,188	0,850	0,178	0,0393	0,00943	5,67	2,948	1,052	0,0310	0,0111	0,00417
	6,04	2,188	0,850	0,178	0,0393	0,00943	6,08	2,955	1,055	0,0305	0,0109	0,00410
	6,47	2,341	0,889	0,168	0,0367	0,00878	6,46	2,955	1,055	0,0305	0,0109	0,00410
	6,59	2,394	0,902	0,161	0,0350	0,00836	6,64	2,959	1,056	0,0303	0,0108	0,00406
	7,18	2,455	0,917	0,155	0,0337	0,00806	7,19	2,960	1,057	0,0301	0,0108	0,00405
A18	5,82	3,009	0,943	0,0956	0,0115	0,00228	5,82	3,268	1,081	0,00676	0,00299	0,00166
	6,04	3,011	0,943	0,0956	0,0115	0,00228	6,05	3,269	1,082	0,00672	0,00297	0,00165
	6,38	3,019	0,949	0,0959	0,0114	0,00224	6,38	3,269	1,082	0,00672	0,00297	0,00165
	6,38	3,020	0,949	0,0959	0,0114	0,00224	6,38	3,269	1,082	0,00672	0,00297	0,00165
	6,82	3,025	0,951	0,0959	0,0114	0,00222	6,82	3,270	1,082	0,00671	0,00296	0,00164
A19	5,54	2,344	0,915	0,00632	0,00251	0,00111	5,54	2,344	0,915	0,00632	0,00251	0,00111
	5,68	2,352	0,919	0,00620	0,00245	0,00108	5,68	2,352	0,919	0,00620	0,00245	0,00108
	5,76	2,352	0,919	0,00620	0,00245	0,00108	5,76	2,352	0,919	0,00620	0,00245	0,00108
	5,87	2,352	0,919	0,00620	0,00245	0,00108	5,87	2,352	0,919	0,00620	0,00245	0,00108
	5,97	2,352	0,919	0,00620	0,00245	0,00108	5,97	2,352	0,919	0,00620	0,00245	0,00108
A20	5,82	1,972	0,943	0,0249	0,00487	0,00228	5,82	2,104	1,007	0,0178	0,00166	0,000846
	6,04	1,973	0,943	0,0249	0,00486	0,00228	6,05	2,107	1,009	0,0177	0,00164	0,000837
	6,38	1,984	0,949	0,0246	0,00477	0,00224	6,38	2,107	1,009	0,0177	0,00164	0,000837
	6,38	1,984	0,949	0,0246	0,00476	0,00224	6,38	2,107	1,009	0,0177	0,00164	0,000837
	6,82	1,989	0,951	0,0245	0,00471	0,00222	6,82	2,108	1,010	0,0177	0,00164	0,000834
A21	5,76	3,701	1,163	0,0139	0,00524	0,00206	5,76	3,701	1,163	0,0139	0,00524	0,00206
	6,10	3,704	1,164	0,0138	0,00520	0,00204	6,10	3,704	1,164	0,0138	0,00520	0,00204
	6,31	3,704	1,164	0,0138	0,00520	0,00204	6,31	3,704	1,164	0,0138	0,00520	0,00204
	6,45	3,704	1,164	0,0138	0,00520	0,00204	6,45	3,704	1,164	0,0138	0,00520	0,00204
	6,83	3,705	1,165	0,0137	0,00519	0,00204	6,83	3,705	1,165	0,0137	0,00519	0,00204
A22	5,64	2,707	0,850	0,218	0,0443	0,00943	5,62	3,330	1,063	0,0140	0,00504	0,00190
	5,64	2,707	0,850	0,218	0,0443	0,00943	5,80	3,330	1,063	0,0140	0,00504	0,00190
	6,23	2,870	0,889	0,207	0,0416	0,00878	6,40	3,337	1,066	0,0138	0,00496	0,00187
	6,36	2,934	0,902	0,197	0,0395	0,00836	6,40	3,337	1,066	0,0138	0,00496	0,00187
	7,04	2,997	0,917	0,192	0,0383	0,00806	7,12	3,341	1,068	0,0136	0,00490	0,00184
A23	5,81	3,576	1,019	0,00570	0,00202	0,000750	5,81	3,576	1,019	0,00570	0,00202	0,000750
	5,99	3,576	1,019	0,00570	0,00202	0,000750	5,99	3,576	1,019	0,00570	0,00202	0,000750
	6,35	3,586	1,023	0,00558	0,00197	0,000734	6,35	3,586	1,023	0,00558	0,00197	0,000734
	6,35	3,586	1,023	0,00558	0,00197	0,000734	6,35	3,586	1,023	0,00558	0,00197	0,000734
	6,80	3,590	1,025	0,00552	0,00195	0,000726	6,80	3,590	1,025	0,00552	0,00195	0,000726
A24	5,81	2,093	1,014	0,0174	0,00202	0,000724	5,81	2,093	1,014	0,0174	0,00202	0,000724
	5,99	2,093	1,014	0,0174	0,00202	0,000724	5,99	2,093	1,014	0,0174	0,00202	0,000724
	6,35	2,103	1,018	0,0173	0,00198	0,000708	6,35	2,103	1,018	0,0173	0,00198	0,000708
	6,35	2,103	1,018	0,0173	0,00198	0,000708	6,35	2,103	1,018	0,0173	0,00198	0,000708
	6,80	2,108	1,020	0,0173	0,00196	0,000700	6,80	2,108	1,020	0,0173	0,00196	0,000700
A25	6,05	3,081	0,804	0,00464	0,00143	0,000472	6,05	3,081	0,804	0,00464	0,00143	0,000472
	6,03	3,081	0,804	0,00464	0,00143	0,000472	6,03	3,081	0,804	0,00464	0,00143	0,000472
	6,23	3,105	0,812	0,00431	0,00132	0,000433	6,23	3,105	0,812	0,00431	0,00132	0,000433
	6,27	3,105	0,812	0,00431	0,00132	0,000433	6,27	3,105	0,812	0,00431	0,00132	0,000433
	6,76	3,122	0,818	0,00418	0,00128	0,000419	6,76	3,122	0,818	0,00418	0,00128	0,000419
A26	6,56	2,745	0,726	0,0171	0,00442	0,00118	6,56	2,745	0,726	0,0171	0,00442	0,00118
	6,62	2,745	0,726	0,0171	0,00442	0,00118	6,62	2,745	0,726	0,0171	0,00442	0,00118
	6,91	2,745	0,726	0,0171	0,00442	0,00118	6,91	2,745	0,726	0,0171	0,00442	0,00118
	6,91	2,745	0,726	0,0171	0,00442	0,00118	6,91	2,745	0,726	0,0171	0,00442	0,00118
	7,26	2,763	0,731	0,0167	0,00431	0,00115	7,26	2,763	0,731	0,0167	0,00431	0,00115
A27	6,75	3,528	0,983	0,00264	0,000959	0,000379	6,75	3,528	0,983	0,00264	0,000959	0,000379
	6,86	3,528	0,983	0,00264	0,000959	0,000379	6,86	3,528	0,983	0,00264	0,000959	0,000379
	7,03	3,528	0,983	0,00264	0,000959	0,000379	7,03	3,528	0,983	0,00264	0,000959	0,000379
	7,10	3,530	0,984	0,00263	0,000955	0,000377	7,10	3,530	0,984	0,00263	0,000955	0,000377
	7,33	3,530	0,984	0,00263	0,000955	0,000377	7,33	3,530	0,984	0,00263	0,000955	0,000377

	minimum for fit high						minimum for fit low					
	$M_{max.i}$	a	b	Caa	Cab	Cbb	$M_{max.i}$	a	b	Caa	Cab	Cbb
A28	6,30	5,142	1,169	0,420	0,0823	0,0163	6,27	4,336	1,059	0,000692	0,000263	0,000107
	6,30	5,142	1,169	0,420	0,0823	0,0163	6,27	4,336	1,059	0,000692	0,000263	0,000107
	6,69	5,381	1,218	0,375	0,0736	0,0145	6,56	4,338	1,060	0,000688	0,000261	0,000107
	6,73	5,381	1,218	0,375	0,0736	0,0145	6,69	4,338	1,060	0,000688	0,000261	0,000107
	7,19	5,443	1,230	0,361	0,0707	0,0140	7,11	4,338	1,060	0,000686	0,000260	0,000107
A29	5,75	3,348	0,804	0,0316	0,00744	0,00187	5,75	3,348	0,804	0,0316	0,00744	0,00187
	5,75	3,348	0,804	0,0316	0,00744	0,00187	5,75	3,348	0,804	0,0316	0,00744	0,00187
	6,03	3,348	0,804	0,0316	0,00744	0,00187	6,03	3,348	0,804	0,0316	0,00744	0,00187
	6,12	3,430	0,828	0,0292	0,00684	0,00172	6,12	3,430	0,828	0,0292	0,00684	0,00172
	6,81	3,532	0,857	0,0260	0,00604	0,00152	6,81	3,532	0,857	0,0260	0,00604	0,00152
A30	5,63	2,306	0,808	0,0106	0,00375	0,00147	5,63	2,306	0,808	0,0106	0,00375	0,00147
	5,85	2,306	0,808	0,0106	0,00375	0,00147	5,85	2,306	0,808	0,0106	0,00375	0,00147
	6,42	2,321	0,814	0,0102	0,00363	0,00143	6,42	2,321	0,814	0,0102	0,00363	0,00143
	6,42	2,321	0,814	0,0102	0,00363	0,00143	6,42	2,321	0,814	0,0102	0,00363	0,00143
	7,12	2,329	0,818	0,0100	0,00354	0,00139	7,12	2,329	0,818	0,0100	0,00354	0,00139
A31	6,94	4,201	0,864	0,0407	0,00808	0,00164	6,94	4,201	0,864	0,0407	0,00808	0,00164
	6,95	4,201	0,864	0,0407	0,00808	0,00164	6,95	4,201	0,864	0,0407	0,00808	0,00164
	7,08	4,339	0,894	0,0367	0,00727	0,00148	7,08	4,339	0,894	0,0367	0,00727	0,00148
	7,17	4,339	0,894	0,0367	0,00727	0,00148	7,17	4,339	0,894	0,0367	0,00727	0,00148
	7,41	4,339	0,894	0,0367	0,00727	0,00148	7,41	4,339	0,894	0,0367	0,00727	0,00148

	minimum for fit high						minimum for fit low					
	$M_{max,i}$	a	b	Caa	Cab	Cbb	$M_{max,i}$	a	b	Caa	Cab	Cbb
B29	6,05	3,081	0,804	0,00464	0,00143	0,000472	6,05	3,081	0,804	0,00464	0,00143	0,000472
	6,03	3,081	0,804	0,00464	0,00143	0,000472	6,03	3,081	0,804	0,00464	0,00143	0,000472
	6,23	3,105	0,812	0,00431	0,00132	0,000433	6,23	3,105	0,812	0,00431	0,00132	0,000433
	6,27	3,105	0,812	0,00431	0,00132	0,000433	6,27	3,105	0,812	0,00431	0,00132	0,000433
	6,76	3,122	0,818	0,00418	0,00128	0,000419	6,76	3,122	0,818	0,00418	0,00128	0,000419
B30	5,80	3,182	1,070	0,0207	0,00745	0,00281	5,81	3,182	1,070	0,0207	0,00745	0,00281
	5,97	3,182	1,070	0,0207	0,00745	0,00281	5,99	3,182	1,070	0,0207	0,00745	0,00281
	6,34	3,189	1,072	0,0203	0,00733	0,00277	6,35	3,189	1,072	0,0203	0,00733	0,00277
	6,34	3,189	1,072	0,0203	0,00733	0,00277	6,35	3,189	1,072	0,0203	0,00733	0,00277
	6,79	3,192	1,074	0,0202	0,00727	0,00274	6,80	3,192	1,074	0,0202	0,00727	0,00274
B31	6,56	2,745	0,726	0,0171	0,00442	0,00118	6,56	2,745	0,726	0,0171	0,00442	0,00118
	6,62	2,745	0,726	0,0171	0,00442	0,00118	6,62	2,745	0,726	0,0171	0,00442	0,00118
	6,91	2,745	0,726	0,0171	0,00442	0,00118	6,91	2,745	0,726	0,0171	0,00442	0,00118
	6,91	2,745	0,726	0,0171	0,00442	0,00118	6,91	2,745	0,726	0,0171	0,00442	0,00118
	7,26	2,763	0,731	0,0167	0,00431	0,00115	7,26	2,763	0,731	0,0167	0,00431	0,00115
B32	6,75	3,528	0,983	0,00264	0,000959	0,000379	6,75	3,528	0,983	0,00264	0,000959	0,000379
	6,86	3,528	0,983	0,00264	0,000959	0,000379	6,86	3,528	0,983	0,00264	0,000959	0,000379
	7,03	3,528	0,983	0,00264	0,000959	0,000379	7,03	3,528	0,983	0,00264	0,000959	0,000379
	7,10	3,530	0,984	0,00263	0,000955	0,000377	7,10	3,530	0,984	0,00263	0,000955	0,000377
	7,33	3,530	0,984	0,00263	0,000955	0,000377	7,33	3,530	0,984	0,00263	0,000955	0,000377
B33	6,30	5,142	1,169	0,420	0,0823	0,0163	6,27	4,336	1,059	0,000692	0,000263	0,000107
	6,30	5,142	1,169	0,420	0,0823	0,0163	6,27	4,336	1,059	0,000692	0,000263	0,000107
	6,69	5,381	1,218	0,375	0,0736	0,0145	6,56	4,338	1,060	0,000688	0,000261	0,000107
	6,73	5,381	1,218	0,375	0,0736	0,0145	6,69	4,338	1,060	0,000688	0,000261	0,000107
	7,19	5,443	1,230	0,361	0,0707	0,0140	7,11	4,338	1,060	0,000686	0,000260	0,000107
B34	5,75	3,348	0,804	0,0316	0,00744	0,00187	5,75	3,348	0,804	0,0316	0,00744	0,00187
	5,75	3,348	0,804	0,0316	0,00744	0,00187	5,75	3,348	0,804	0,0316	0,00744	0,00187
	6,03	3,348	0,804	0,0316	0,00744	0,00187	6,03	3,348	0,804	0,0316	0,00744	0,00187
	6,12	3,430	0,828	0,0292	0,00684	0,00172	6,12	3,430	0,828	0,0292	0,00684	0,00172
	6,81	3,532	0,857	0,0260	0,00604	0,00152	6,81	3,532	0,857	0,0260	0,00604	0,00152
B35	5,63	2,306	0,808	0,0106	0,00375	0,00147	5,63	2,306	0,808	0,0106	0,00375	0,00147
	5,85	2,306	0,808	0,0106	0,00375	0,00147	5,85	2,306	0,808	0,0106	0,00375	0,00147
	6,42	2,321	0,814	0,0102	0,00363	0,00143	6,42	2,321	0,814	0,0102	0,00363	0,00143
	6,42	2,321	0,814	0,0102	0,00363	0,00143	6,42	2,321	0,814	0,0102	0,00363	0,00143
	7,12	2,329	0,818	0,0100	0,00354	0,00139	7,12	2,329	0,818	0,0100	0,00354	0,00139
B36	6,94	4,201	0,864	0,0407	0,00808	0,00164	6,94	4,201	0,864	0,0407	0,00808	0,00164
	6,95	4,201	0,864	0,0407	0,00808	0,00164	6,95	4,201	0,864	0,0407	0,00808	0,00164
	7,08	4,339	0,894	0,0367	0,00727	0,00148	7,08	4,339	0,894	0,0367	0,00727	0,00148
	7,17	4,339	0,894	0,0367	0,00727	0,00148	7,17	4,339	0,894	0,0367	0,00727	0,00148
	7,41	4,339	0,894	0,0367	0,00727	0,00148	7,41	4,339	0,894	0,0367	0,00727	0,00148

	minimum for fit high						minimum for fit low					
	$M_{max.i}$	a	b	Caa	Cab	Cbb	$M_{max.i}$	a	b	Caa	Cab	Cbb
C099	5,63	3,080	1,052	0,0549	0,00515	0,00113	5,63	2,440	1,040	0,00691	0,00136	0,000552
	5,89	3,080	1,052	0,0549	0,00515	0,00113	5,87	2,440	1,040	0,00691	0,00136	0,000552
	6,45	3,091	1,056	0,0548	0,00509	0,00111	6,45	2,446	1,043	0,00685	0,00134	0,000543
	6,46	3,091	1,056	0,0548	0,00509	0,00111	6,45	2,446	1,043	0,00685	0,00134	0,000543
	7,14	3,100	1,059	0,0546	0,00504	0,00110	7,14	2,450	1,044	0,00681	0,00132	0,000537
C100	6,92	2,211	0,593	0,0319	0,00702	0,00162	6,93	2,211	0,593	0,0319	0,00702	0,00162
	7,06	2,320	0,621	0,0288	0,00630	0,00145	6,93	2,211	0,593	0,0319	0,00702	0,00162
	6,94	2,211	0,593	0,0319	0,00702	0,00162	7,03	2,211	0,593	0,0319	0,00702	0,00162
	7,11	2,320	0,621	0,0288	0,00630	0,00145	7,11	2,320	0,621	0,0288	0,00630	0,00145
	7,34	2,320	0,621	0,0288	0,00630	0,00145	7,33	2,320	0,621	0,0288	0,00630	0,00145
C101	6,30	1,928	0,834	0,0290	0,0104	0,00415	6,29	2,440	1,049	0,00329	0,000228	0,000101
	6,30	1,928	0,834	0,0290	0,0104	0,00415	6,32	2,440	1,049	0,00329	0,000228	0,000101
	6,70	1,933	0,836	0,0287	0,0103	0,00409	6,72	2,442	1,050	0,00329	0,000226	0,000100
	6,72	1,933	0,836	0,0287	0,0103	0,00409	6,72	2,442	1,050	0,00329	0,000226	0,000100
	7,18	1,936	0,837	0,0285	0,0102	0,00406	7,19	2,442	1,050	0,00328	0,000226	0,000098
C102	5,61	3,007	0,798	0,0359	0,00794	0,00199	5,61	3,007	0,798	0,0359	0,00794	0,00199
	5,61	3,007	0,798	0,0359	0,00794	0,00199	5,61	3,007	0,798	0,0359	0,00794	0,00199
	6,16	3,081	0,820	0,0336	0,00735	0,00184	6,16	3,081	0,820	0,0336	0,00735	0,00184
	6,31	3,081	0,820	0,0336	0,00735	0,00184	6,31	3,081	0,820	0,0336	0,00735	0,00184
	7,05	3,210	0,856	0,0292	0,00623	0,00155	7,05	3,210	0,856	0,0292	0,00623	0,00155
C103	5,64	2,041	0,718	0,00388	0,00146	0,000668	5,64	2,041	0,718	0,00388	0,00146	0,000668
	5,64	2,041	0,718	0,00388	0,00146	0,000668	5,64	2,041	0,718	0,00388	0,00146	0,000668
	6,18	2,053	0,724	0,00377	0,00141	0,000645	6,18	2,053	0,724	0,00377	0,00141	0,000645
	6,33	2,053	0,724	0,00377	0,00141	0,000645	6,33	2,053	0,724	0,00377	0,00141	0,000645
	7,00	2,058	0,727	0,00371	0,00138	0,000633	7,00	2,058	0,727	0,00371	0,00138	0,000633
C104	5,61	2,744	0,798	0,0341	0,00741	0,00199	5,61	2,744	0,798	0,0341	0,00741	0,00199
	5,61	2,744	0,798	0,0341	0,00741	0,00199	5,61	2,744	0,798	0,0341	0,00741	0,00199
	6,16	2,814	0,820	0,0319	0,00684	0,00184	6,16	2,814	0,820	0,0319	0,00684	0,00184
	6,31	2,814	0,820	0,0319	0,00684	0,00184	6,31	2,814	0,820	0,0319	0,00684	0,00184
	7,05	2,935	0,856	0,0278	0,00575	0,00155	7,05	2,935	0,856	0,0278	0,00575	0,00155
C105	6,92	2,639	0,712	0,0387	0,00831	0,00196	6,93	2,481	0,675	0,0128	0,00211	0,000482
	7,06	2,699	0,728	0,0358	0,00764	0,00181	6,93	2,481	0,675	0,0128	0,00211	0,000482
	6,94	2,639	0,712	0,0387	0,00831	0,00196	7,03	2,481	0,675	0,0128	0,00211	0,000482
	7,11	2,699	0,728	0,0358	0,00764	0,00181	7,11	2,556	0,695	0,0119	0,00192	0,000438
	7,34	2,699	0,728	0,0358	0,00764	0,00181	7,33	2,556	0,695	0,0119	0,00192	0,000438
C106	6,30	2,398	0,915	0,00489	0,00226	0,00124	6,29	2,398	0,915	0,00489	0,00226	0,00124
	6,30	2,398	0,915	0,00489	0,00226	0,00124	6,32	2,398	0,915	0,00489	0,00226	0,00124
	6,70	2,399	0,915	0,00486	0,00225	0,00123	6,72	2,399	0,915	0,00486	0,00225	0,00123
	6,72	2,399	0,915	0,00486	0,00225	0,00123	6,72	2,399	0,915	0,00486	0,00225	0,00123
	7,18	2,400	0,916	0,00486	0,00225	0,00123	7,19	2,400	0,916	0,00486	0,00225	0,00123
C107	6,30	2,847	1,075	0,00410	0,00218	0,00132	6,29	2,847	1,075	0,00410	0,00218	0,00132
	6,30	2,847	1,075	0,00410	0,00218	0,00132	6,32	2,847	1,075	0,00410	0,00218	0,00132
	6,70	2,847	1,075	0,00409	0,00217	0,00132	6,72	2,847	1,075	0,00409	0,00217	0,00132
	6,72	2,847	1,075	0,00409	0,00217	0,00132	6,72	2,847	1,075	0,00409	0,00217	0,00132
	7,18	2,847	1,075	0,00409	0,00217	0,00131	7,19	2,847	1,075	0,00409	0,00217	0,00131

	minimum for fit high						minimum for fit low					
	$M_{max,i}$	a	b	Caa	Cab	Cbb	$M_{max,i}$	a	b	Caa	Cab	Cbb
D099	6,83	2,908	0,749	0,0283	0,00629	0,00154	6,82	2,648	0,688	0,0125	0,00227	0,000523
	6,83	2,908	0,749	0,0283	0,00629	0,00154	6,84	2,648	0,688	0,0125	0,00227	0,000523
	6,96	2,908	0,749	0,0283	0,00629	0,00154	6,93	2,648	0,688	0,0125	0,00227	0,000523
	7,00	2,908	0,749	0,0283	0,00629	0,00154	7,00	2,648	0,688	0,0125	0,00227	0,000523
	7,26	2,956	0,763	0,0266	0,00586	0,00144	7,25	2,717	0,706	0,0117	0,00207	0,000478
D100	6,83	2,538	0,632	0,0226	0,00507	0,00119	6,82	2,538	0,632	0,0226	0,00507	0,00119
	6,83	2,538	0,632	0,0226	0,00507	0,00119	6,84	2,538	0,632	0,0226	0,00507	0,00119
	6,96	2,538	0,632	0,0226	0,00507	0,00119	6,93	2,538	0,632	0,0226	0,00507	0,00119
	7,00	2,538	0,632	0,0226	0,00507	0,00119	7,00	2,538	0,632	0,0226	0,00507	0,00119
	7,26	2,631	0,655	0,0206	0,00460	0,00108	7,25	2,631	0,655	0,0206	0,00460	0,00108
D101	5,68	1,878	0,794	0,00856	0,00352	0,00174	5,68	1,878	0,794	0,00856	0,00352	0,00174
	6,12	1,885	0,798	0,00840	0,00343	0,00170	6,12	1,885	0,798	0,00840	0,00343	0,00170
	6,46	1,885	0,798	0,00840	0,00343	0,00170	6,46	1,885	0,798	0,00840	0,00343	0,00170
	6,67	1,888	0,799	0,00831	0,00339	0,00168	6,67	1,888	0,799	0,00831	0,00339	0,00168
	7,19	1,889	0,800	0,00827	0,00337	0,00167	7,19	1,889	0,800	0,00827	0,00337	0,00167
D102	5,65	1,565	0,900	0,0167	0,00188	0,000713	5,62	1,821	1,000	0,0139	0,000840	0,000335
	5,65	1,565	0,900	0,0167	0,00188	0,000713	5,80	1,821	1,000	0,0139	0,000840	0,000335
	6,29	1,585	0,909	0,0165	0,00181	0,000686	6,40	1,828	1,003	0,0139	0,000826	0,000329
	6,34	1,585	0,909	0,0165	0,00181	0,000686	6,40	1,828	1,003	0,0139	0,000826	0,000329
	7,06	1,599	0,914	0,0164	0,00175	0,000664	7,12	1,831	1,005	0,0138	0,000816	0,000325
D103	5,74	2,825	0,724	0,0356	0,00830	0,00210	5,74	3,021	0,775	0,0208	0,00475	0,00125
	5,95	2,825	0,724	0,0356	0,00830	0,00210	5,95	3,021	0,775	0,0208	0,00475	0,00125
	5,74	2,825	0,724	0,0356	0,00830	0,00210	5,74	3,021	0,775	0,0208	0,00475	0,00125
	6,04	2,825	0,724	0,0356	0,00830	0,00210	6,04	3,021	0,775	0,0208	0,00475	0,00125
	6,66	3,017	0,781	0,0286	0,00654	0,00165	6,66	3,168	0,820	0,0178	0,00394	0,00104
D104	5,74	2,786	0,775	0,0228	0,00475	0,00125	5,74	2,786	0,775	0,0228	0,00475	0,00125
	5,95	2,786	0,775	0,0228	0,00475	0,00125	5,95	2,786	0,775	0,0228	0,00475	0,00125
	5,74	2,786	0,775	0,0228	0,00475	0,00125	5,74	2,786	0,775	0,0228	0,00475	0,00125
	6,04	2,786	0,775	0,0228	0,00475	0,00125	6,04	2,786	0,775	0,0228	0,00475	0,00125
	6,66	2,933	0,820	0,0198	0,00394	0,00104	6,66	2,933	0,820	0,0198	0,00394	0,00104
D105	6,28	3,222	0,984	0,0123	0,000873	0,000269	6,29	3,411	1,043	0,0108	0,000435	0,000140
	6,28	3,222	0,984	0,0123	0,000873	0,000269	6,29	3,411	1,043	0,0108	0,000435	0,000140
	6,59	3,227	0,986	0,0123	0,000867	0,000265	6,62	3,412	1,044	0,0108	0,000434	0,000139
	6,71	3,227	0,986	0,0123	0,000867	0,000265	6,73	3,412	1,044	0,0108	0,000434	0,000139
	7,13	3,229	0,987	0,0123	0,000864	0,000264	7,15	3,412	1,044	0,0108	0,000433	0,000138
D106	6,83	2,088	0,713	0,0238	0,00265	0,000628	6,82	1,979	0,688	0,0224	0,00227	0,000523
	6,83	2,088	0,713	0,0238	0,00265	0,000628	6,84	1,979	0,688	0,0224	0,00227	0,000523
	6,96	2,088	0,713	0,0238	0,00265	0,000628	6,93	1,979	0,688	0,0224	0,00227	0,000523
	7,00	2,088	0,713	0,0238	0,00265	0,000628	7,00	1,979	0,688	0,0224	0,00227	0,000523
	7,26	2,159	0,732	0,0228	0,00243	0,000577	7,25	2,048	0,706	0,0215	0,00207	0,000478

	minimum for fit high						minimum for fit low					
	$M_{max,i}$	a	b	Caa	Cab	Cbb	$M_{max,i}$	a	b	Caa	Cab	Cbb
E085	6,56	2,934	0,914	0,194	0,0336	0,00652	6,56	1,762	0,715	0,0249	0,00585	0,00166
	6,66	2,934	0,914	0,194	0,0336	0,00652	6,64	1,762	0,715	0,0249	0,00585	0,00166
	6,94	2,934	0,914	0,194	0,0336	0,00652	6,93	1,762	0,715	0,0249	0,00585	0,00166
	6,94	2,934	0,914	0,194	0,0336	0,00652	6,93	1,762	0,715	0,0249	0,00585	0,00166
	7,28	2,979	0,923	0,188	0,0324	0,00627	7,27	1,791	0,724	0,0241	0,00563	0,00160
E086	6,30	3,805	1,004	0,0135	0,000965	0,000188	6,29	3,726	1,054	0,00272	0,00103	0,000420
	6,30	3,805	1,004	0,0135	0,000965	0,000188	6,32	3,726	1,054	0,00272	0,00103	0,000420
	6,68	3,803	1,006	0,0135	0,000962	0,000186	6,71	3,728	1,054	0,00270	0,00102	0,000418
	6,72	3,803	1,006	0,0135	0,000962	0,000186	6,71	3,728	1,054	0,00270	0,00102	0,000418
	7,18	3,803	1,007	0,0136	0,000961	0,000185	7,19	3,729	1,055	0,00270	0,00102	0,000417
E087	6,94	1,887	0,680	0,0940	0,00816	0,00142	6,93	1,771	0,661	0,0187	0,00259	0,000616
	6,94	1,887	0,680	0,0940	0,00816	0,00142	6,93	1,771	0,661	0,0187	0,00259	0,000616
	7,07	2,053	0,715	0,0909	0,00752	0,00129	7,06	1,854	0,682	0,0177	0,00235	0,000559
	7,14	2,053	0,715	0,0909	0,00752	0,00129	7,13	1,854	0,682	0,0177	0,00235	0,000559
	7,38	2,053	0,715	0,0909	0,00752	0,00129	7,36	1,854	0,682	0,0177	0,00235	0,000559
E088	5,63	1,446	0,670	0,0118	0,00419	0,00182	5,63	1,446	0,670	0,0118	0,00419	0,00182
	5,68	1,446	0,670	0,0118	0,00419	0,00182	5,68	1,446	0,670	0,0118	0,00419	0,00182
	6,32	1,462	0,678	0,0114	0,00401	0,00174	6,32	1,462	0,678	0,0114	0,00401	0,00174
	6,32	1,462	0,678	0,0114	0,00401	0,00174	6,32	1,462	0,678	0,0114	0,00401	0,00174
	7,06	1,474	0,684	0,0110	0,00386	0,00167	7,06	1,474	0,684	0,0110	0,00386	0,00167
E089	6,94	4,802	1,056	0,292	0,0571	0,0112	6,93	2,870	0,700	0,0206	0,00440	0,00103
	6,94	4,802	1,056	0,292	0,0571	0,0112	6,93	2,870	0,700	0,0206	0,00440	0,00103
	7,07	4,959	1,087	0,270	0,0526	0,0104	7,06	2,934	0,718	0,0191	0,00402	0,000941
	7,14	4,959	1,087	0,270	0,0526	0,0104	7,13	2,934	0,718	0,0191	0,00402	0,000941
	7,38	4,959	1,087	0,270	0,0526	0,0104	7,36	2,934	0,718	0,0191	0,00402	0,000941
E090	6,56	3,139	0,914	0,129	0,0283	0,00652	6,56	2,260	0,715	0,0407	0,00753	0,00166
	6,66	3,139	0,914	0,129	0,0283	0,00652	6,64	2,260	0,715	0,0407	0,00753	0,00166
	6,94	3,139	0,914	0,129	0,0283	0,00652	6,93	2,260	0,715	0,0407	0,00753	0,00166
	6,94	3,139	0,914	0,129	0,0283	0,00652	6,93	2,260	0,715	0,0407	0,00753	0,00166
	7,28	3,179	0,923	0,125	0,0273	0,00627	7,27	2,293	0,724	0,0399	0,00730	0,00160
E091	6,94	2,211	0,593	0,0319	0,00702	0,00162	6,93	2,211	0,593	0,0319	0,00702	0,00162
	6,94	2,211	0,593	0,0319	0,00702	0,00162	6,93	2,211	0,593	0,0319	0,00702	0,00162
	7,07	2,320	0,621	0,0288	0,00630	0,00145	7,06	2,320	0,621	0,0288	0,00630	0,00145
	7,14	2,320	0,621	0,0288	0,00630	0,00145	7,13	2,320	0,621	0,0288	0,00630	0,00145
	7,38	2,320	0,621	0,0288	0,00630	0,00145	7,36	2,320	0,621	0,0288	0,00630	0,00145
E092	6,30	2,906	1,076	0,0433	0,0159	0,00610	6,29	2,906	1,076	0,0433	0,0159	0,00610
	6,30	2,906	1,076	0,0433	0,0159	0,00610	6,32	2,906	1,076	0,0433	0,0159	0,00610
	6,68	2,908	1,077	0,0431	0,0158	0,00607	6,71	2,908	1,077	0,0431	0,0158	0,00607
	6,72	2,908	1,077	0,0431	0,0158	0,00607	6,71	2,908	1,077	0,0431	0,0158	0,00607
	7,18	2,908	1,077	0,0430	0,0158	0,00606	7,19	2,908	1,077	0,0430	0,0158	0,00606
E093	6,30	1,720	0,750	0,00938	0,00362	0,00170	6,29	1,720	0,750	0,00938	0,00362	0,00170
	6,30	1,720	0,750	0,00938	0,00362	0,00170	6,32	1,720	0,750	0,00938	0,00362	0,00170
	6,68	1,725	0,752	0,00925	0,00356	0,00168	6,71	1,725	0,752	0,00925	0,00356	0,00168
	6,72	1,725	0,752	0,00925	0,00356	0,00168	6,71	1,725	0,752	0,00925	0,00356	0,00168
	7,18	1,727	0,753	0,00919	0,00353	0,00166	7,19	1,727	0,753	0,00919	0,00353	0,00166
E094	6,68	3,292	0,848	0,0264	0,00641	0,00173	6,68	3,081	0,793	0,0149	0,00313	0,000801
	6,68	3,292	0,848	0,0264	0,00641	0,00173	6,68	3,081	0,793	0,0149	0,00313	0,000801
	6,99	3,292	0,848	0,0264	0,00641	0,00173	6,99	3,081	0,793	0,0149	0,00313	0,000801
	7,02	3,292	0,848	0,0264	0,00641	0,00173	7,02	3,081	0,793	0,0149	0,00313	0,000801
	7,40	3,319	0,857	0,0254	0,00613	0,00166	7,40	3,119	0,804	0,0142	0,00295	0,000756
E095	6,68	2,871	0,740	0,0287	0,00631	0,00153	6,68	3,081	0,793	0,0149	0,00313	0,000801
	6,68	2,871	0,740	0,0287	0,00631	0,00153	6,68	3,081	0,793	0,0149	0,00313	0,000801
	6,99	2,871	0,740	0,0287	0,00631	0,00153	6,99	3,081	0,793	0,0149	0,00313	0,000801
	7,02	2,871	0,740	0,0287	0,00631	0,00153	7,02	3,081	0,793	0,0149	0,00313	0,000801
	7,40	2,922	0,755	0,0268	0,00586	0,00142	7,40	3,119	0,804	0,0142	0,00295	0,000756
E096	6,30	2,687	1,004	0,0396	0,000601	0,000188	6,29	2,765	1,029	0,0389	0,000363	0,000116
	6,30	2,687	1,004	0,0396	0,000601	0,000188	6,32	2,765	1,029	0,0389	0,000363	0,000116
	6,68	2,689	1,006	0,0397	0,000599	0,000186	6,71	2,766	1,030	0,0389	0,000362	0,000115
	6,72	2,689	1,006	0,0397	0,000599	0,000186	6,71	2,766	1,030	0,0389	0,000362	0,000115
	7,18	2,690	1,007	0,0397	0,000598	0,000185	7,19	2,766	1,030	0,0389	0,000362	0,000114
E097	6,30	2,687	1,004	0,0396	0,000601	0,000188	6,29	2,765	1,029	0,0389	0,000363	0,000116
	6,30	2,687	1,004	0,0396	0,000601	0,000188	6,32	2,765	1,029	0,0389	0,000363	0,000116
	6,68	2,689	1,006	0,0397	0,000599	0,000186	6,71	2,766	1,030	0,0389	0,000362	0,000115
	6,72	2,689	1,006	0,0397	0,000599	0,000186	6,71	2,766	1,030	0,0389	0,000362	0,000115
	7,18	2,690	1,007	0,0397	0,000598	0,000185	7,19	2,766	1,030	0,0389	0,000362	0,000114

Tables 5-2. The parameters a and b of the frequency-magnitude relation with the parameters of the covariance matrix as measure of the uncertainty for the different $M_{max,i}$ for the CSS model of the Lower Rhine graben. The parameters are given for both variants of the minimum for fit.

	minimum for fit high						minimum for fit low					
	$M_{max,i}$	a	b	Caa	Cab	Cbb	$M_{max,i}$	a	b	Caa	Cab	Cbb
BECS001	6.69	1.014	0.858	0.0141	0.0044	0.00184	6.69	0.898	0.810	0.0099	0.0025	0.00101
	6.82	1.014	0.858	0.0141	0.0044	0.00184	6.82	0.898	0.810	0.0099	0.0025	0.00101
	6.94	1.017	0.858	0.0141	0.0044	0.00184	6.94	0.901	0.810	0.0099	0.0025	0.00101
	7.07	1.021	0.860	0.0140	0.0043	0.00182	7.07	0.903	0.812	0.0098	0.0025	0.00100
	7.24	1.023	0.860	0.0140	0.0043	0.00182	7.24	0.906	0.812	0.0098	0.0025	0.00100
BECS002	6.69	1.038	0.858	0.0141	0.0044	0.00184	6.69	0.922	0.810	0.0099	0.0025	0.00101
	6.82	1.038	0.858	0.0141	0.0044	0.00184	6.82	0.922	0.810	0.0099	0.0025	0.00101
	6.94	1.041	0.858	0.0141	0.0044	0.00184	6.94	0.925	0.810	0.0099	0.0025	0.00101
	7.07	1.045	0.860	0.0140	0.0043	0.00182	7.07	0.927	0.812	0.0098	0.0025	0.00100
	7.24	1.047	0.860	0.0140	0.0043	0.00182	7.24	0.930	0.812	0.0098	0.0025	0.00100
DECS001	6.69	1.647	0.858	0.0560	0.0089	0.00184	6.69	1.029	0.791	0.0348	0.0109	0.00368
	6.82	1.641	0.858	0.0560	0.0089	0.00184	6.82	1.023	0.791	0.0348	0.0109	0.00368
	6.94	1.641	0.858	0.0560	0.0089	0.00184	6.94	1.023	0.791	0.0348	0.0109	0.00368
	7.07	1.644	0.860	0.0559	0.0088	0.00182	7.07	1.026	0.794	0.0342	0.0107	0.00360
	7.24	1.644	0.860	0.0559	0.0088	0.00182	7.24	1.026	0.794	0.0342	0.0107	0.00360
DECS002	6.39	1.570	0.858	0.0560	0.0089	0.00184	6.39	0.952	0.791	0.0348	0.0109	0.00368
	6.53	1.565	0.858	0.0560	0.0089	0.00184	6.53	0.946	0.791	0.0348	0.0109	0.00368
	6.66	1.564	0.858	0.0560	0.0089	0.00184	6.66	0.946	0.791	0.0348	0.0109	0.00368
	6.80	1.568	0.860	0.0559	0.0088	0.00182	6.80	0.950	0.794	0.0342	0.0107	0.00360
	7.01	1.567	0.860	0.0559	0.0088	0.00182	7.01	0.949	0.794	0.0342	0.0107	0.00360
DECS003	6.88	1.981	0.858	0.0560	0.0089	0.00184	6.88	1.029	0.810	0.0099	0.0025	0.00101
	7.00	1.975	0.858	0.0560	0.0089	0.00184	7.00	1.028	0.810	0.0099	0.0025	0.00101
	7.10	1.975	0.858	0.0560	0.0089	0.00184	7.10	1.032	0.810	0.0099	0.0025	0.00101
	7.20	1.979	0.860	0.0559	0.0088	0.00182	7.20	1.034	0.812	0.0098	0.0025	0.00100
	7.32	1.978	0.860	0.0559	0.0088	0.00182	7.32	1.037	0.812	0.0098	0.0025	0.00100
DECS004	6.88	1.145	0.858	0.0141	0.0044	0.00184	6.88	1.363	0.791	0.0348	0.0109	0.00368
	7.00	1.144	0.858	0.0141	0.0044	0.00184	7.00	1.357	0.791	0.0348	0.0109	0.00368
	7.10	1.148	0.858	0.0141	0.0044	0.00184	7.10	1.357	0.791	0.0348	0.0109	0.00368
	7.20	1.151	0.860	0.0140	0.0043	0.00182	7.20	1.360	0.794	0.0342	0.0107	0.00360
	7.32	1.154	0.860	0.0140	0.0043	0.00182	7.32	1.360	0.794	0.0342	0.0107	0.00360
DECS005	6.39	1.579	0.858	0.0560	0.0089	0.00184	6.39	0.961	0.791	0.0348	0.0109	0.00368
	6.53	1.574	0.858	0.0560	0.0089	0.00184	6.53	0.955	0.791	0.0348	0.0109	0.00368
	6.66	1.574	0.858	0.0560	0.0089	0.00184	6.66	0.956	0.791	0.0348	0.0109	0.00368
	6.80	1.577	0.860	0.0559	0.0088	0.00182	6.80	0.959	0.794	0.0342	0.0107	0.00360
	7.01	1.576	0.860	0.0559	0.0088	0.00182	7.01	0.958	0.794	0.0342	0.0107	0.00360
DECS006	6.29	1.425	0.858	0.0560	0.0089	0.00184	6.29	0.807	0.791	0.0348	0.0109	0.00368
	6.43	1.419	0.858	0.0560	0.0089	0.00184	6.43	0.801	0.791	0.0348	0.0109	0.00368
	6.56	1.419	0.858	0.0560	0.0089	0.00184	6.56	0.801	0.791	0.0348	0.0109	0.00368
	6.70	1.423	0.860	0.0559	0.0088	0.00182	6.70	0.804	0.794	0.0342	0.0107	0.00360
	6.91	1.422	0.860	0.0559	0.0088	0.00182	6.91	0.804	0.794	0.0342	0.0107	0.00360
DECS007	6.09	1.257	0.858	0.0560	0.0089	0.00184	6.09	0.639	0.791	0.0348	0.0109	0.00368
	6.23	1.251	0.858	0.0560	0.0089	0.00184	6.23	0.633	0.791	0.0348	0.0109	0.00368
	6.36	1.251	0.858	0.0560	0.0089	0.00184	6.36	0.633	0.791	0.0348	0.0109	0.00368
	6.50	1.254	0.860	0.0559	0.0088	0.00182	6.50	0.636	0.794	0.0342	0.0107	0.00360
	6.71	1.254	0.860	0.0559	0.0088	0.00182	6.71	0.636	0.794	0.0342	0.0107	0.00360
DECS008	6.39	1.554	0.858	0.0560	0.0089	0.00184	6.39	0.936	0.791	0.0348	0.0109	0.00368
	6.53	1.548	0.858	0.0560	0.0089	0.00184	6.53	0.930	0.791	0.0348	0.0109	0.00368
	6.66	1.548	0.858	0.0560	0.0089	0.00184	6.66	0.930	0.791	0.0348	0.0109	0.00368
	6.80	1.552	0.860	0.0559	0.0088	0.00182	6.80	0.933	0.794	0.0342	0.0107	0.00360
	7.01	1.551	0.860	0.0559	0.0088	0.00182	7.01	0.933	0.794	0.0342	0.0107	0.00360
NLCS001	6.88	1.538	0.858	0.0141	0.0044	0.00184	6.88	1.422	0.810	0.0099	0.0025	0.00101
	7.00	1.537	0.858	0.0141	0.0044	0.00184	7.00	1.421	0.810	0.0099	0.0025	0.00101
	7.10	1.540	0.858	0.0141	0.0044	0.00184	7.10	1.425	0.810	0.0099	0.0025	0.00101
	7.20	1.544	0.860	0.0140	0.0043	0.00182	7.20	1.427	0.812	0.0098	0.0025	0.00100
	7.32	1.547	0.860	0.0140	0.0043	0.00182	7.32	1.430	0.812	0.0098	0.0025	0.00100
NLCS002	6.69	1.824	0.858	0.0560	0.0089	0.00184	6.69	1.206	0.791	0.0348	0.0109	0.00368
	6.82	1.819	0.858	0.0560	0.0089	0.00184	6.82	1.200	0.791	0.0348	0.0109	0.00368
	6.94	1.818	0.858	0.0560	0.0089	0.00184	6.94	1.200	0.791	0.0348	0.0109	0.00368
	7.07	1.822	0.860	0.0559	0.0088	0.00182	7.07	1.204	0.794	0.0342	0.0107	0.00360
	7.24	1.821	0.860	0.0559	0.0088	0.00182	7.24	1.203	0.794	0.0342	0.0107	0.00360
NLCS003	6.39	1.504	0.858	0.0560	0.0089	0.00184	6.39	0.886	0.791	0.0348	0.0109	0.00368
	6.53	1.499	0.858	0.0560	0.0089	0.00184	6.53	0.880	0.791	0.0348	0.0109	0.00368
	6.66	1.499	0.858	0.0560	0.0089	0.00184	6.66	0.881	0.791	0.0348	0.0109	0.00368
	6.80	1.502	0.860	0.0559	0.0088	0.00182	6.80	0.884	0.794	0.0342	0.0107	0.00360
	7.01	1.501	0.860	0.0559	0.0088	0.00182	7.01	0.883	0.794	0.0342	0.0107	0.00360

6. Depth distributions

The depth distributions were calculated for a model of nine respective superzones (cf. chapter 8.3 of *Grünthal et al. 2018*). This superzone model is shown in Fig. 6-1. Also, this superzone model consists of a subsumption of the LASZ model A. It is identical to the superzone model of kernels as shown in Fig. 3-7. The polygon traces of the superzones of depth distributions are also part of the electronic annex. Fig. 6-2 presents the frequency of depth data in classes of 5 km for each superzone, the cumulative depth distributions and the mathematically optimized discretization of the depth occurrences according to *Miller and Rice (1983)* in form of three data pairs of respective depth values and corresponding weights. Additionally, these data are given for each depth distribution superzone in Tab. 6-1.

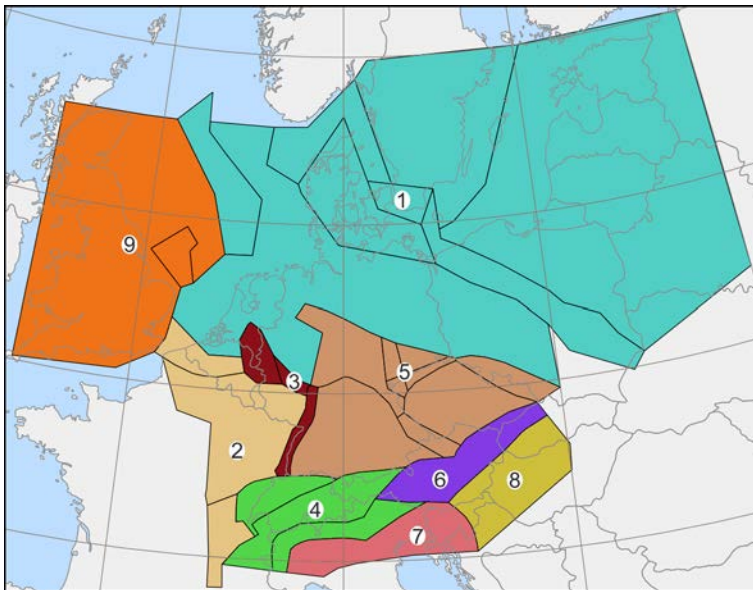


Figure 6-1. The depth superzone model.

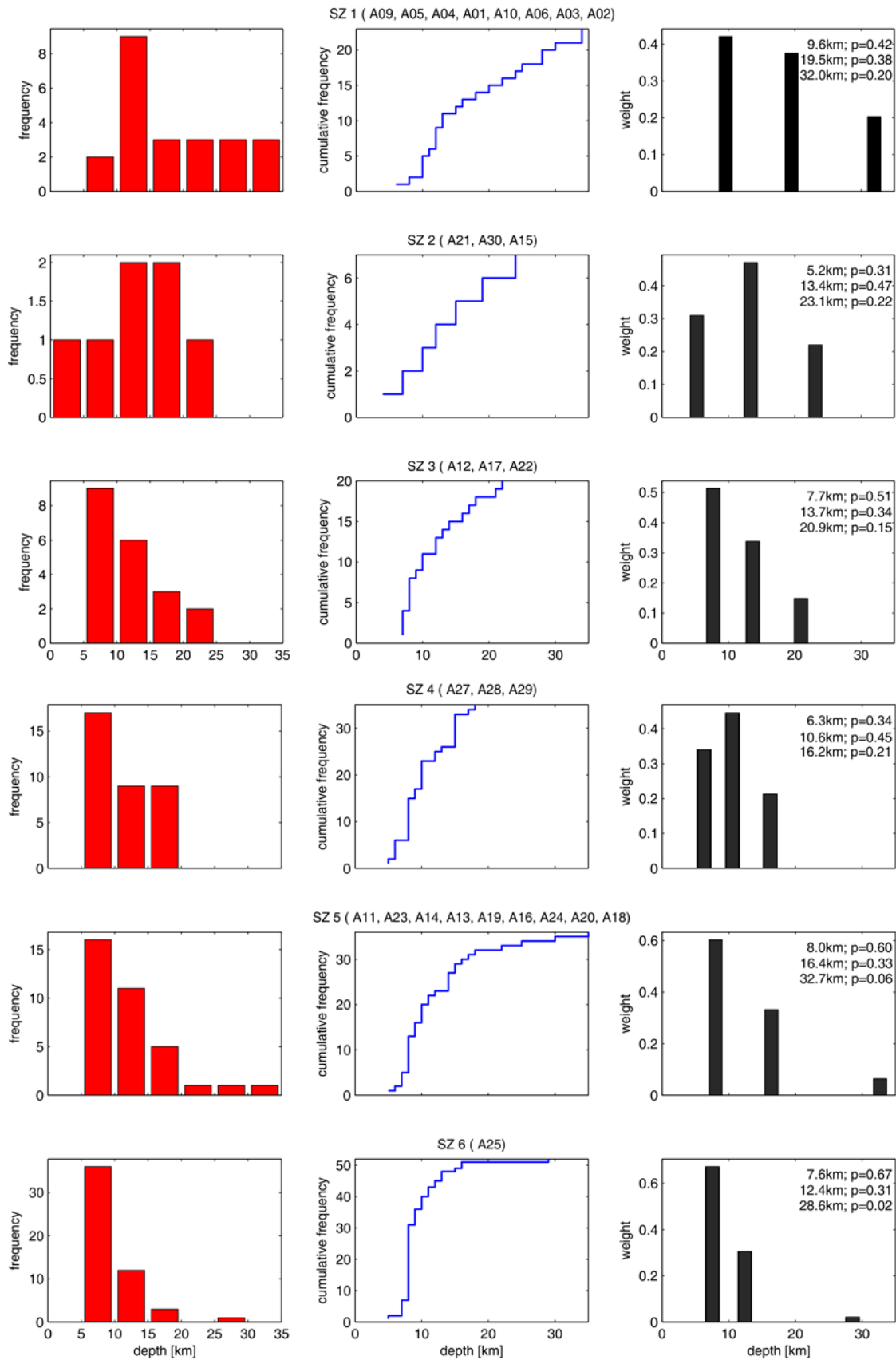


Figure 6-2. The depth distributions of the superzones. The frequency of depth data in classes of 5 km for each superzone (left), the cumulative depth distributions (middle) and the mathematically optimized discretization of the depth occurrences according to *Miller & Rice* (1983) in form of three data pairs of respective depth values and corresponding weights.

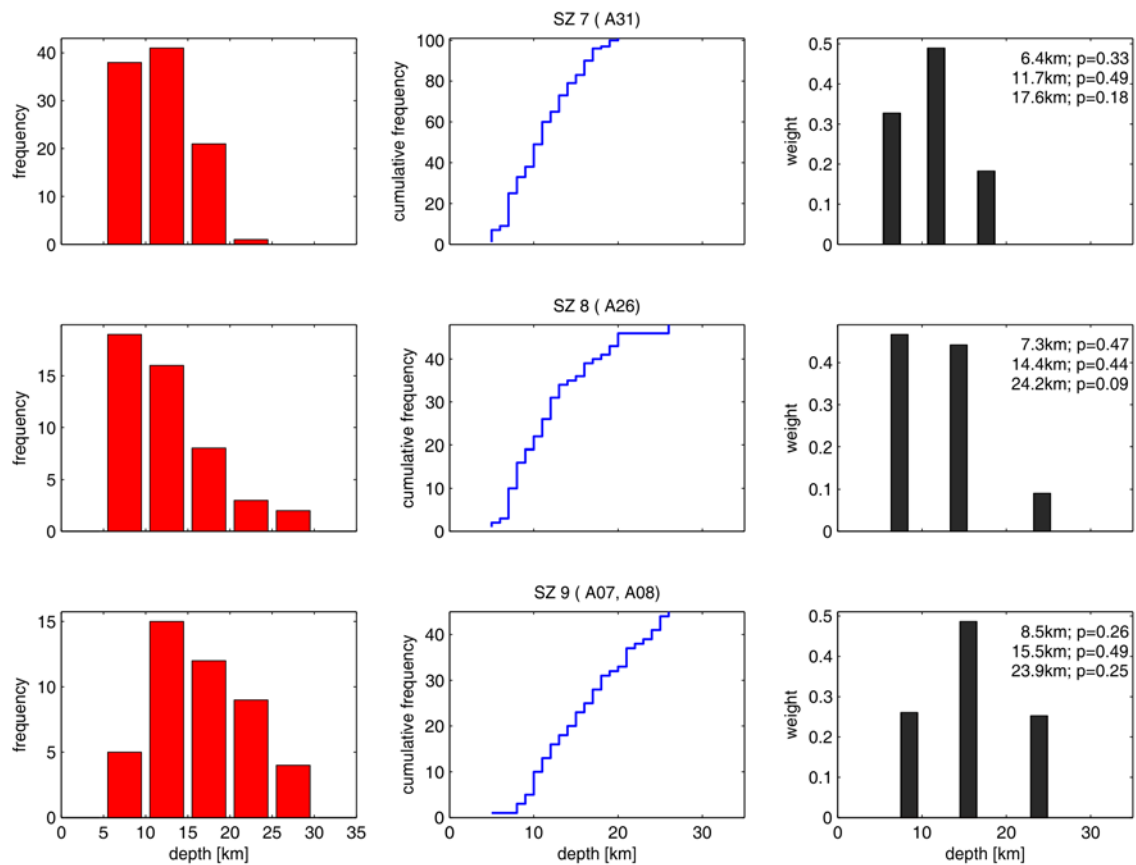


Figure 6-2. Continued.

Table 6-1. Combination of LASZs of model A to build nine depth superzones DSZ. Sampled depths distribution for each DSZ at three optimally selected depths with their corresponding weights.

DSZ	LASZ (model A)	depths [km]			weights		
		1	2	3	1	2	3
1	A09, A05, A04, A01, A10, A06, A03, A02	9.6	19.5	32.0	0.421	0.376	0.203
2	A21, A30, A15	5.2	13.4	23.1	0.309	0.470	0.221
3	A12, A17, A22	7.7	13.7	20.9	0.513	0.338	0.149
4	A27, A28, A29	6.3	10.6	16.2	0.341	0.446	0.213
5	A11, A23, A14, A13, A19, A16, A24, A20, A18	8.0	16.4	32.7	0.603	0.333	0.064
6	A25	7.6	12.4	28.6	0.672	0.306	0.022
7	A31	6.4	11.7	17.6	0.327	0.490	0.183
8	A26	7.3	14.4	24.2	0.467	0.442	0.091
9	A07, A08	8.5	15.5	23.9	0.261	0.486	0.253

7. Tectonic regimes

The parameters of the tectonic regime were derived for a model of eleven respective superzones (cf. chapter 8.5 of *Grünthal et al. 2018*), which are presented in Fig. 7-1 with the polygon traces as part of the electronic annex. The data source for deriving these parameters is the World Stress Map Database Release 2016 (*Heidbach et al. 2016*). The percentages of the occurrence of style-of-faulting within each of these eleven superzones are provided in Tab. 7-1.

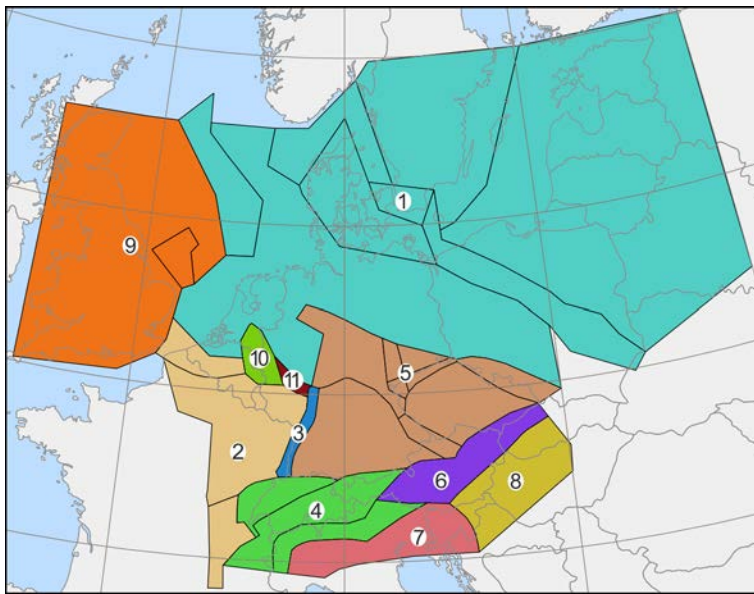


Figure 7-1. The superzone model used to derive the tectonic regime parameters.

Table 7-1. Combination of LASZs of model A to build eleven tectonic superzones TSZ. Weights of style-of-faulting for each TSZ according to the WSM database

TSZ	LASZ (model A)	strike-slip	normal	thrust
1	A09, A05, A04, A01, A10, A06, A03, A02	0.632	0.263	0.105
2	A21, A30, A15	0.571	0.214	0.214
3	A22	0.500	0.500	-
4	A27, A28, A29	0.538	0.299	0.167
5	A11, A23, A14, A13, A19, A16, A24, A20, A18	0.727	0.258	0.015
6	A25	0.816	0.053	0.132
7	A31	0.315	0.076	0.609
8	A26	0.520	0.080	0.400
9	A07, A08	0.594	0.250	0.156
10	A12	0.267	0.733	-
11	A17	-	0.750	0.250

8. Additional results of the probabilistic seismic hazard assessment

The results of the reassessment of the probabilistic seismic hazard of Germany are described in chapter 9 of *Grünthal et al.* (2018). Here we provide additional probabilistic seismic hazard maps and deaggregation results for several selected sites.

8.1. Probabilistic seismic hazard maps

While a selection of a few seismic hazard maps could be presented by *Grünthal et al.* (2018) only, we here show a more comprehensive set of maps. The hazard calculations were accomplished for rock underground conditions and characterized by an average shear wave velocity of the upper 30m $v_{S30} = 800\text{m/s}$, for the hazard levels of occurrence or exceedance probabilities of 10%, 5% and 2% within 50 years. These hazard levels correspond to the mean return periods $RP = 475, 975$ and 2475 years (a). The horizontal 5% damped Uniform Hazard response Spectra (UHS) were computed for the spectral range of periods T of 0.02s-3.0s, for the weighted arithmetic mean of the results per each logic tree branch, the median, the 84th and the 16th percentile. The seismic hazard maps were generated for (1) the mean and the aforementioned percentiles for selected spectral response accelerations (SRA) of the UHS, (2) for the mean of the amplitudes of periods T in the UHS representing the plateau (0.1s, 0.15s, 0.2s), and (3) for peak ground accelerations (PGA).

Here we present the seismic hazard maps for selected amplitudes of the UHS; i.e. for 0.1s for $RP = 475\text{a}$ in form of the mean, the median with the 84th percentile (Fig. 8-1) and accordingly for $RP = 975\text{a}$ (Fig. 8-2) and $RP = 2475\text{a}$ (Fig. 8-3). The corresponding set of maps for 0.15s is shown in Figs. 8-4 to 8.6 as well as for 0.2s (Figs. 8-7 to 8-9). The PGA maps in the mentioned configuration are shown in Figs. 8-10 to 8-12. The mean of the amplitudes of periods T in the UHS representing the plateau (0.1s, 0.15s, 0.2s) at a grid point, abbreviated as meanSRA, are presented for the given results from the logic tree branches in Figs. 8-13 to 8-15. The corresponding maxSRA maps; i.e. the maxima of the amplitudes at the given three values of T at a grid point, are subject of the Figs. 8-16 to 8-18.

Figure 8-1. Seismic hazard maps for the response acceleration amplitudes at 0.1s spectral period for the mean return period $RP = 475a$; mean values of the logic tree (top left), median (bottom left) with the related 84th percentile (bottom right).

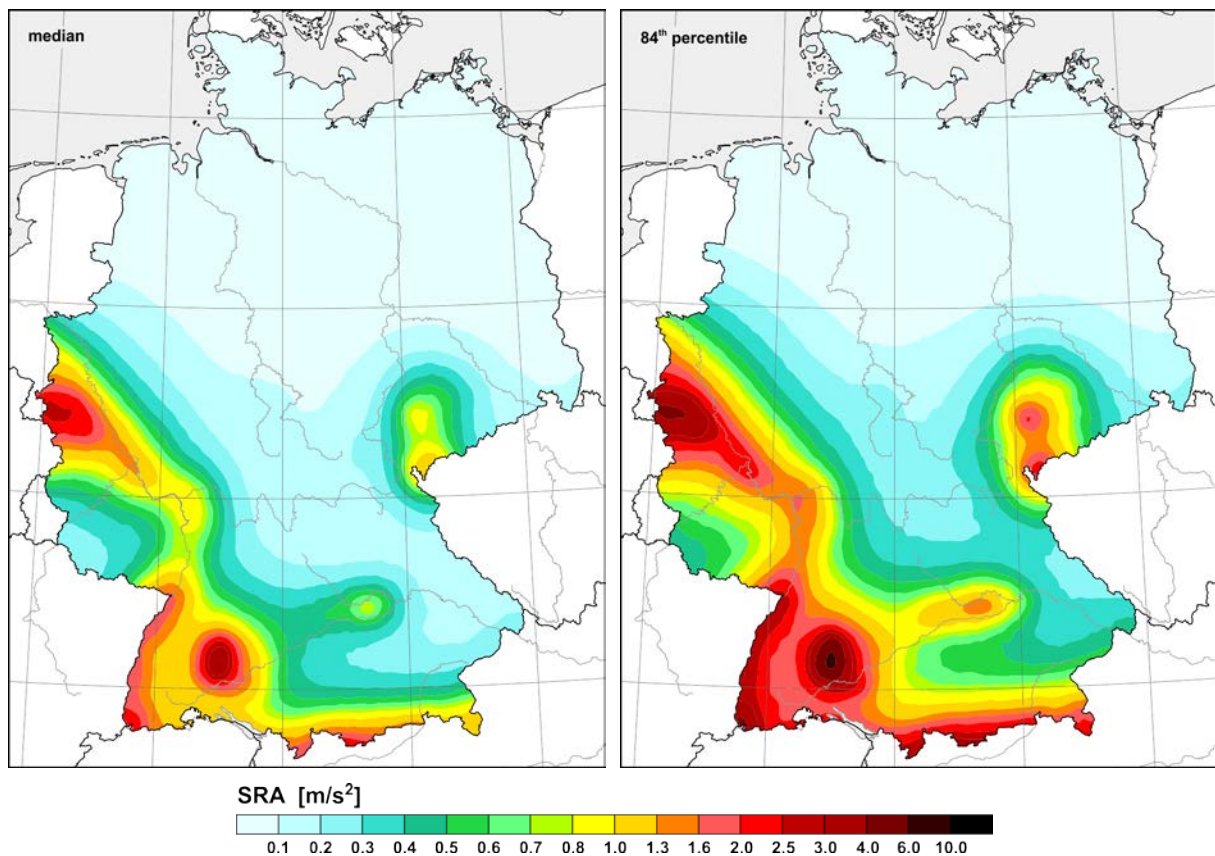


Figure 8-2. Seismic hazard maps for the response acceleration amplitudes at 0.1 s spectral period for the mean return period $RP = 975a$; mean values (top left), median (bottom left) with the related 84th percentile (bottom right).

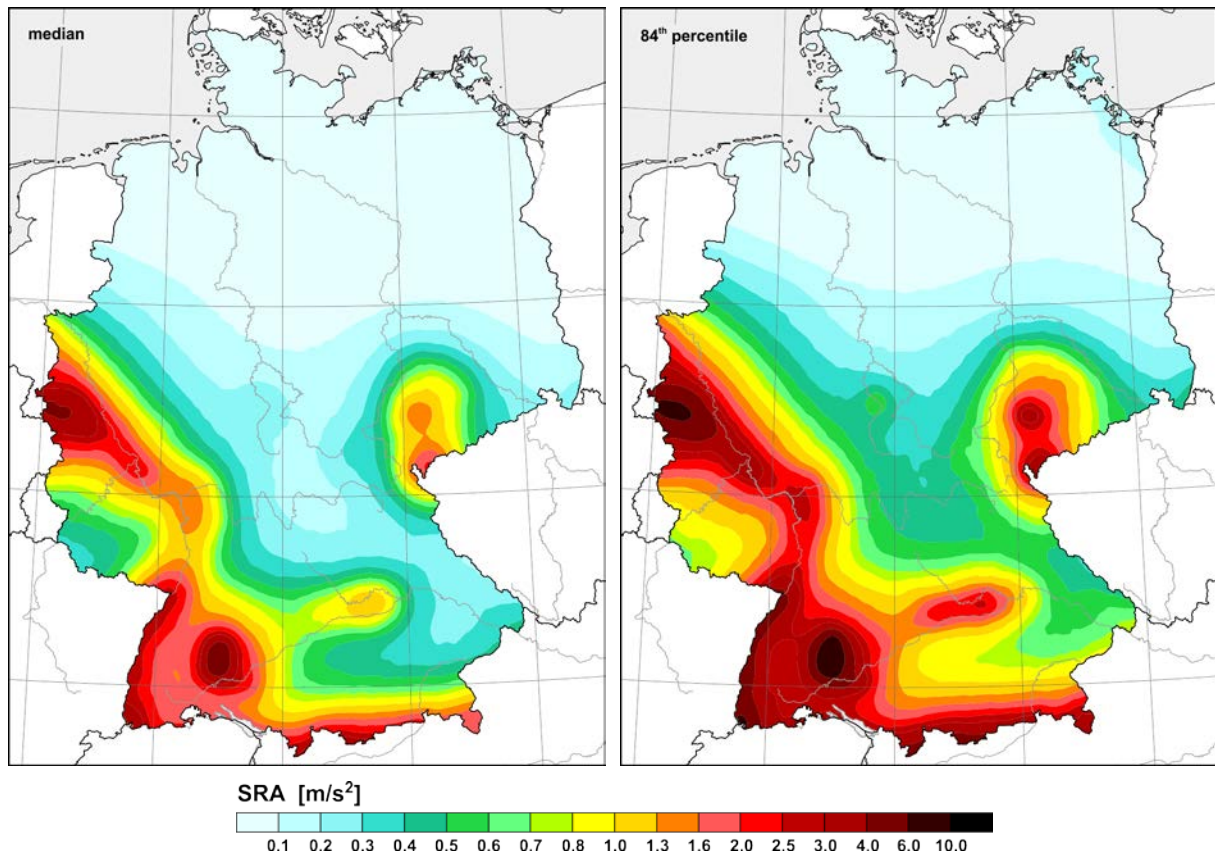


Figure 8-3. Seismic hazard maps for the response acceleration amplitudes at 0.1s spectral period for the mean return period $RP = 2475a$; mean values of the logic tree (top left), median (bottom left) with the related 84th percentile (bottom right).

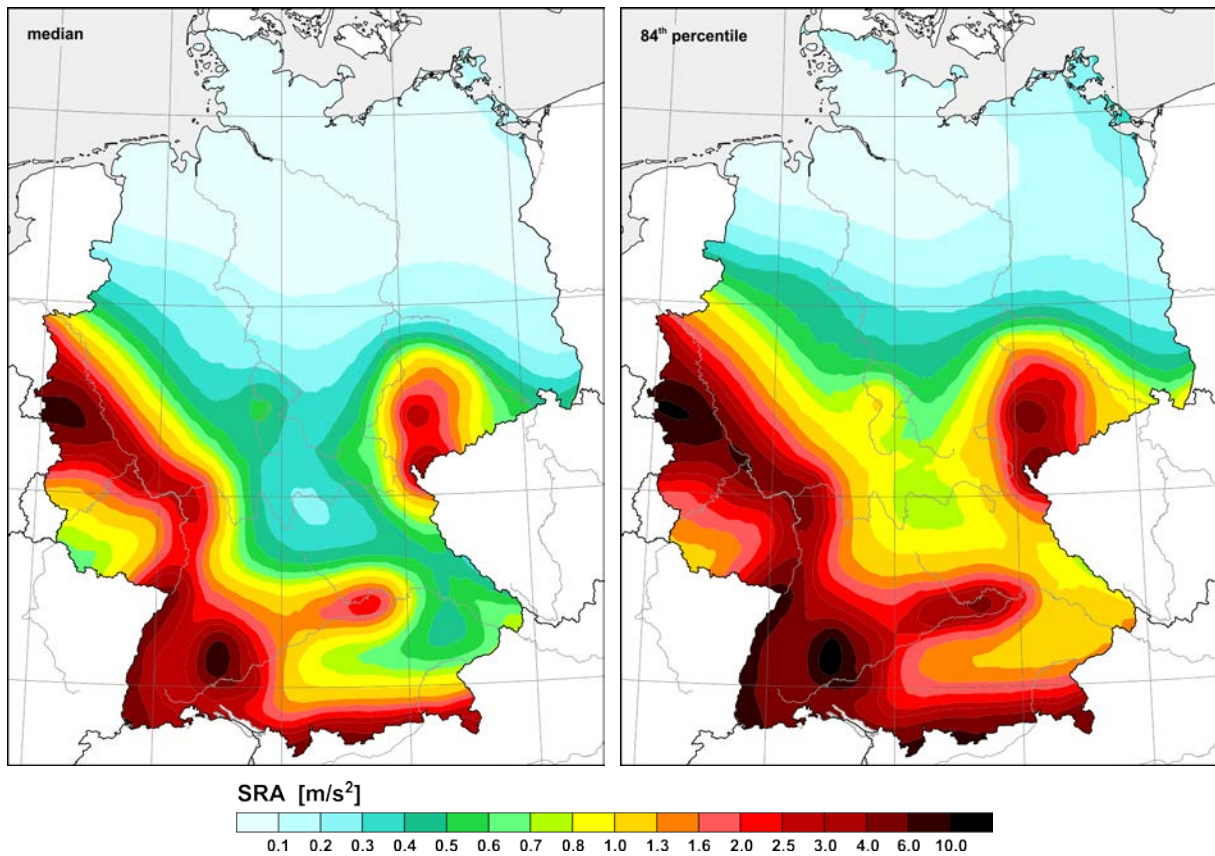


Figure 8-4. Seismic hazard maps for the response acceleration amplitudes at 0.15 s spectral period for the mean return period $RP = 475a$; mean values (top left), median (bottom left) with the related 84th percentile (bottom right).

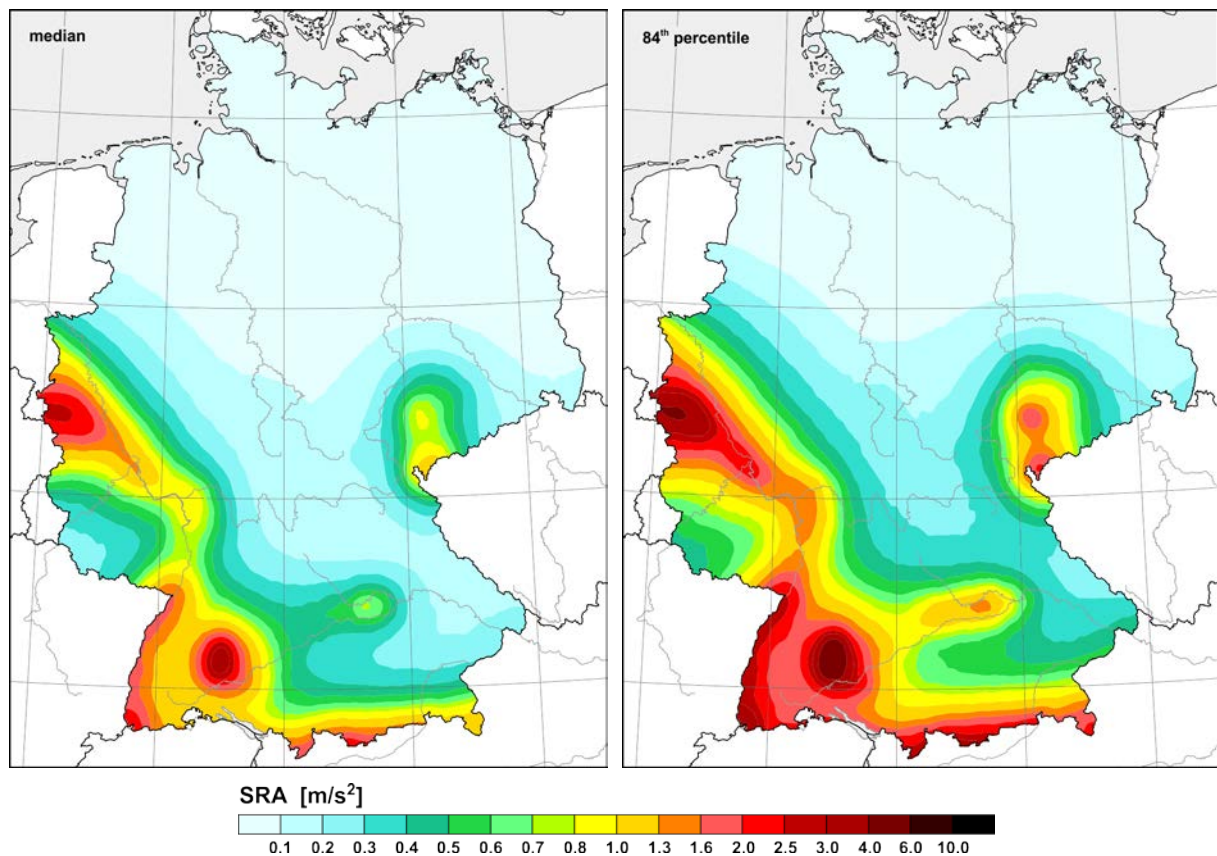


Figure 8-5. Seismic hazard maps for the response acceleration amplitudes at 0.15 s spectral period for the mean return period $RP = 975a$; mean values (top left), median (bottom left) with the related 84th percentile (bottom right).

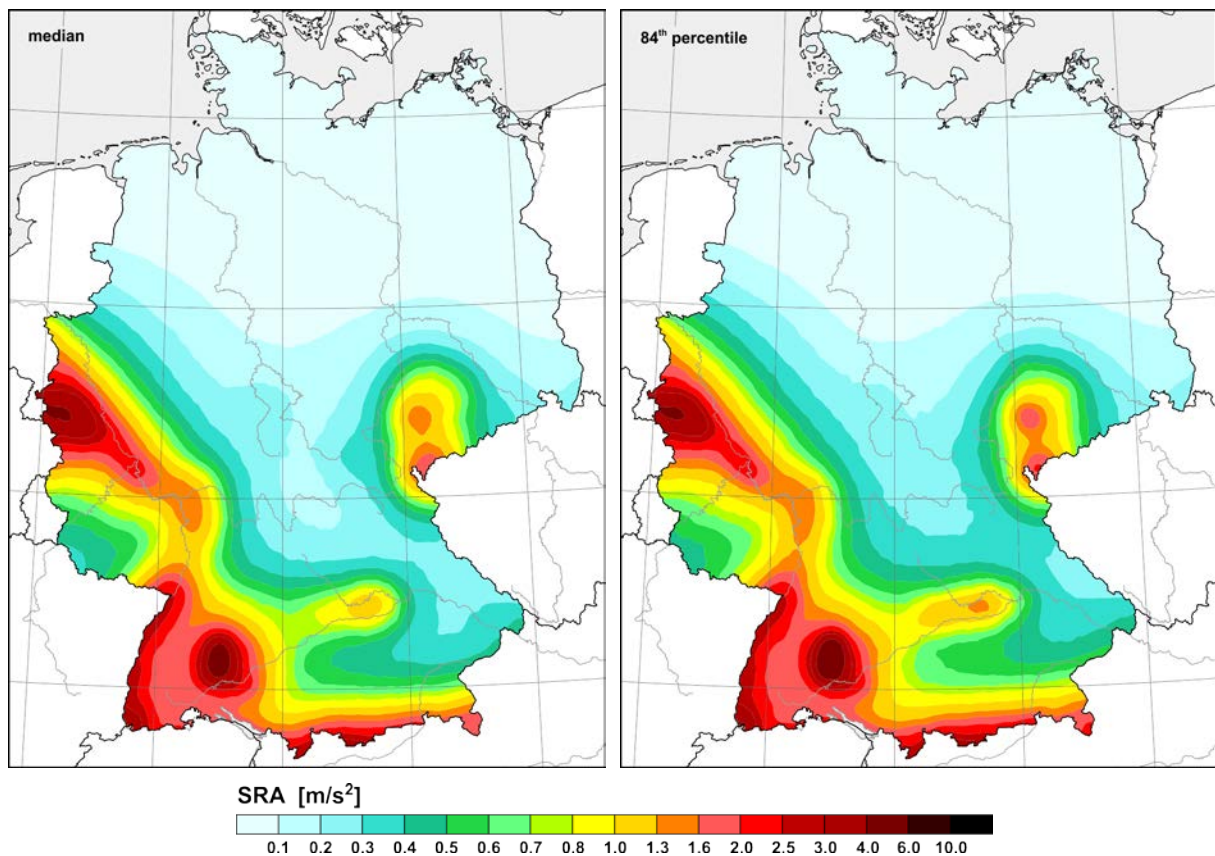


Figure 8-6. Seismic hazard maps for the response acceleration amplitudes at 0.15 s spectral period for the mean return period $RP = 2475a$; mean values (top left), median (bottom left) with the related 84th percentile (bottom right).

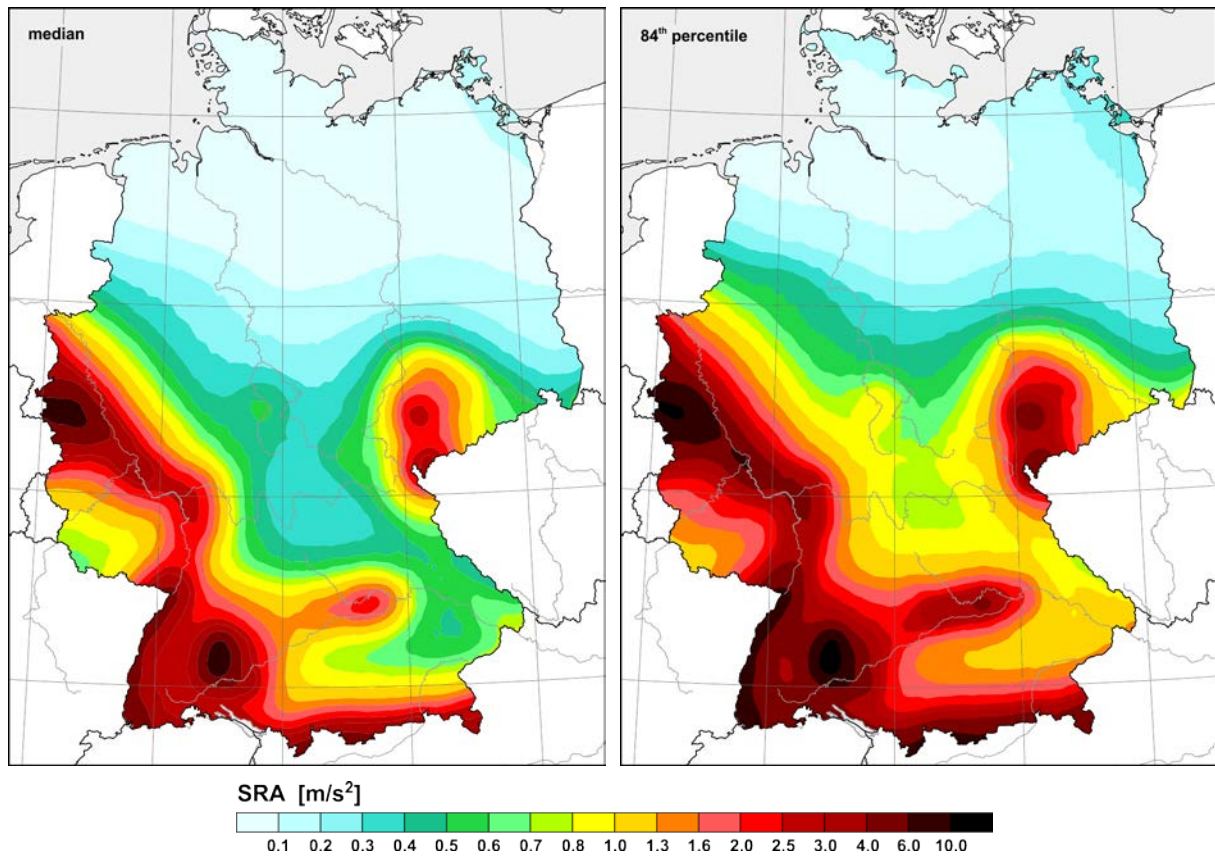


Figure 8-7. Seismic hazard maps for the response acceleration amplitudes at 0.20 s spectral period for the mean return period $RP = 475a$; mean values (top left), median (bottom left) with the related 84th percentile (bottom right).

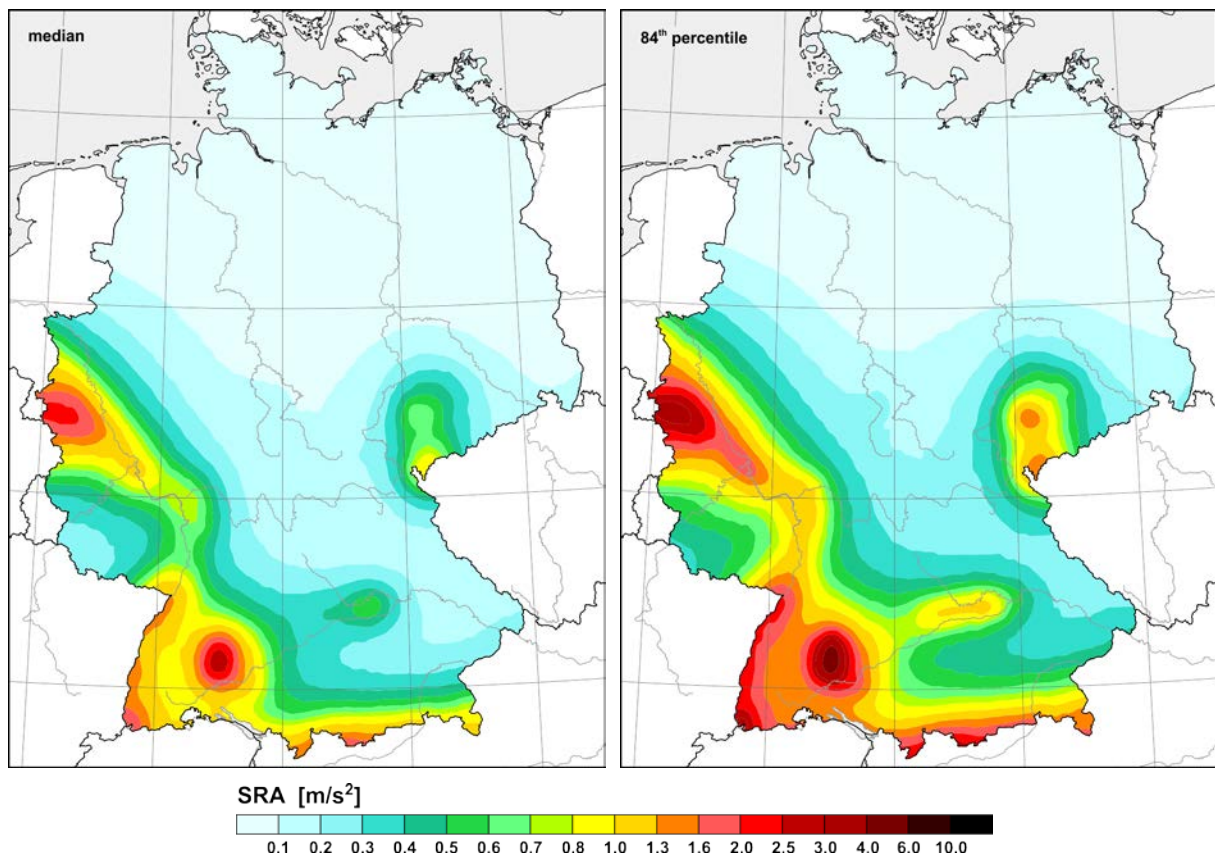


Figure 8-8. Seismic hazard maps for the response acceleration amplitudes at 0.20 s spectral period for the mean return period $RP = 975a$; mean values (top left), median (bottom left) with the related 84th percentile (bottom right).

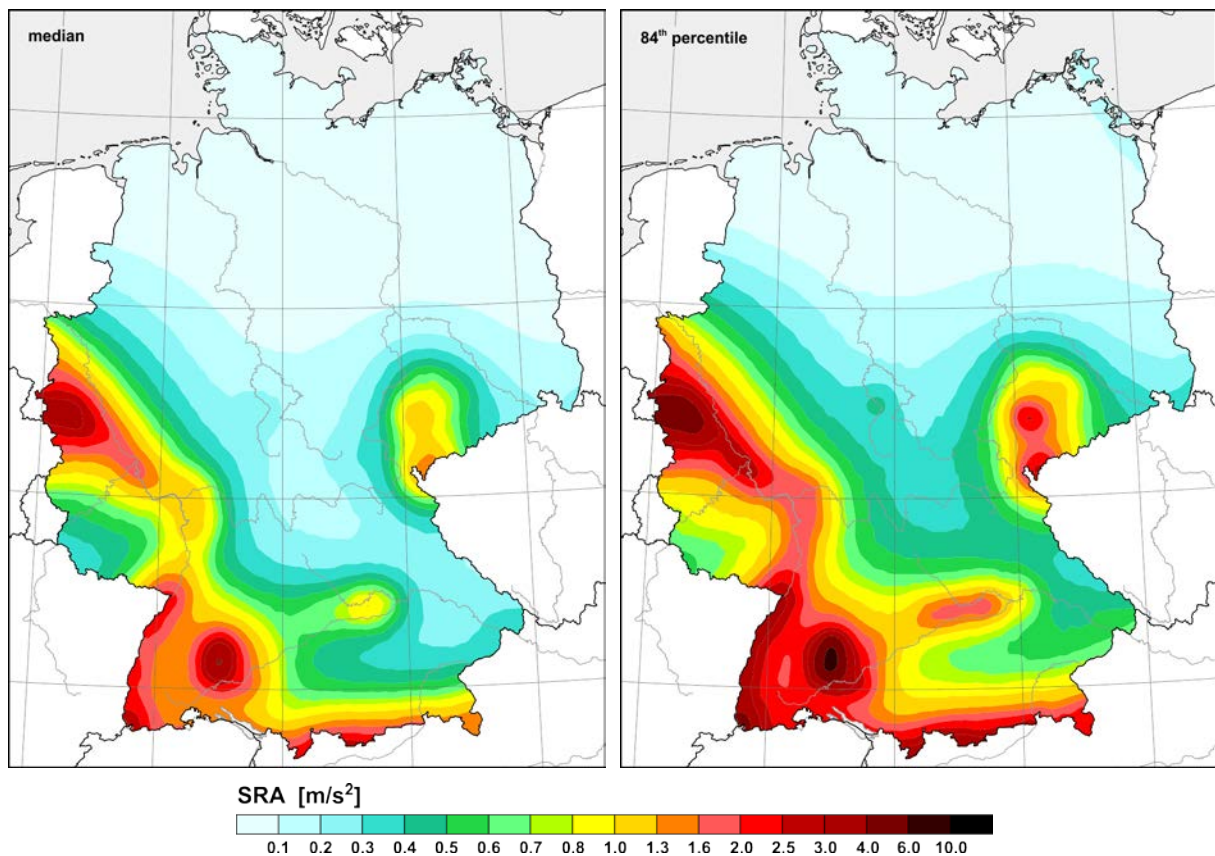


Figure 8-9. Seismic hazard maps for the response acceleration amplitudes at 0.20 s spectral period for the mean return period $RP = 2475a$; mean values (top left), median (bottom left) with the related 84th percentile (bottom right).

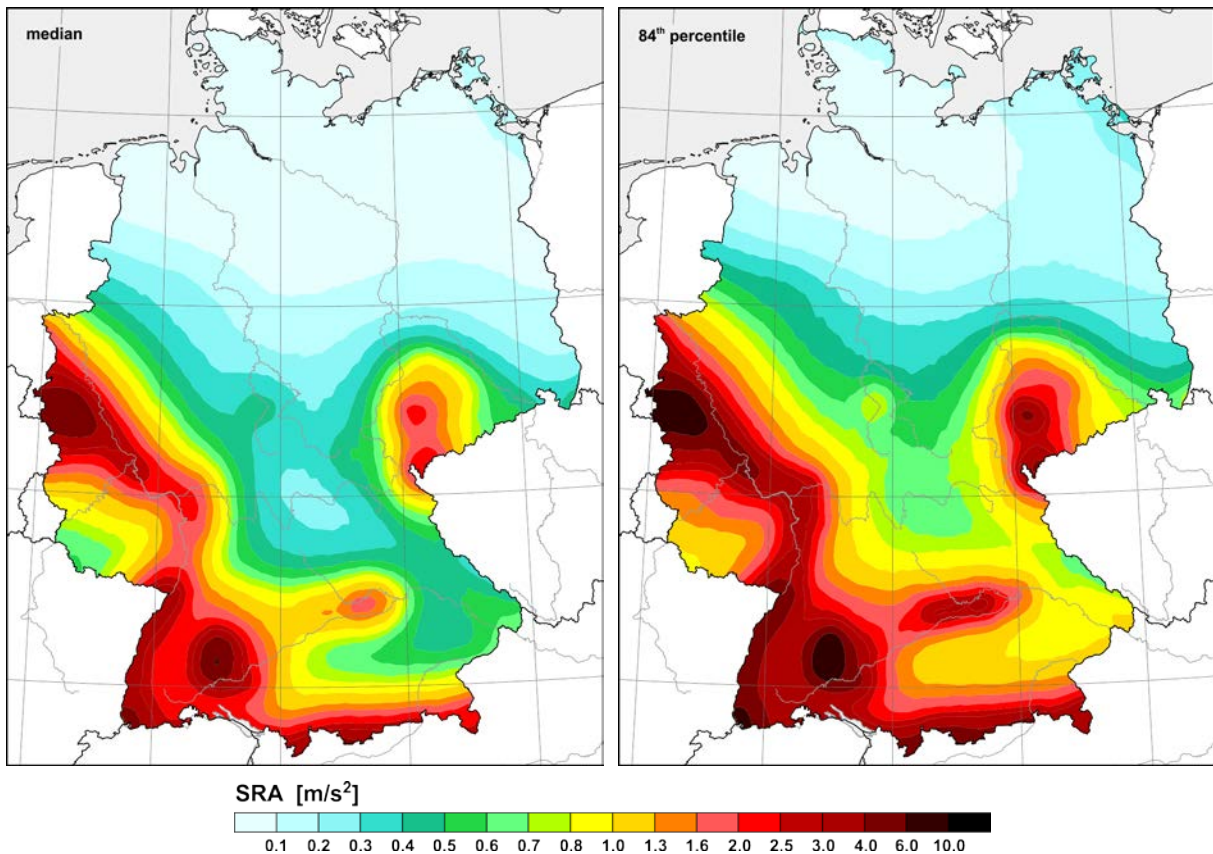


Figure 8-10. Seismic hazard maps for peak ground acceleration (PGA) for the mean return period $RP = 475a$; mean values (top left), median (bottom left) with the related 84th percentile (bottom right).

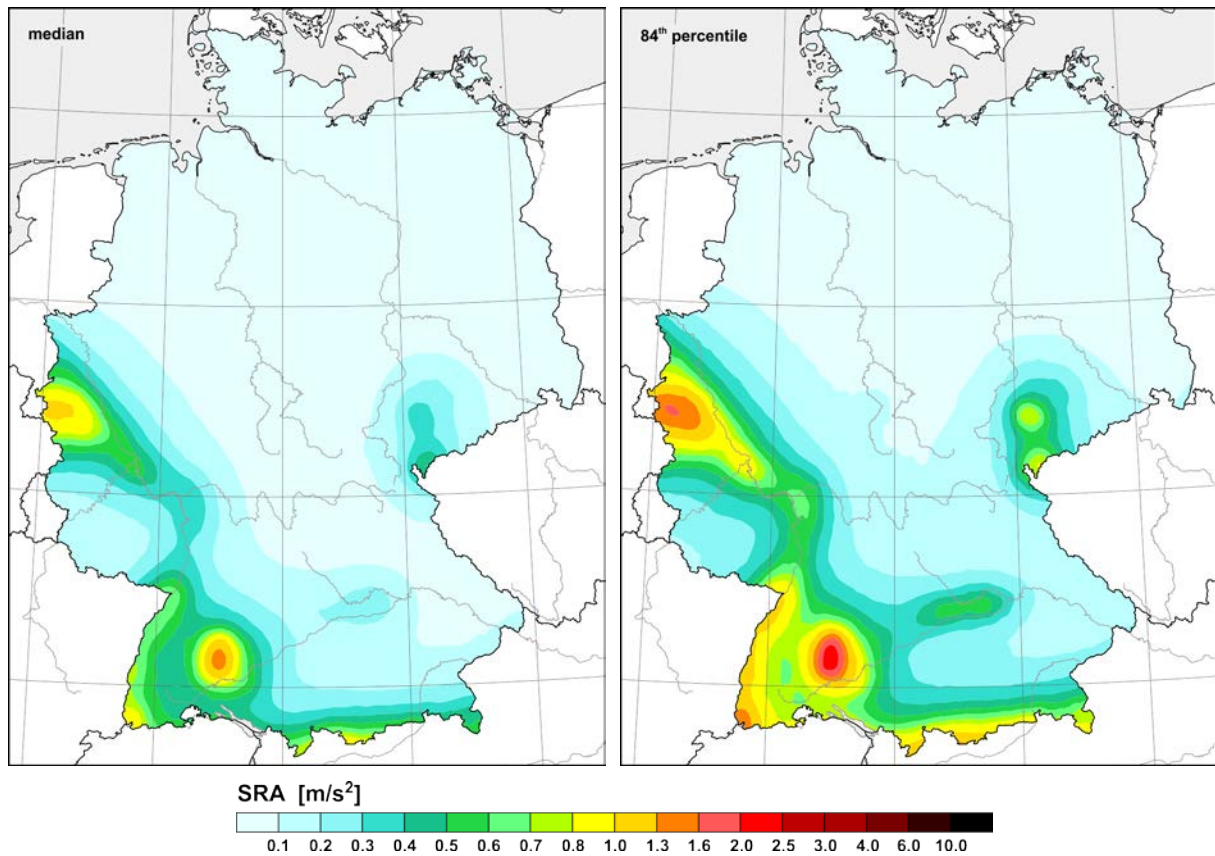


Figure 8-11. Seismic hazard maps for peak ground acceleration (PGA) for the mean return period $RP = 975a$; mean values (top left), median (bottom left) with the related 84th percentile (bottom right).

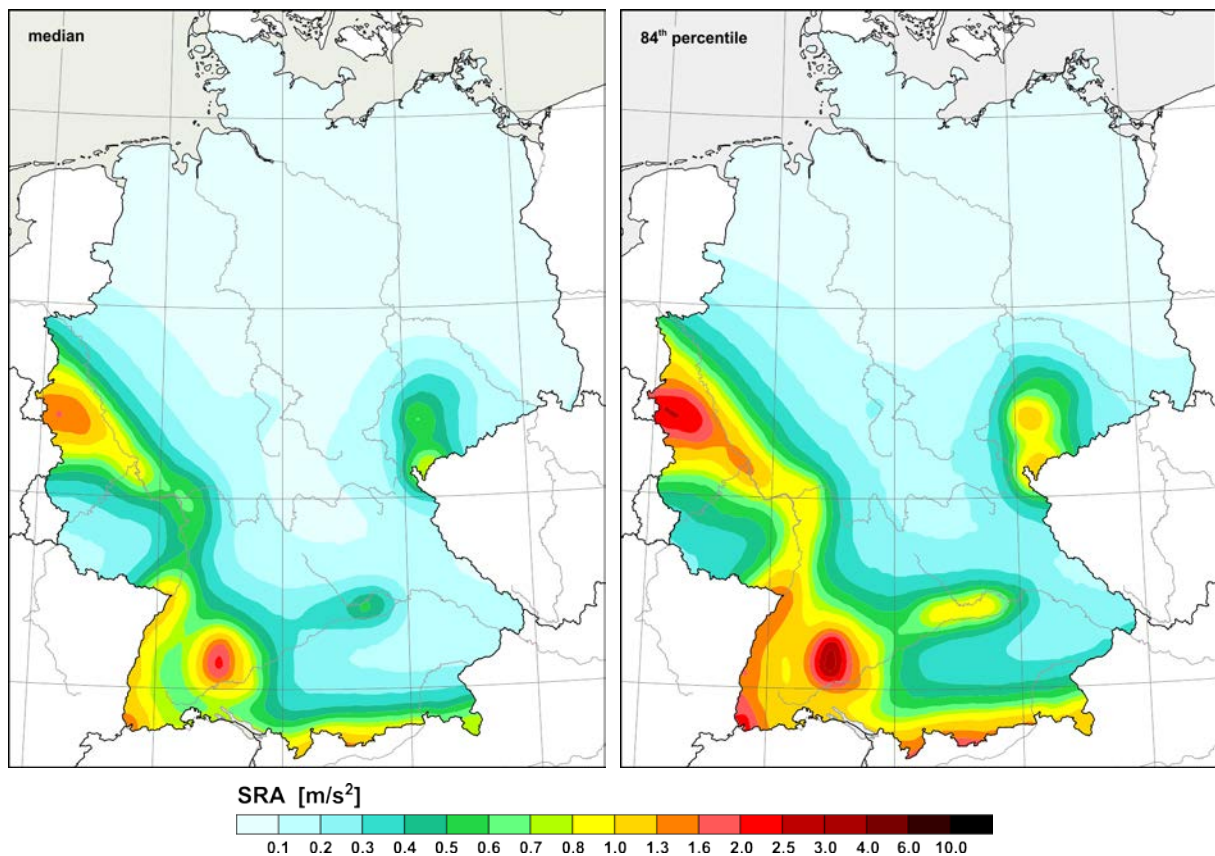


Figure 8-12. Seismic hazard maps for peak ground acceleration (PGA) for the mean return period $RP = 2475$ a; mean values (top left), median (bottom left) with the related 84th percentile (bottom right).

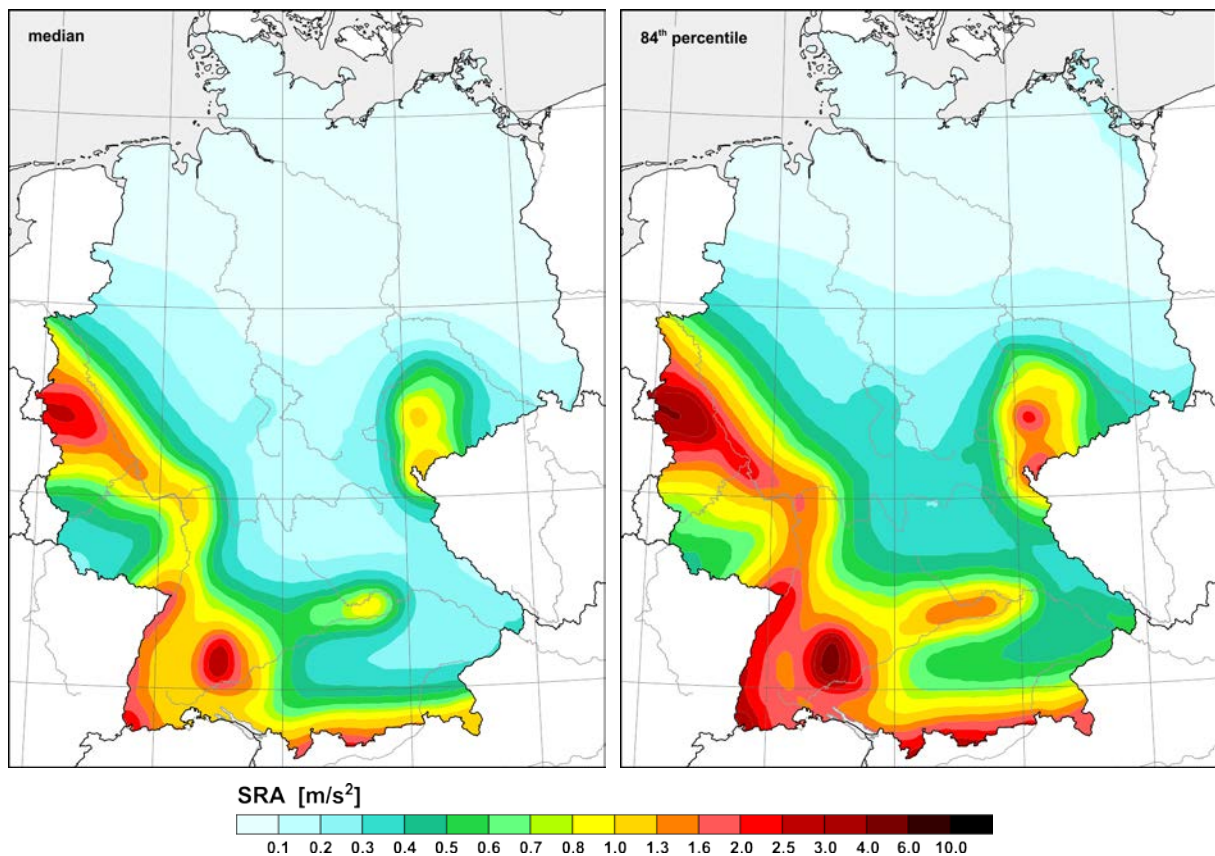


Figure 8-13. Seismic hazard maps for the mean values of the response acceleration amplitudes at the spectral periods of 0.1s, 0.15s and 0.2s (mean SRA) for the mean return period $RP = 475a$; mean values (top left), median (bottom left) with the related 84th percentile (bottom right).

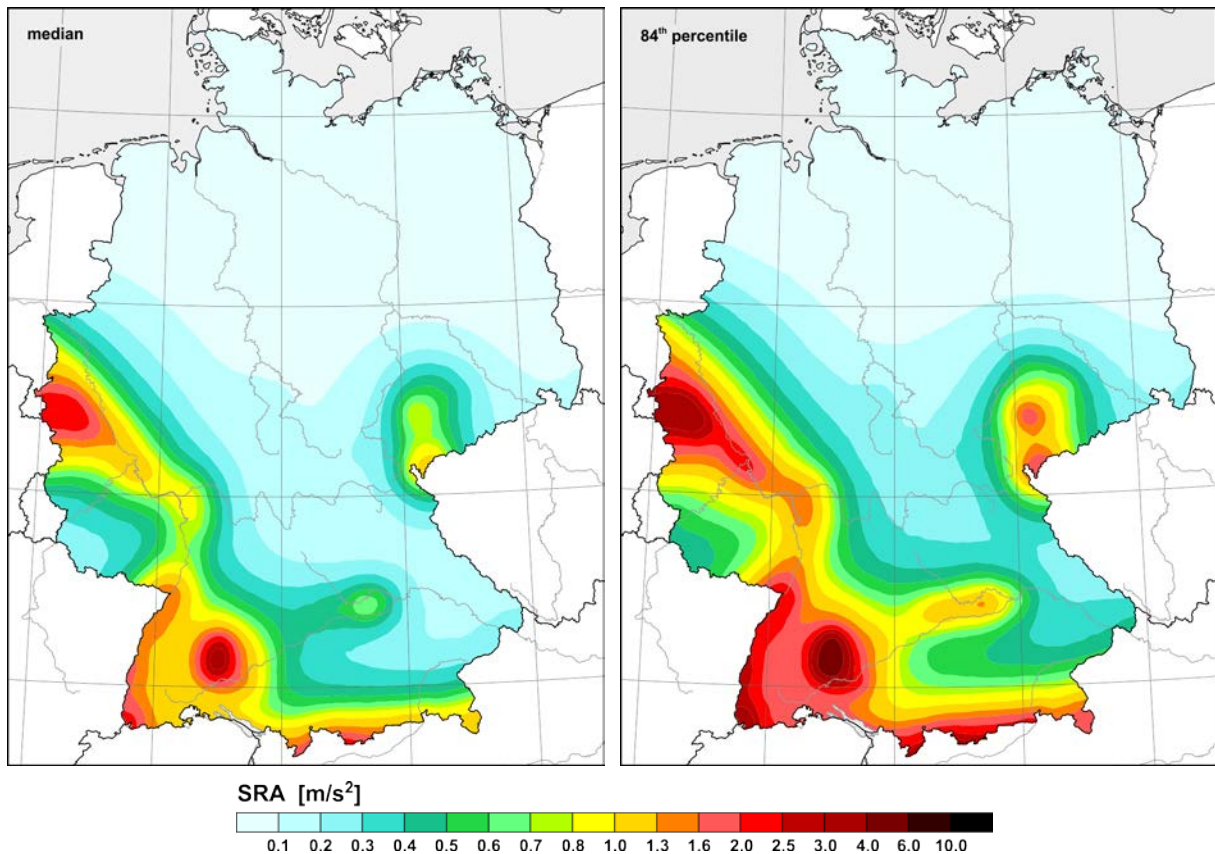


Figure 8-14. Seismic hazard maps for the mean values of the response acceleration amplitudes at the spectral periods of 0.1s, 0.15s and 0.2s (mean SRA) for the mean return period $RP = 975a$; mean values (top left), median (bottom left) with the related 84th percentile (bottom right).

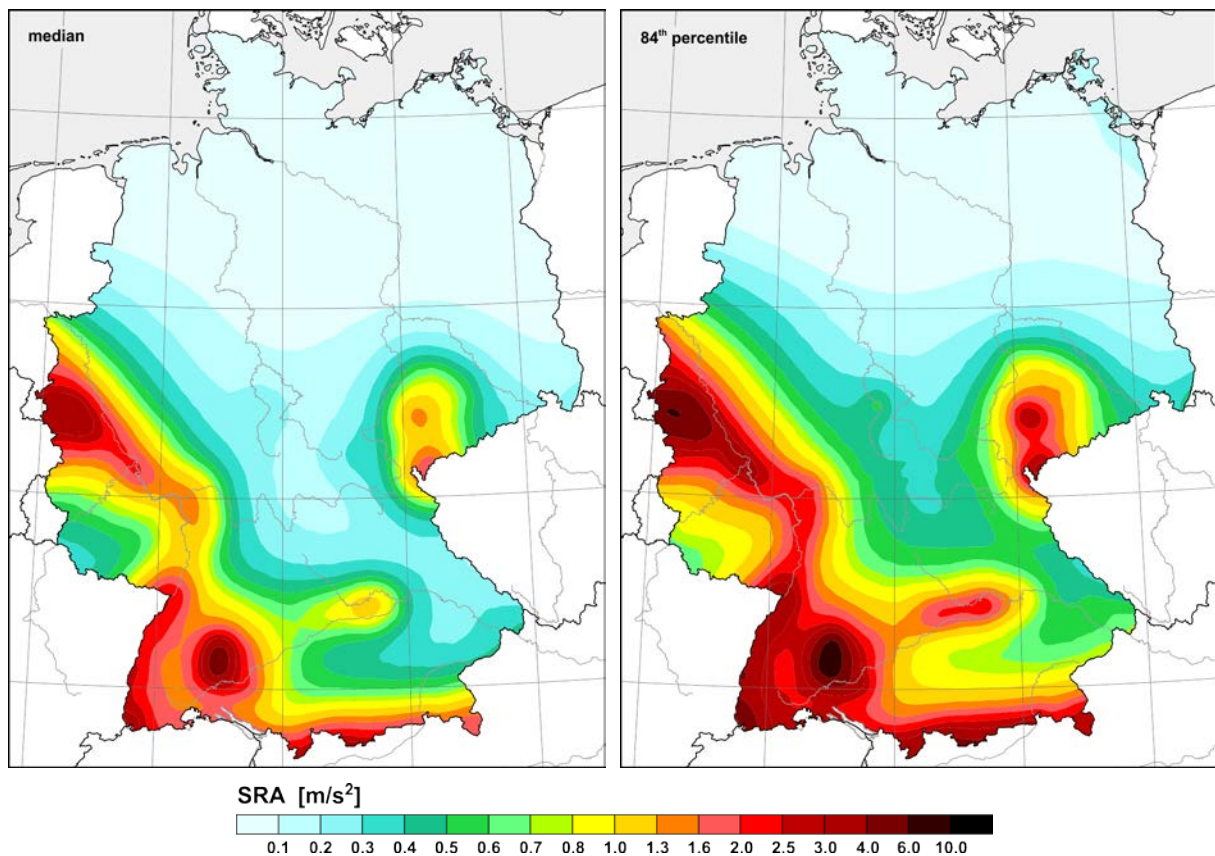


Figure 8-15. Seismic hazard maps for the mean values of the response acceleration amplitudes at the spectral periods of 0.1s, 0.15s and 0.2s (mean SRA) for the mean return period $RP = 2475a$; mean values (top left), median (bottom left) with the related 84th percentile (bottom right).

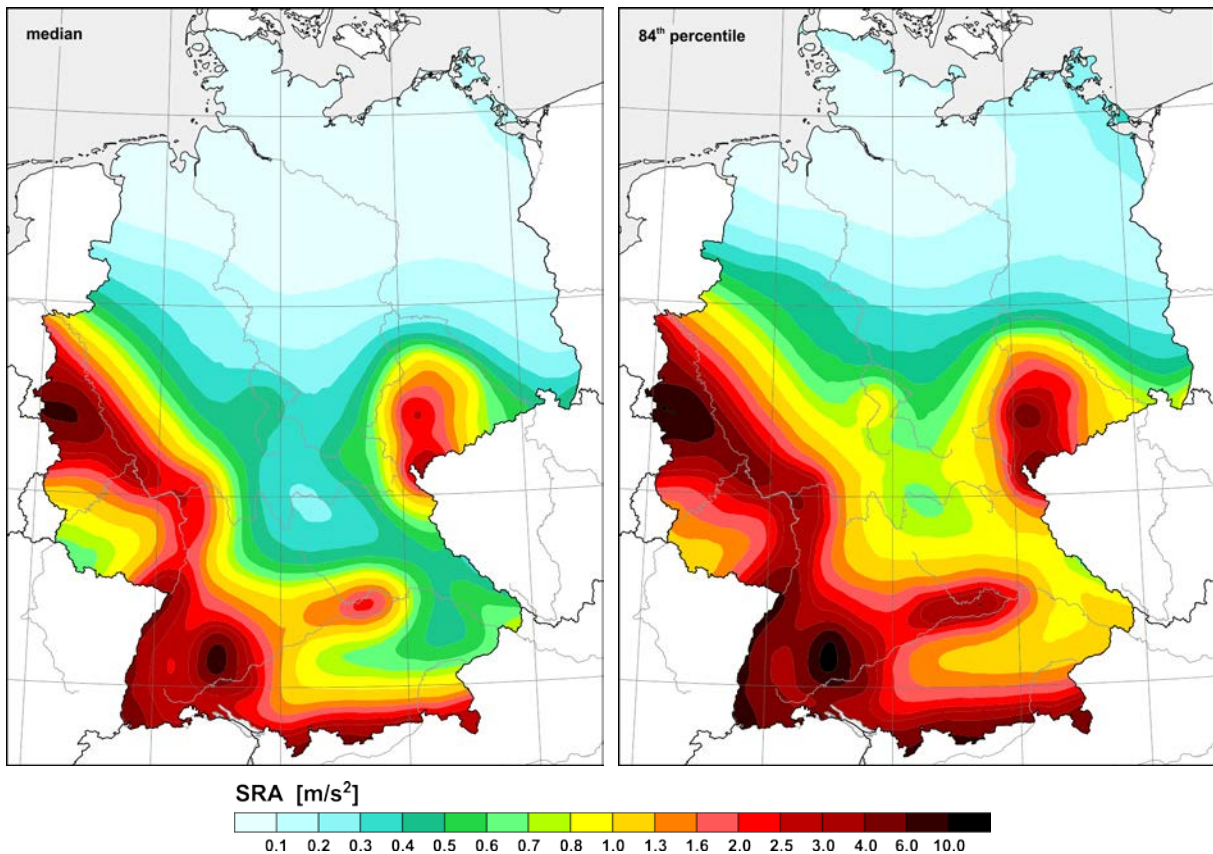


Figure 8-16. Seismic hazard maps for the maximal values of the response acceleration amplitudes at the spectral periods of 0.1s, 0.15s and 0.2s (max SRA) for the mean return period $RP = 475a$; mean values (top left), median (bottom left) with the related 84th percentile (bottom right).

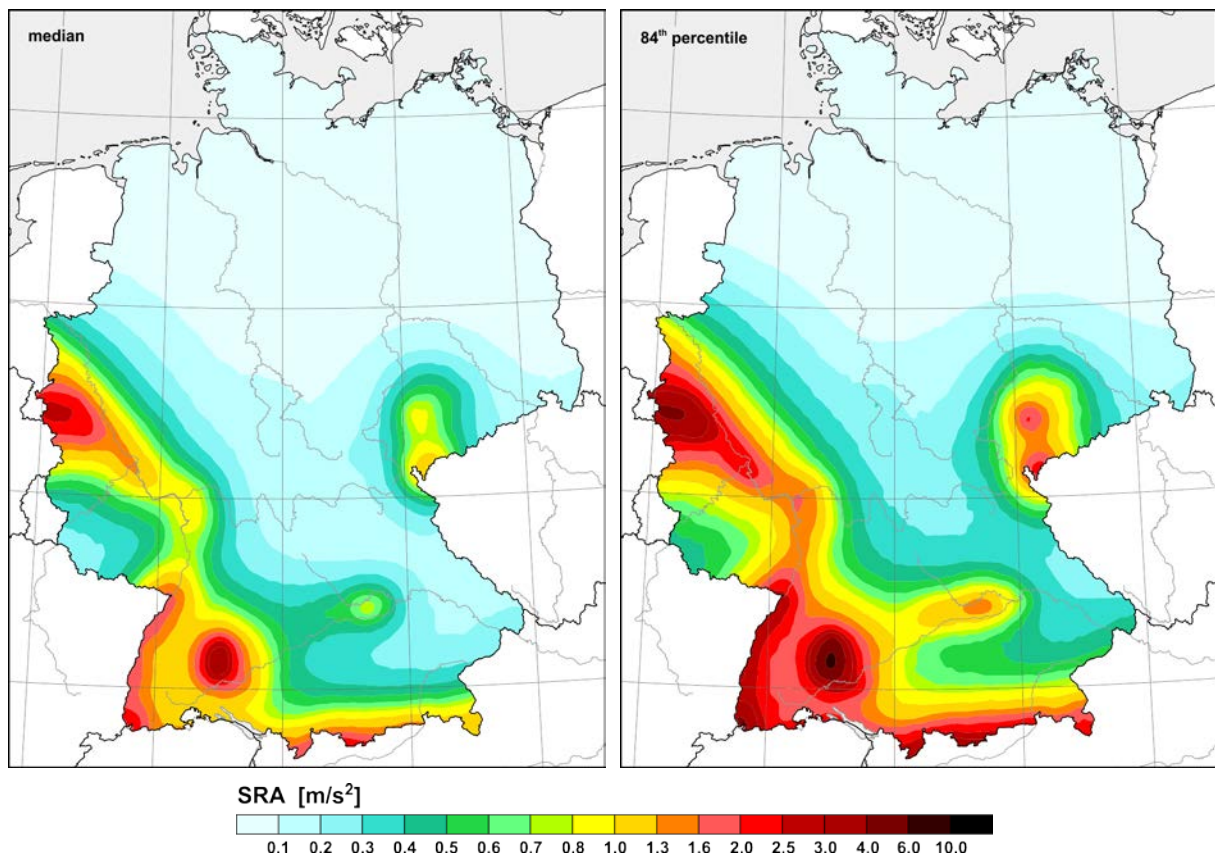


Figure 8-17. Seismic hazard maps for the maximal values of the response acceleration amplitudes at the spectral periods of 0.1s, 0.15s and 0.2s (max SRA) for the mean return period $RP = 975a$; mean values (top left), median (bottom left) with the related 84th percentile (bottom right).

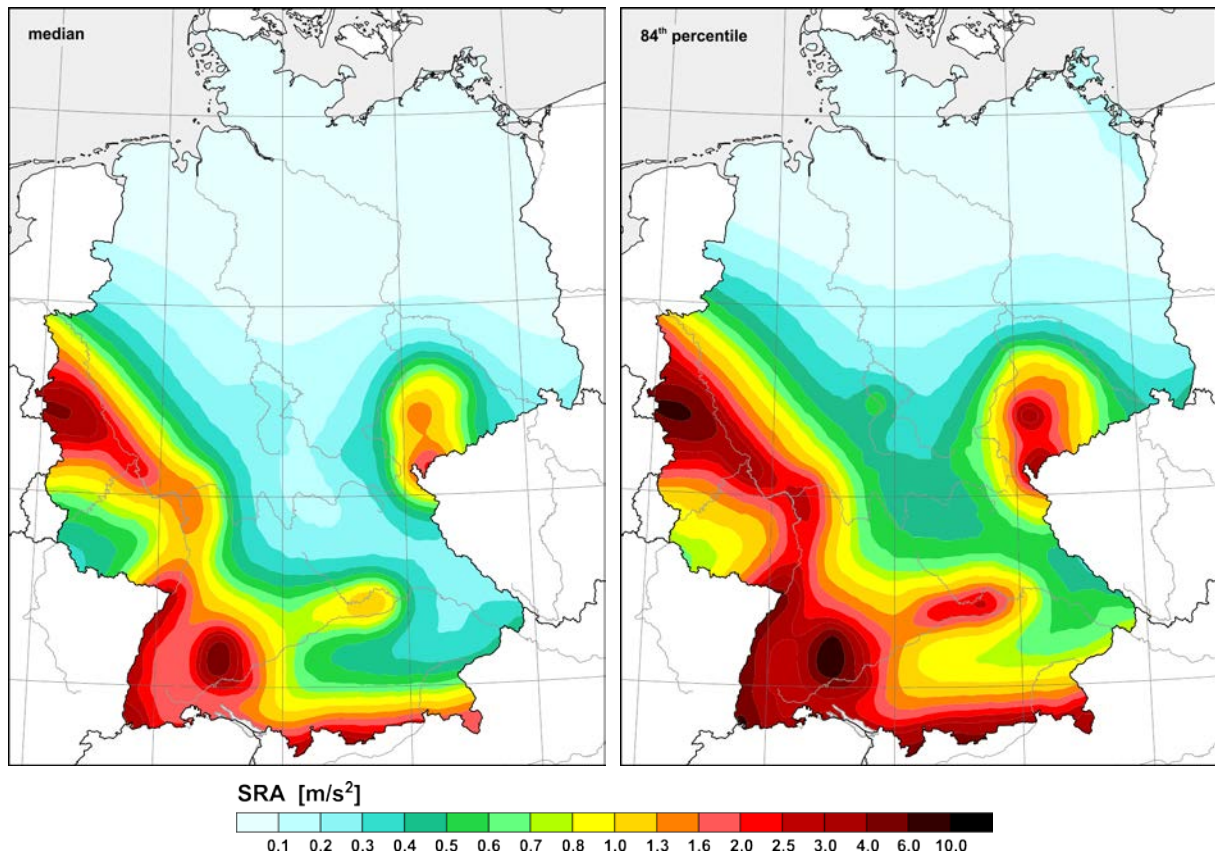
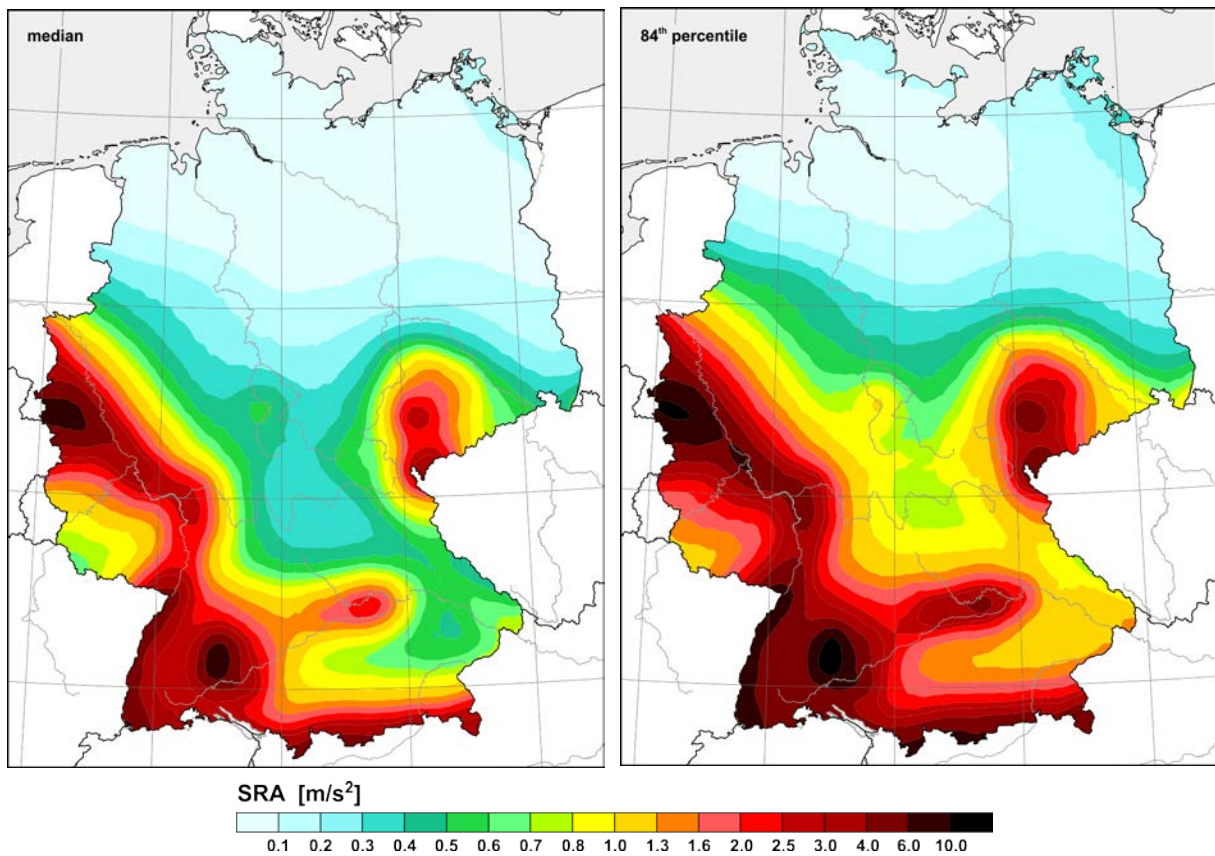


Figure 8-18. Seismic hazard maps for the maximal values of the response acceleration amplitudes at the spectral periods of 0.1s, 0.15s and 0.2s (max SRA) for the mean return period $RP = 2475a$; mean values (top left), median (bottom left) with the related 84th percentile (bottom right).



8.2. Deaggregations

Deaggregations provide an interesting insight into the composition of the seismic hazard at a site for respective hazard levels and ground motion parameters (cf. chapter 9.1 of Grünthal *et al.* 2018); i.e. which rates of magnitude-distance bins govern the seismic hazard for the given parameters. As an example, we here provide the deaggregations for the centres of Aachen, Cologne, Gera, Karlsruhe, Stuttgart and Tuttlingen (Fig. 8-19).

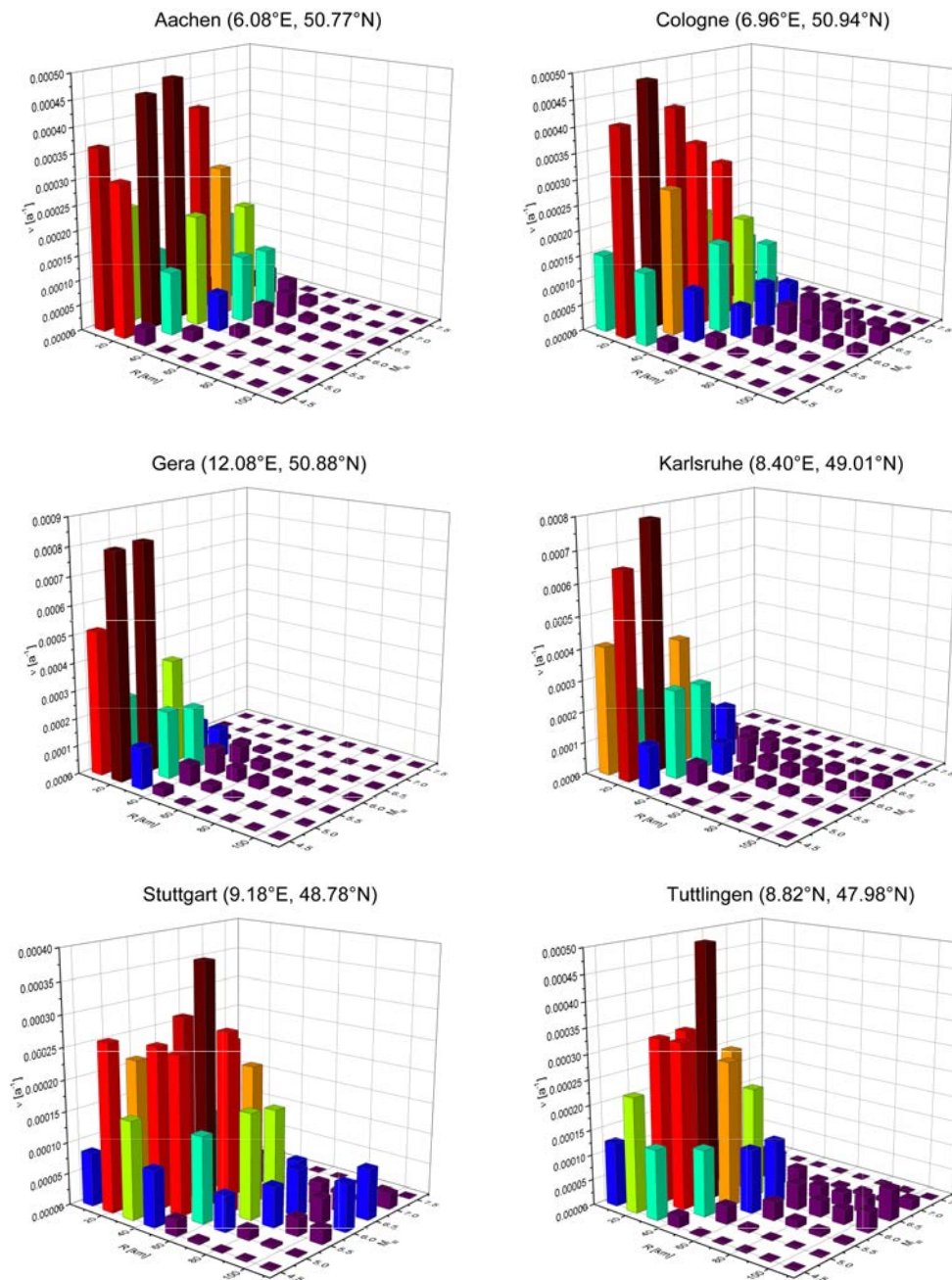


Figure 8-19. Deaggregations in form of the rates of magnitude-distance bins for the centres of Aachen, Gera, Cologne, Karlsruhe, Stuttgart and Tuttlingen for PGA and $RP = 475a$.

8.3. The parameters of the EC 8 elastic design spectral shapes

The central result of the PSHA concerning the project presented here are UHS for any geographic point within Germany (cf. chapter 9.1 in *Grünthal et al. 2018*). These UHS are accessible under the specific project related web portal http://www.gfz-potsdam.de/EqHaz_D2016, wherefrom the UHS can also be downloaded. The 19 calculated spectral periods in the range of 0.02-3.0 s as backbone for constructing the UHS were also used for the fit according to the shape of the EC 8 elastic design spectra.

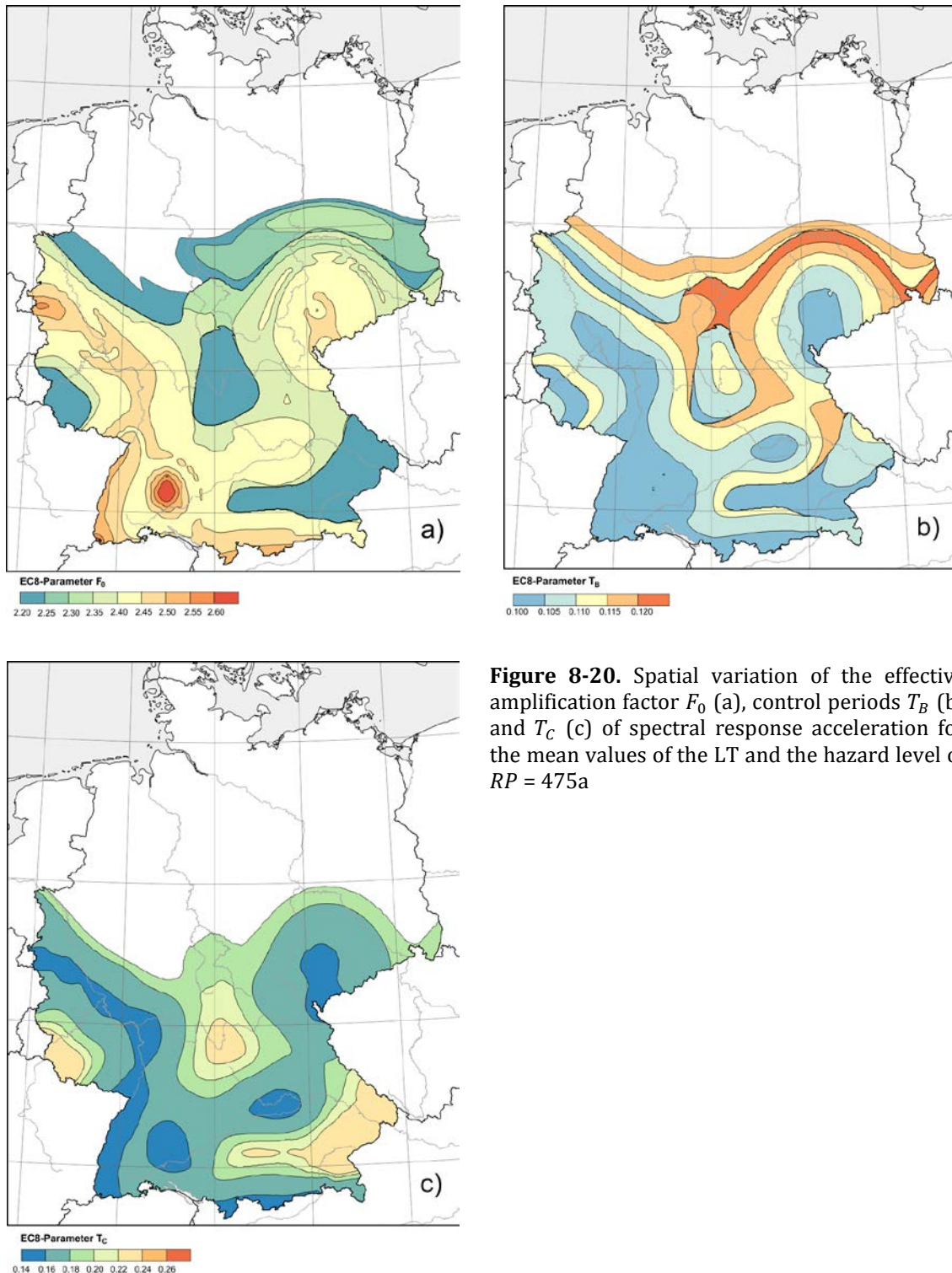


Figure 8-20. Spatial variation of the effective amplification factor F_0 (a), control periods T_B (b) and T_C (c) of spectral response acceleration for the mean values of the LT and the hazard level of $RP = 475a$

These EC 8 spectra are characterized by the following parameters: the effective amplification factor F_0 ; i.e. the ratio between the plateau of the design spectra and PGA, and the control periods T_B , T_C and T_D . The parameters F_0 , T_B and T_C show a significant spatial pattern within the target area, which is depicted in Figs. 8-20a-c for the mean values of the LT and the hazard level of $RP = 475a$. T_D , the transition period from constant velocity to constant displacement within the spectrum, can only be accessed with large uncertainties mainly due to missing calculated spectral data for larger periods since respective parameters for additional periods are not provided with the GMPE adopted in this analysis.

9. Comparison with results of the new Swiss earthquake hazard model

A comparison of the new earthquake hazard model CH2015 for Switzerland (*Wiemer et al. 2016*) with the new German model D2016 has already been made in *Grünthal et al. (2018)* in terms of median PGA maps for $RP = 475a$ and for $v_{S30} = 800\text{m/s}$ north and south of the common state border. Both maps coincide very well.

Further comparisons are presented in the following concerning UHS and hazard curves at points within Germany near to the common border. We selected two sites, one immediately north of Basel (46.6°N, 7.6°E) and another one east of Schaffhausen (47.7°N, 8.7°E).

The first comparison is made for seismic hazard curves in form of exceedance probabilities within 50 years for the spectral response acceleration of $T = 0.2\text{ s}$ (Fig. 9-1) in terms of g ; i.e. the gravitational acceleration, and for $v_{S30} = 1105\text{ m/s}$, which is used as the basis for the results according to the new Swiss project (*Wiemer et al. 2016*) provided via the link as part of the given reference. The curves are shown for median and mean values. Their coincidence is striking. None of them lies above the other, but they cross each other two or three times within the probability range up to 10^{-4} .

The comparison of the UHS according to both projects are shown in Fig. 9-2 in form of the response spectra for the median, the 84th and the 16th percentile for RP = 475 a. The UHS are also provided in terms of g and for $v_{S30} = 1105$ m/s. For both locations, which

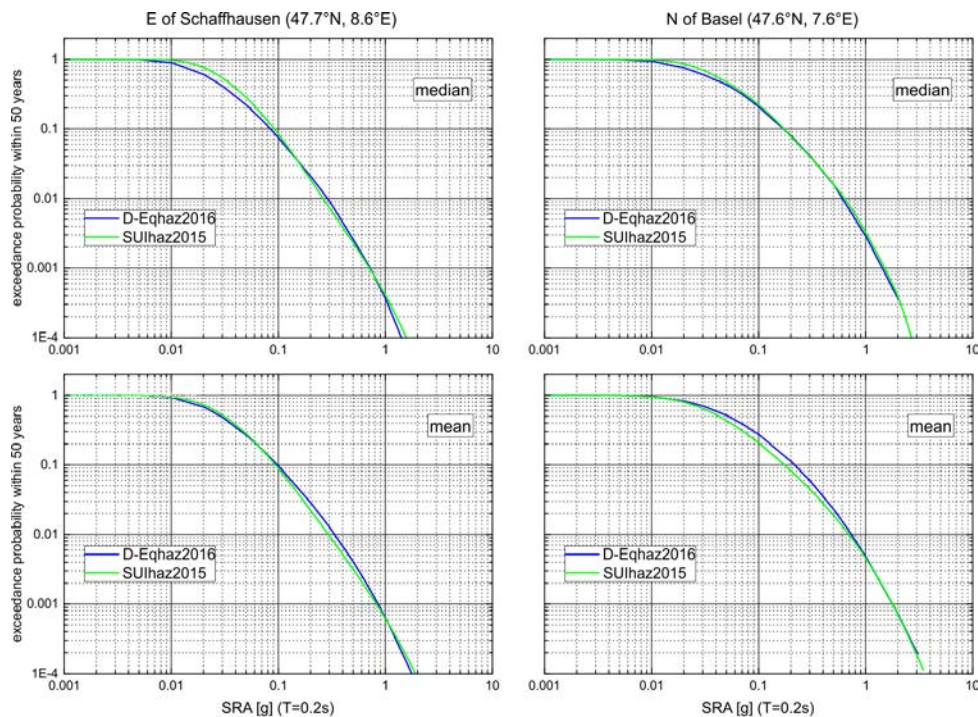


Figure 9-1. Seismic hazard curves for two sites immediately north of Basel (left) and east of Schaffhausen (right) as exceedance probabilities within 50 years for the spectral response acceleration of $T = 0.2$ s in terms of g ; i.e. the gravitational acceleration, for $v_{S30} = 1105$ m/s according to the new Swiss project CH2015 (Wiemer *et al.* 2016; <http://www.efehr.org/en/hazard-data-access/hazard-curves/c>) compared with the curves after the D2016 model (Grünthal *et al.* 2018). The curves are shown for median and mean values.

are the same as shown and discussed above in terms of the hazard curves, the peaks of the median curves are slightly higher according to the D2016 model and significantly higher for the 84th percentile. The shape of the 16th percentile curve is in one of the two cases practically the same. The maximum spectral amplitudes are reached at almost the same periods, but with slightly lower values for the D2016 model. However, the UHS according to the D2016 model are narrower than those after the Swiss model CH2015, which results in two crossing points of the spectra in case that the one model shows larger peak values. The intersecting points of the median spectral curves are, in both cases, at or near to 0.06 s and at or near to 0.2 s; i.e. just the spectral period used for the graphs of Fig. 9-1. The third spectral period, where the values are almost identical, is for both cases the spectral point which defines the median PGA.

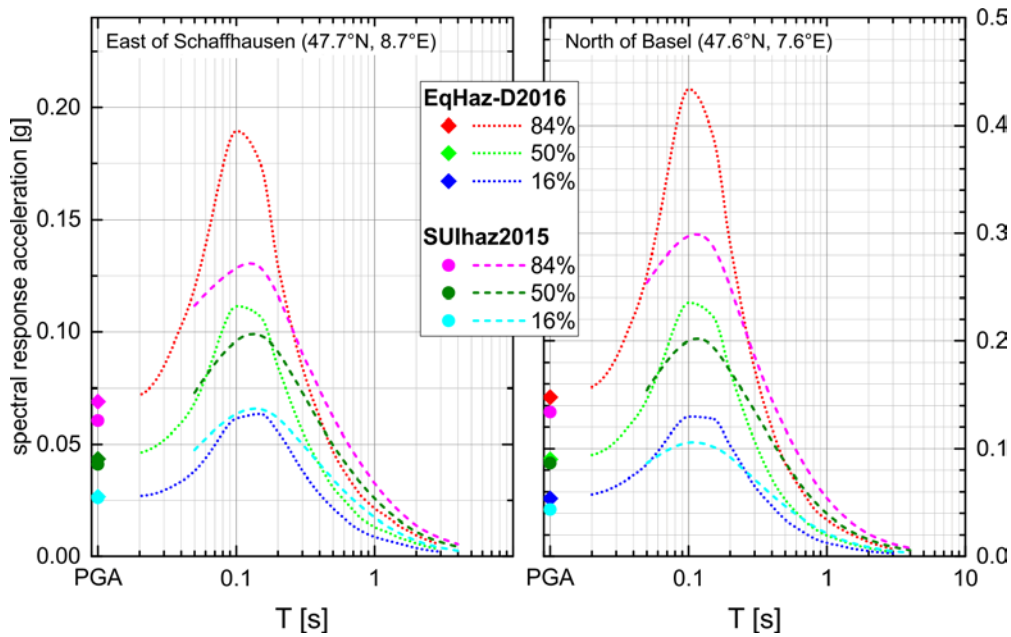


Figure 9-2. Comparison of UHS according to the new Swiss project SU1haz2015 (Wiemer *et al.* 2016) with those after the D2016 model (Grünthal *et al.* 2018). The response spectra are shown for the median, the 84th and the 16th percentile, for RP = 475 a, in terms of g and for $v_{S30} = 1105$ m/s.

10. Available Datasets

The main input data of the earthquake model for the probabilistic seismic hazard assessment of Germany, version 2016, are: (1) the geometry of five SSZ models A, B, C, D, E and of the CSS model; (2) the assignment of individual sources to the different superzone models (M_{max} , b -value, depth, tectonic regime and smoothing kernel) and (3) the seismicity rates of all sources given as M_{max} depending Gutenberg-Richter parameters a and b with their covariances C_{aa} , C_{ab} and C_{bb} (Grünthal *et al.* 2018, Chapter 5.2). These data are published via GFZ Data Services by Grünthal *et al.* (2018a).

The geometry data of the five SSZ models are provided by ESRI shapefiles (Model_A.shp, Model_B.shp, Model_C.shp, Model_D.shp, Model_E.shp). Each individual area source of a SSZ model is given by a polygon with geographic coordinates (reference system WGS84) and several describing attributes (Table 9-1). The CSS model of the Lower Rhine graben is described by the shapefile CSS_Lower_Rhine_Top.shp in form of polylines with geographic coordinates (reference system WGS84), each representing the trace of a fault plane upper edge. The

poly-lines are taken from the European Database of Seismogenic Faults (EDSF) compiled in the framework of the Project SHARE, WP3 Task 3.2 (Basili *et al.*, 2013). The additional CSS attributes of the shape file are explained in Tab. 9-2.

Table 9-1. Shapefile attributes of SSZ models. Attributes marked by (*) are only related to model A.

Attribute	Description	Typ
Name	source name built from model name and source number within the model (e.g. C05)	string
SourceNo	source number within a SSZ model (e.g. 5)	integer
DepthGr	depth group number according to Fig. 6-1 and Table 6-1	integer
TectGr	tectonic group number according to Fig. 7-1 and Table 7-1	integer
bGr*	common b-value group number according to Fig. 5-1	integer
MmaxGr*	M_{max} group number according to Fig. 4-2 and Table 4-1	integer
KernelGr*	kernel group number according to Fig. 3-7 and Tab. 3-2	integer
TerraneGr*	tectonic terrane group number according to Fig. 4-1	integer

Table 9-2. Shapefile attributes of the CSS models. Related values are given in Tab. 3-1.

Attribute	Description	Typ
Name	CSS name according to EDSF	string
TotalL	CSS total length [km]	double
TotalW	CSS total depth [km]	double
TotalA	CSS total area [km ²]	double
MaxDepth	maximal depth of CSS	double
FaultType	fault type	string
MaxMw	M_{max} of CSS	double
SigMw	standard deviation of M_{max}	double

The parameters a and b of the frequency-magnitude relation (Tab. 5-1a-e, Tab. 5-2) are provided by EXCEL files (Model_A_Param.xlsx, Model_B_Param.xlsx, Model_C_Param.xlsx, Model_D_Param.xlsx, Model_E_Param.xlsx, CSS_Param.xlsx). These files contain the two versions of the minimum magnitude for fit in two different table sheets (high and low).

11. References

- Basilic, R., Kastelic, V., Demircioglu, M. B., Garcia Moreno, D., Nemser, E. S., Petricca, P., Sboras, S. P., Besana-Ostman, G. M., Cabral, J., Camelbeeck, T., Caputo, R., Danciu, L., Domac, H., Fonseca, J., García-Mayordomo, J., Giardini, D., Glavatovic, B., Gulen, L., Ince, Y., Pavlides, S., Sesetyan, K., Tarabusi, G., Tiberti, M. M., Utkucu, M., Valensise, G., Vanneste, K., Vilanova, S., Wössner, J. (2013): The European Database of Seismogenic Faults (EDSF) compiled in the framework of the Project SHARE, (Share - The European Database of Seismogenic Faults). DOI: <http://doi.org/10.6092/INGV.IT-SHARE-EDSF>
- DIN EN 1998-1:2010-12 (2010) Eurocode 8: Auslegung von Bauwerken gegen Erdbeben – Teil 1: Grundlagen, Erdbebeneinwirkungen und Regeln für Hochbauten. DIN Deutsches Institut für Normung e.V. Berlin
- DIN EN 1998-1/NA:2011-01 (2011) National Annex - Nationally determined parameters - Eurocode 8: Design of structures for earthquake resistance - Part 1: General rules, Seismic actions and rules for buildings. DIN Deutsches Institut für Normung e.V. Berlin
- Grünthal G (2014) Induced seismicity related to geothermal projects versus natural tectonic earthquakes and other types of induced seismic events in Central Europe. *Geothermics* 52: 22-35; <http://doi.org/10.1016/j.geothermics.2013.09.009>
- Grünthal G, Mayer-Rosa D, Lenhardt W (1998) Abschätzung der Erdbebengefährdung für die D-A-CH-Staaten - Deutschland, Österreich, Schweiz. *Bautechnik* 75(10): 753-767
- Grünthal G, Stromeyer D, Bosse C, Cotton F, Bindi D (2018) The probabilistic seismic hazard assessment of Germany: version 2016, considering the range of epistemic uncertainties and aleatory variability. *Bull Earthquake Engineering* :1-57, <http://doi.org/10.1007/s10518-018-0315-y>
- Grünthal,G, Stromeyer D, Bosse C (2018a): The Source Model of the Probabilistic Seismic Hazard Assessment (PSHA) of Germany - Version 2016. V. 1.0. GFZ Data Services, <http://doi.org/10.5880/GFZ.2.6.2018.001>
- Hakimhashemi A, Grünthal G (2012) A statistical method for estimating catalog completeness applicable to long-term nonstationary seismicity data. *Bull Seismol Soc Am* 102(6): 2530-2546; <http://doi.org/10.1785/0120110309>

- Heidbach O, Custodio S, Kingdon A, Mariucci MT, Montone P, Müller B, Pierdominici S, Rajabi M, Reinecker J, Reiter K, Tingay M, Williams J, Ziegler M (2016) World Stress Map Database Release 2016. GFZ Data Services, <http://doi.org/10.5880/WSM.2016.001>
- Miller AC, Rice TR (1983) Discrete approximation of probability distributions. *Management Science* 29(3): 352–362. <http://doi.org/10.1287/mnsc.29.3.352>
- Vanneste K, Camelbeeck T, Verbeek K (2013) A model of composite seismic sources for the Lower Rhine Graben, Northwest Europe. *Bull Seismol Soc Am* 103(2A): 984-1007, <http://doi.org/10.1785/0120120037>
- Wiemer St, Danciu L, Edwards B, Marti M, Fäh D, Hiemer St, Wössner J, Cauzzi C, Kästli Ph, Kremer K (2016) Seismic Hazard Model 2015 for Switzerland (SUIhaz2015). Technical Report, Swiss Seismological Service (SED) at ETH Zurich, <http://doi.org/10.12686/a2>



ISSN 2190-7110